Barts and The London School of Medicine and Dentistry

Queen Mary University of London

Evaluation of the anti-tumour potency and biodistribution of vaccinia virus mutants in solid tumour models

PhD Thesis

Jonathan Hughes BSc MBChB FRCS

Barts Cancer Institute
Barts and The London School of Medicine and Dentistry
Queen Mary University of London

Acknowledgements

I am most grateful to Yaohe Wang, Ghassan Alusi and Nick Lemoine for their support and guidance during this project.

The provision of viruses by Istvan Fodor (VVIL110), Steve Thorne (WRLuc) and Andrea McCart (WRDD) is greatly appreciated. I would like to acknowledge the assistance of Jennelle Francis and Vipul Bhakta in virus production, and Gary Martin with the animal experiments.

All histology and immunohistochemistry was performed by the Barts Cancer Institute Pathology Service.

This project was supported by Barts and The London Charity, Cancer Research UK and The Royal College of Surgeons of England.

Abstract

The survival of many patients with advanced solid tumours has remained poor over the past 40 years, despite improvements in existing therapies. Progress in the field of molecular biology has made gene therapy a feasible treatment modality. Viruses are the most promising vectors, with an adenovirus the first to receive a government licence in 2003. However, the efficacy of adenoviral monotherapy has been disappointing in clinical trials. Vaccinia virus is an attractive alternative, with many superior characteristics. There are several strains of vaccinia virus, some of which have established safety profiles following their use as smallpox vaccines in millions of humans. The dominant strain in cancer research, Western Reserve, has been reported as the most potent oncolytic virus for cancer treatment, but is a non-vaccine strain. Other strains, such as the European vaccine Lister strain, are largely untested.

This study evaluated the anti-tumour potency and biodistribution of different vaccinia virus strains using *in vitro* and *in vivo* models of cancer.

Lister strain vaccinia virus demonstrated superior anti-tumour potency and cancer-selective replication *in vitro* and *in vivo*, compared to Western Reserve; especially in human cancer cell lines. Studies examining the safety of the virus following local and systemic delivery to immunocompetent mice bearing tumours confirmed favourable viral biodistribution of the Lister strain; with higher viral titres in the tumours. Examination of the serum from a mouse cancer model found lower levels of pro-inflammatory cytokines following Lister strain treatment.

Strategies to further improve the Lister strain virus were considered, and a Lister strain virus expressing the anti-inflammatory cytokine IL10 was shown to increase anti-tumour potency and viral titres within treated tumours.

This study suggests that the Lister strain is a more promising vaccinia virus strain than the Western Reserve strain for oncolytic viral gene therapy. IL10 expressed as a transgene enhances intratumoural viral persistence and anti-tumour potency.

Contents

List of Figures

List of Tables

List of Abbreviations

APC	antigen presenting cells
ATCC	American Type Culture Collection
ATP	adenosine triphosphate
BEGM	Bronchial Epithelial Growth Medium
BSA	bovine serum albumin
CAR	coxsackievirus and adenovirus receptor
CEV	cell associated enveloped viruses
CO_2	carbon dioxide
CPE	cytopathic effect
CRUK	Cancer Research UK
CRUK CCS	CR UK Central Cell Services
C_T	cycle threshold
CTL	cytotoxic T lymphocytes
DAB	3,3'-diaminobenzidine tetrahydrochloride
DC	dendritic cells
DMEM	Dulbecco's modified Eagle's medium
DNA	deoxyribonucleic acid
ds	doubled stranded
EC_{50}	viral dose required to kill 50% of cells
ECM	extracellular matrix
EEV	extracellular enveloped viruses
EGF	epidermal growth factor
eIF2α	eukaryotic translation initiation factor 2α
ELISA	enzyme linked immunosorbent assay
EMEM	Earle's minimal essential medium
FCS	heat-inactivated foetal calf serum
GDEPT	gene-directed enzyme prodrug therapy
GFP	green fluorescence protein
GMP	good manufacturing process
HBSS	Hank's balanced salt solution
H&E	hematoxylin and eosin
HNSCC	head and neck squamous cell carcinoma
HRP	horseradish peroxidase
IEV	intracellular enveloped viruses
IFN	interferon
IL	interleukin
IMV	intracellular mature viruses
IP	intraperitoneal
IT	intratumoural

ITR	inverted terminal repetitions
IV	immature viruses or intravenous
JAK	Janus kinases
JH	Jonathan Hughes
kbp	kilobase-pairs
LIVP	Lister virus from the Institute of Viral Preparations
MGB	minor groove binder
MHC	major histocompatability complex
MOI	multiplicity of infection
MMP	matrix metalloproteinase
MTS	3-(4,5-dimethylthiazol-2-yl)-5-(3-carboxymethoxyphenyl)-2-
MVA	Modified Vaccinia virus Ankara
NHBE	normal human bronchial epithelial cells
NK	natural killer
NYVAC	New York vaccinia virus
OD	optical density
PAMPS	pathogen associated molecular patterns
PBS	phosphate buffered saline
PFU	plaque forming units
PMS	phenazine methosulfate
PSA	prostate specific antigen
qRT-PCR	quantitative real-time polymerase chain reaction
RCT	randomised controlled trial
rIL10	recombinant IL10
RNA	ribonucleic acid
ROI	region of interest
rpm	revolutions per minute
SCID	severe combined immunodeficiency
SEM	standard error of mean
SFDA	State Food and Drug Administration
SPI	serine protease inhibitor
STAT	signal transducers and activators of transcription
TAA	tumour-associated antigen
$TCID_{50}$	50% tissue culture infective dose
TGF-α	transforming growth factor-α
TK	thymidine kinase
TLR	toll-like receptor
Tm	Melting temperature
TNF	tumour necrosis factor
TSG	tumour suppressor gene
USA	United States of America
UK	United Kingdom

VCP	vaccinia complement control protein
VEGF	vascular endothelial growth factor
VGF	vaccinia growth factor
VLTF-1	vaccinia late transcription factor-1
VVL15	Lister vaccinia virus armed with firefly luciferase
VVLister	Lister vaccinia virus vaccinia strain
VVlacZ	Lister vaccinia virus armed with lacZ
VVIL10	Lister vaccinia virus armed with murine IL10
WR	Western Reserve vaccinia virus
WRLuc	Western Reserve vaccinia virus with deletion of thymidine kinase
WRDD	WRLuc with VEGF deletion

1. Introduction

1.1. Cancer

Cancer was responsible for 7.6 million human deaths in 2007 globally; and is the second highest cause of death in the developed world, behind cardiovascular disease. [1] This figure is expected to increase to 17.5 million by 2050 due to population growth and aging. From a UK perspective, the most recent figures document 293,000 new cancer diagnoses and 155,000 cancer deaths in 2007. In the UK, breast, lung, colorectal and prostate are the most common forms of cancer; accounting for 54% of all new cancer diagnoses. From 1977 to 2006 cancer incidence rates have increased by 25%; however, more recently this rate has stabilised. In terms of survival, there is evidence of improvements in some cancer types (Figure 1.) due to advances in disease detection and treatment. However for many cancers (such as head and neck, pancreatic and lung) the prognosis for patients is largely unchanged. To address this impasse, cancer has become the main focus of medical research globally. [2]

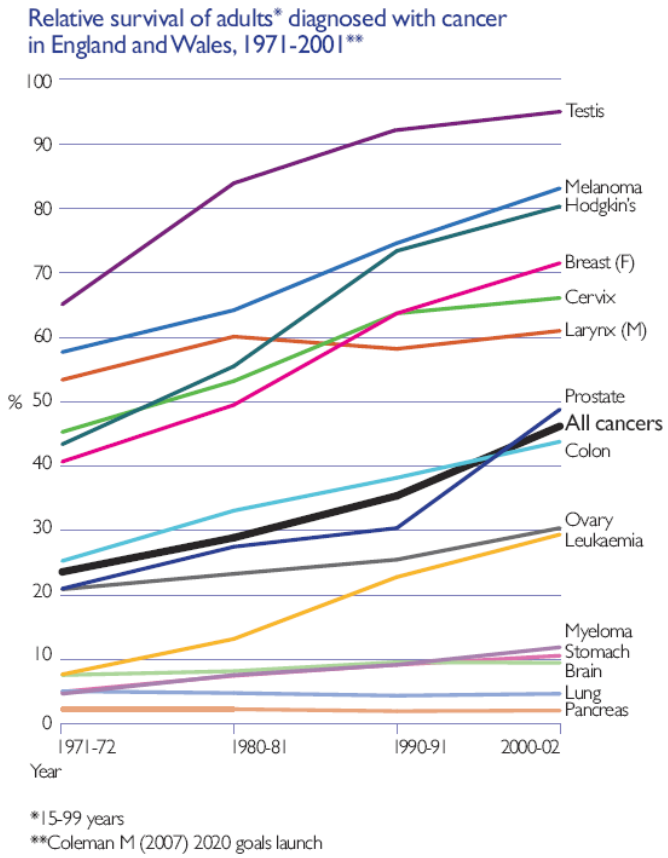

Figure 1. Comparison of relative survival rates for major cancers over 30 years. [3]

Advances in the field of molecular biology have allowed a greater understanding of the process of carcinogenesis; enabling progress in cancer prevention and treatment. Genetic changes, either inherited or acquired later in life, are the basis for uncontrolled cell proliferation that causes cancer. Gene therapy aims to treat cancer by delivering genetic sequences to patient's cells. The mechanism for this gene delivery relies on vectors, of which viruses are the most promising type; with the world's first gene therapy product (an engineered adenovirus) licensed for clinical application in 2003. [4]

Currently the greatest challenge for gene therapy is developing efficacious vectors that selectively replicate in cancer cells and are safe for human application. As a result many different species of virus are being evaluated, with adenovirus being the most extensively investigated. However the potency of adenovirus is limited by its dependence on a specific receptor for entry into the host cell, which can be altered during malignant transformation. [5] Consequently alternative vectors are being examined. One such alternative is vaccinia virus, of which there are many strains. A number of strains of vaccinia virus were used around the world as part of the smallpox eradication programme in the 1950s. The uses of vaccine-derived strains in cancer therapy have the major benefit in that they have been used extensively in human populations, and hence are relatively safe. Comparison of the *in vitro* and *in vivo* efficacy and safety between the dominant laboratory strain (Western Reserve), which has undergone minimal human testing, and the European smallpox vaccine strain (Lister) shall be made. Efficacy of viral gene therapy depends on the interaction between the host immune system and the virus. A new Lister strain vaccinia virus mutant (VVIL10) encoding an immune-modulating gene (IL10) will also be evaluated for efficacy and safety *in vitro* and *in vivo*.

1.2. Cancer cell biology

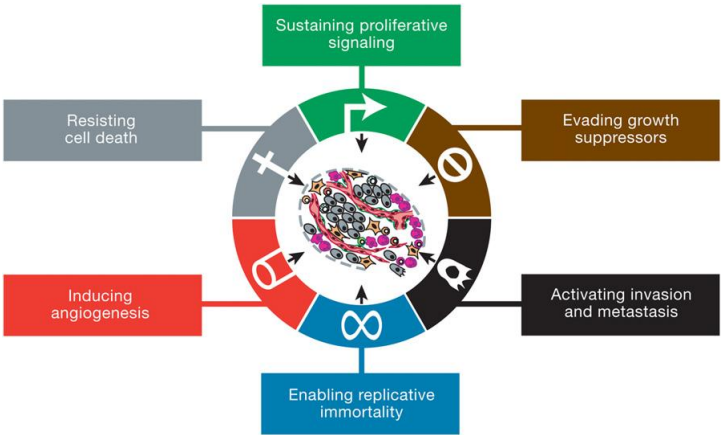

Figure 2. The Hallmarks of Cancer.[6]

Carcinogenesis is an onco-evolutionary process by which normal cells acquire, through a multi-step process, a succession of biological capabilities to become malignant. These six capabilities have been defined as the "Hallmarks of Cancer" and provide a robust framework to our understanding of neoplastic disease. [7] Acquisition of these hallmarks is made possible due to two enabling characteristics: genomic instability, caused by disruption of genome-maintenance and surveillance systems, and tumour immunoevasion. Additionally, recruited normal tumour surrounding cells (tumour-associated stroma) play a vital role in the development of cancer.

1. Sustaining Proliferative Signalling

Malignant tissues develop the ability to deregulate growth signals, leading to uncontrolled cell proliferation and growth compared to normal tissues; thus disrupting tissue architecture and function. Cancer cells can acquire this capability through production of growth factor ligands (autocrine proliferation); signalling to tumour-associated stroma, which in turn produce tumour proliferating signals; overexpression/structural alteration of receptor proteins leading to hyper-responsiveness; constitutive activation of the downstream signalling pathways; and disruption of negative feed-back signalling mechanisms. For example, RAS oncogene mutations abrogate Ras GTPase activity, which physiologically results in negative feedback on proliferation signalling.

2. Evading Growth Suppressors

Tumour suppressor genes, such as Retinoblastoma (Rb) and p53, encode proteins that acts as cellular gatekeepers; controlling proliferation through activation of senescence or apoptosis in response to extracellular signals, intracellular stresses or genomic damage. Additionally, abrogations of the mechanisms of cellular growth contact inhibition are seen in many cancers, with involvement of Merlin (NF2 gene product) and LKB1 proteins recently elucidated. These proteins in normal cells maintain tissue integrity and suppress mitogenic signals. [8,9]

3. Resisting Cell Death

Subversion of apoptosis by cancer cells despite cellular stresses is an important hurdle in tumourigenesis. [10] The apoptotic machinery is divided into upstream regulators and downstream effectors; with the regulators are further divided into an extrinsic death receptor pathway (responding to extracellular signals, such as Fas ligand and TNFα) and an intrinsic stress pathway (responding to intracellular signals, primarily regulated by the Bcl-2 family). A final common pathway involves activation of either caspase 8 and 9, activation of effector caspases (3, 6, 7), and subsequent cellular destruction. [10] Apoptosis initiation is triggered by the balance of pro- (Bax and Bak) and anti- (Bcl-2, Bcl-X_L, Bcl-w, Mcl-1 and A1) apoptotic members of the Bcl-2 protein family. Bax and Bak activation results in cytochrome c release, and downstream caspase-mediated proteolysis. Stimulation of the intrinsic stress pathway is thought to be most important in cancer development, [6] and several stress sensors, including the TP53 DNA-damage sensor, have been implicated in tumourigenesis. Additionally under-expression of cell survival factors, such as insulin-like growth factor 1/2 in epithelial cells, or hyperactive oncoprotein signalling, such as Myc, can induce apoptosis. [11] Cancer cells avoid induction of apoptosis by reducing expression of these stress sensors and pro-apoptotic regulators or, conversely, increasing expression of cell survival and anti-apoptotic proteins.

More recently further mechanisms of cell death, other than apoptosis, have unfolded. Autophagy is a process of lysosome-mediated cellular organelle breakdown in response to nutrient restricted environments, such as those found within cancers. The resultant catabolites are then available for more essential processes ensuring cell survival.[12] Beclin-1 protein has been demonstrated to be a key autophagy regulatory protein; with

mice bearing inactivated Beclin-1 genes more susceptible to cancer. [12] However the role of autophagy in cancer is conflicting with evidence of autophagy resulting in a pro-cancer survival state, allowing tumour re-growth in the presence of more favourable conditions.[13] Necrosis cell death differs from apoptosis and autophagy in that the dead cells contents are released into the tissue microenvironment. This induces recruitment of immune cells to clear up the necrotic debris. However there is evidence of a tumour promoting role of these recruited immune cells, releasing pro-proliferative factors, such as IL-1α, to act on neighbouring cells and induce neoplasia. [14]

4. Enabling Replicative Immortality

Non-malignant cells have a limited number of cell-cycles, in contrast to cancer cells which possess the ability to propagate almost indefinitely – immortalisation. Tandem TTAGGG repeats at the end of chromosomes, called telomeres, shorten progressively with each cell cycle in normal cells until the ends of the chromosomes can no longer be protected from fatal DNA fusions; resulting in senescence or cell death. [15] Specialised DNA polymerases, called telomerases, are over-expressed in the majority of cancers, but absent in normal cells, are able to add telomeres to DNA; thereby allowing almost limitless replication.

In contrast to the dogma that all malignancies over-express telomerase, recent evidence has shown that some early stage malignancies are unable to express significant levels of telomerase and undergo cell death. [16] As such these cells are unable to progress to later stage malignancies. Transient telomere deficiency may even facilitate malignant progression, by increasing genomic instability, and therefore mutations of oncogenes and tumour suppressor genes. This has been demonstrated to occur in mice lacking TP53-mediated genomic surveillance and telomerase.[17] Therefore it has been proposed that in the early stages of carcinogenesis telomere deficiency allow tumour promoting mutations to occur, whereas at later points in the development of cancer telomerase function stabilises the malignant genome allowing limitless replication. [6] Furthermore telomerase may have tumour-promoting roles by enhancing cell proliferation and apoptosis resistance. [18]

5. Inducing Angiogenesis

Tumours are able to switch on physiologically quiescent angiogenesis to provide vasculature for their ever increasing metabolic requirements early on in their

development. This "angiogenic switch" is governed by the balance of stimulatory and inhibitory factors on vascular endothelial cells,[19] as well as peri-tumoural inflammatory cells.[20] The prototypal stimulator of angiogenesis is vascular endothelial growth factor-A (VEGF-A), via tyrosine kinase receptors (VEGFR- 1-3). VEGF expression can be upregulated by hypoxia and oncogene signalling. Conversely thrombospondin-1 (TSP-1) can bind to transmembrane receptors on endothelial cells and inhibit angiogenesis. [21] Other endogenous inhibitors of angiogenesis include angiostatin (plasmin fragment) and endostatin (type 18 collagen fragment) have a role in wound healing and act to prevent angiogenesis in neoplasia.[21]

6. Activating invasion and metastasis

The "invasion and metastasis cascade" encompasses a multistep process of cancer cells, [22] and is associated with changes in shape, attachment to other cancer cells and the extracellular matrix (ECM) of cancer cells. E-cadherin is a key cell to cell adhesion molecule and is frequently downregulated in human carcinomas. [23] Conversely adhesion molecules normally associated with cell migration are upregulated in invasive cancers; such as N-cadherin. [6]

The "epithelial-mesenchymal transition" (EMT) is a developmental regulatory program that is crucial for embryogenesis and wound healing. [24] This program can be activated by cancer cells allowing invasion and metastasis. EMT-inducing transcription factors identified as controlling the program include Snail, Slug, Twist and Zeb1/2; with overexpression of some eliciting metastasis experimentally.[25]

Yet again the importance of tumour stromal cells in carcinogenesis is apparent, with evidence that these cells, in addition to stimulating angiogenesis, have a role in cancer cell invasion and metastasis. [26] For example, tumour associated macrophages (TAMs) produce matrix-degrading enzymes that facilitate local invasion. [27]

Dissemination of cancer cells from the primary tumour must be followed by survival and growth in the new tissue microenvironment for metastasis to be successful; this, however, does not always occur. [22] Some metastases remain dormant until treatment or after long periods of time following treatment. Causes for this include: failure to activate angiogenesis, [28] induction of autophagy due to starvation, [29] anti-growth signals of normal extracellular matrix, [30] and immune tumour-suppressive actions. [31] The

timing and location (primary or secondary site) of the acquisition of the capability of metastases to establish themselves in the new tissues is unclear.

In addition to the six core hallmarks first described in 2000, [7] two emerging hallmarks have been described: reprogramming of energy metabolism and evasion of immune destruction. [6] The importance and mechanistic independence from those initially described has yet to be definitively established.

Reprogramming of glucose-dependent ATP production from oxidative phosphorylation to the glycolysis, even in the presence of ample oxygen, – the so-called "Warburg effect", [32] or "aerobic glycolysis" - has been observed in many cancers. This method of energy metabolism is 18 times less efficient, however it allows for the diversion of glycolytic intermediates into biosynthetic pathways that are of vital importance for rapidly proliferating cells. [33]

The role of the immune system, in particular the innate arm, has historically been thought to attempt to destroy cancer cells through immunosurveillance. Better prognoses have been demonstrated in patients with tumours showing heavy CTL and NK infiltration. [34] Cancer cells themselves have been shown to secrete TGF-β and other immunosuppressive cytokines to evade the host immune system. [35]

1.3. Gene Therapy

Gene therapy has been defined in the 2003 United Kingdom Government white paper, "Our inheritance, our future – realising the potential of genetics in the NHS", as "the deliberate introduction of genetic material into patient's cells in order to treat or prevent a disease". [36] This document suggested that gene therapy would have diverse applications from "cancer to coronary artery disease"; and gave hope for licensed treatments "within five to ten years".

Gene therapy was initially applied to inherited diseases with single gene mutations (monogenic); such as Severe Combined Immunodeficiency Disease (SCID), Cystic Fibrosis and Haemophilia. However permanent corrective gene expression in such

illnesses has been unsuccessful. This together with the development of leukaemia in children with SCID, and the death of a patient with ornithine transcarbamylase deficiency following viral gene therapy highlighted the potential risks of such treatments. [37] With this in mind new applications for gene therapy, such as cancer and cardiovascular disease, were considered; where transient gene delivery would be more likely to be achieved, and provide a safe and clinically significant effect. [38]

Cancer is a genetic disease, with normal cells undergoing multiple mutations, as part of an "onco-evolutionary process", to transform into malignant cells. Mutations in the cell behaviour regulating genes (proto-oncogenes and tumour suppressor genes) lead to cell growth self-sufficiency, insensitivity to anti-growth signals, evasion of apoptosis, sustained angiogenesis, limitless replicative potential and tissue invasion and metastases – the hallmarks of cancer, as previously described. [7] All of these changes are potential targets for gene therapy and has resulted in cancer gene therapy dominating the gene therapy research field; with two-thirds of clinical trials for cancer applications. [39] However success at clinical trial has been disappointing mainly due to poor efficiency of gene transfer rather than a paucity of potential therapeutic genes. [40] Strategies to overcome this have focused on modulating the host immune response to the virus, optimising existing viruses, discovering/creating new viruses and, finally, identifying tumour-associated genes that can improve viral potency.

1.4. Choice of genes for cancer therapy

Following the mapping of the human genome in 2008, there is an extensive array of genes available as potential therapeutic transgenes for cancer gene therapy. There are three main strategies that characterise the type of gene used: corrective, cytoreductive and immunomodulatory.

1.4.1. Corrective

Cancer is caused by mutations in oncogenes and tumour suppressor genes (TSG) resulting in uncontrolled cell growth. Corrective gene therapy attempts to block oncogene or replace TSG function, thereby returning cells to normal cell growth. p53 TSG mutations are implicated in over 50% of all cancers, and is thus is considered to be a potential magic bullet for corrective cancer gene therapy. [41] In 2003 the world's first government licensed gene therapy product featured a recombinant adenovirus

expressing p53 (Gendicine™; SiBiono Schenzhen, China). [4] Oncogenes can be overexpressed or amplified in cancer; and their action can be blocked therapeutically at either the transcriptional or translational level.

1.4.2. Cytoreductive

Cytoreductive gene therapy aims to directly or indirectly kill cancer cells, rather than correct the underlying genetic defect. This can be achieved by augmenting the effects of chemotherapy, by introducing a transgene that can convert an inactive pro-drug to a potent anti-cancer agent, for example the nitroreductase gene and CB1954. [7] Other strategies include inhibiting angiogenesis, [42] or inducing apoptosis. [4]

1.4.3. Immunomodulatory

The host immune response detects tumour associated antigens (TAA) which allows CD8+ cytotoxic T cells to induce tumour lysis. Cancer cells can subvert this immuno-surveillance through three broad strategies of tumour escape; which have been suggested to represent a "seventh hallmark of cancer". [43] One common strategy is to reduce the immunogenicity of the cancer cells by modulating the interaction of peptides, MHC molecules and T cell receptors – a process termed antigenic drift. [44] Also MHC class I down–regulation by tumour cells reduces the cancer cell sensitivity to CTL mediated lysis.[45] A second strategy is to develop resistance to immune-mediated killing by impairing perforin binding, [46] down-regulation or mutation of Fas, [47] and mutations in TNF-related apoptosis-inducing ligand receptors in tumours.[48] A final strategy is to subvert the immune response through failure to produce danger signals that activate DCs (which can lead to development of immunosuppressive Tregs),[49,50] down-regulation of endothelial adhesion molecules,[51] induction of tryptophan deficiency (which inhibits T cell proliferation),[52] secretion of immunosuppressive mediators (such as nitric oxide, TGFβ, IL10),[53-55] tumour expression of Fas ligand (which can kill infiltrating immune cells),[56] and induction of myeloid suppressor cells (which inhibit CD8+ T cell/ NK activity and DC maturation).[57]

Gene therapy can reverse this tumour-induced immuno-tolerance by increasing TAA presentation or upregulating MHC I expression. [40] This has been achieved by using cytokines as transgenes, with resulting enhanced antitumour efficacy; for example IL2 and IL12 delivery by vaccinia virus in a glioma mouse model. [58] Furthermore, clearance

of the viral vector or oncolytic virus by the host immune response can also be reduced by this approach. [59]

1.5. Vectors for Gene Therapy

The greatest limitation to cancer gene therapy becoming an effective everyday clinical treatment modality is the accuracy and efficiency of gene transfer to the target cells. [40] The ideal vector should be efficient, safe and tumour selective; preferentially affecting cancer cells and sparing normal cells. Tumour selectivity can be achieved by administering the vector directly into the tumour, or through engineering the vector physically or genetically. The latter strategy is more attractive as this would allow for systemic administration which would be able to treat inaccessible or multiple lesions. However to reach its target the vector would have to overcome clearance of circulating virus by complement and the reticulo-endothelial cell-based mechanisms, leading to phagocytosis of viral particles by macrophages or liver Kupffer cells. [60]

The two main groups of vectors used in cancer gene therapy research are viral and non-viral. Approximately 70% of clinical trials and the majority of research to date have used viral vectors. [38] Non-viral vectors use either physical transfection or particle-mediated systems to introduce foreign DNA into the target cells. They are generally less immunogenic than viral vectors which allows for repeated administration. [61] Additionally they are cheaper to produce, and can carry more DNA; however their major disadvantage is low transfection rates.

Viruses are obligate intracellular pathogens which require host cell machinery to complete their life cycles. They have evolved over millions of years to be highly effective at infecting, replicating within and generally lysing host cells. Viruses have also developed mechanisms that allow them to subvert the host immune system and thereby increase their infectivity, such as expressing interferon γ decoy receptors. Viral vectors commonly induce mild flu-like illnesses, but have the potential for causing acute life-threatening toxicity. Some “oncolytic” viruses can also exert an anti-cancer directly themselves. Apart from different viral species, a common classification of viral vectors is whether they have the ability to replicate. Non-replicating viruses were the first vector systems for the delivery of foreign genes and most research to date has

utilised such viruses. [62] However, the efficacy of gene transfer of these viruses is poor, and for successful cancer treatment every tumour cell would have to be infected.

In contrast replicating viruses allow more cancer cells to be infected as their progeny can go on to infect more cells and destroy the host cell as a direct consequence of their replication. [62] Replication-selective viruses have the ability to replicate in tumour cells, but not normal cells. Some viruses exhibit inherent tumour selectivity, such as Reovirus and Newcastle virus; whereas other viruses can be genetically modified to improve tumour selectivity. This can be achieved by inserting tumour-specific promoters, such as prostate-specific antigen (PSA) or deleting genes that are needed for viral replication in normal cells but not tumour cells, such as thymidine kinase.

The most commonly used virus for gene therapy is the adenovirus. It is non-integrative, has high transfection efficiency and can be produced in high titres to good manufacturing process (GMP) standards. However the anti-tumour efficacy in many clinical trials has been poor. [4,63]

1.6. Oncolytic viruses

Oncolytic viruses are self-replicating, tumour-selective viruses that are able to lyse cancer cells. [64] In this way they differ from our original notion of viral gene therapy whereby a viral vector is used to deliver specific gene expression to a host tissue to correct an underlying genetic defect. However, oncolytic viruses can also be armed with therapeutic genes, such as anti-angiogenic or immunomodulatory genes, to enhance their anti-tumour potency.

At the beginning of the last century the oncolytic effects of viral infections were first noted, whereby periods of clinical remission were observed in patients with leukaemia following influenza infection. [65] Oncolysis is achieved through multiple mechanisms, including direct lysis, apoptosis, expression of toxic proteins, autophagy, protein synthesis shut-down and induction of anti-tumoural immunity. [66] The 1950s and 1960s saw clinical trials of several wild-type oncolytic viruses (first generation) including reovirus, adenovirus, vaccinia virus and Newcastle disease virus. However it wasn't until 1991 that advances in molecular biology allowed the development of the first genetically-engineered, replication-selective oncolytic virus (second generation), using a herpes simplex virus. [67] Subsequent research has continued investigation into genetic

modifications to the viral backbone to improve tumour selectivity and anti-tumour potency, including arming of viruses with transgenes (third generation). In 2005 China approved the world's first oncolytic virus treatment, the genetically modified adenovirus Onyx015/dl1520, or H101, for late-stage refractory nasopharyngeal cancer in combination with chemotherapy. [68]

Adenovirus has been the most extensively researched of the oncolytic viruses. Adenoviruses are double stranded DNA viruses, whose natural pathogenicity is associated with only mild respiratory infections. The main strategy used to achieve adenoviral tumour selectivity has been through deletion of the E1B-55K region, which normally encodes a p53 binding protein that prevents virally induced apoptosis or cell cycle arrest in normal cells. [62] As approximately half of all malignancies are p53 deficient, [41] E1B-55K deletion confers restricted adenoviral replication to tumour cells, sparing normal tissue. Onyx015 or *dl*1520 virus has shown to be well tolerated in phase I and II clinical trials alone or in combination with chemotherapy; however objective tumour responses have been disappointing. [69,70] It has been postulated that poor adenoviral anti-tumour potency could be due to downregulation of CAR receptors on the tumour cell surface, thus limiting adenoviral cellular infection. [71] Further limitations of adenovirus arise due to the fact that adenoviruses are common pathogens; with most adults exposed to the most widely used serotype 5 adenovirus (Ad5). [72] Neutralising antibodies to systemically administered adenovirus attenuate its efficacy as an oncolytic virus through rapid viral clearance.

Systemic delivery is compromised not only by circulating neutralising antibodies, but also by due to Kupffer cell-mediated liver sequestration and complement; [73] limiting current adenovirus therapy to intratumoural injection and, therefore, making the treatment of disseminated disease difficult.

Recent research has identified carcinoembryonic antigen-related cell adhesion molecule 6 (CEACAM6) expressed by some cancer cells as having a role in limiting the ability of adenovirus to infect cancer cells. [74] CEACAM6 has been shown to block adenovirus trafficking via the Src pathway which interferes with the cytoskeleton of cancer cells.

Finally, the lack of immunocompetent mouse models for investigating the *in vivo* efficacy of adenovirus is a major barrier to developing adenoviruses suitable for clinical

trial. These limitations of adenovirus have led researchers to consider other oncolytic viruses, such as vaccinia.

1.7. Vaccinia Virus

Vaccinia virus has a long history of medical use in humans. In 1796 Edward Jenner isolated cowpox from the hand of a milk-maid, and subsequent inoculation of a boy conferred protection to small pox. [75] Vaccination against smallpox continued and in 1980 smallpox eradication was declared complete at the 33rd World Health Assembly. The exact origin of the vaccinia virus strain has not been definitively established, but it is thought to be derived from the cowpox. [76,77]

Vaccinia has several characteristics that make it a more attractive vector compared to adenovirus. It has a much larger cloning capacity of 25kb, compared to 7kb for adenovirus, and has strong promoters to drive high levels of transgene expression. It has a wide host range and a natural tumour tropism; infecting cells through membrane fusion rather than a defined cell surface receptor. [78] Four to six hours following vaccinia infection host protein synthesis is shut down, facilitating rapid viral replication with ~10 000 copies of the viral genomes produced within 12 hours. [79] Vaccinia does not integrate DNA into the host genome, which is a safety concern of other viral vectors; instead replicating in viral factories within the cytoplasm. The short life cycle compares favourably with the 48-72 hours life cycle for adenovirus; resulting in rapid cell death. [80] During its life cycle, vaccinia virus exists in different forms; however the extracellular enveloped virion (EEV) form is derived from host cells membrane and therefore has limited antigenicity allowing unharmed passage through the host bloodstream to distant tumours following systemic delivery. Vaccinia virus has also been shown recently to replicate well in the hypoxic environments often present in solid tumours. [81] Further advantages include rapid cell to cell spread, strong lytic ability and reliance on its own encoded proteins for replication, rather than the host cell. This latter advantage is in contrast to adenovirus which depends on many host encoded proteins for its replication, which can be lost during tumourigenesis. Finally, its safety profile is well established following its use globally as a smallpox vaccine, with established antiviral agents available to treat adverse responses, such as vaccinia immunoglobulin and cidofovir.

1.7.1. Vaccinia virus biology

Vaccinia virus is a member of the genus *Orthopoxvirus* from the *Poxviridae* family. There are many strains of vaccinia virus, some of which are smallpox vaccine strains developed in different countries during the global eradication programme and consequently have considerable data regarding their safety in humans. Other strains are considered of limited oncolytic potential in humans due to their inability to replicate in mammalian cells or toxicity. [60] Certain strains show higher levels of inherent tumour selectivity making these strains preferable for anti-cancer treatments.

The New York City Board of Health (NYCBH) or Wyeth strain was obtained from England in 1856 and was used as the smallpox vaccine strain in North America. [77] The Western Reserve (WR) strain is derived from the NYCBH strain following serial passage in mice brains; and has demonstrated superior virulence and anti-tumour potency *in vitro*. [82] However WR is not a vaccine strain and therefore its safety in humans is largely unknown. Additionally WR has been show to exhibit significant off-target replication in ovaries and bone marrow, [83] and may cause death by overwhelming pulmonary replication. [84,85] These safety concerns have led to research into identifying and modifying other vaccinia virus strains for cancer therapy.

The Modified Vaccinia Ankara (MVA) and New York Vaccinia (NYVAC) are highly attenuated and consequently have a good safety profile; however they do not replicate in mammalian cells. [60] The Tian Tian strain is the Chinese vaccine strain and was used extensively during smallpox eradication. It has been used as a cancer vaccine, but has unknown potential as an oncolytic agent. [60] The Copenhagen strain was the Northern European vaccine strain, but was withdrawn due to toxicity. The other European vaccine strain is the Lister strain. The Lister strain was developed in the Elstree laboratories at the Lister Institute in London. Both Lister and WR can be cost-effectively mass produced to high titres. Despite the Lister virus having been fully sequenced, [86] this strain has not been extensively researched in terms of its oncolytic potential and may represent a promising virus strain for such an application.

This study will compare the perceived gold standard laboratory WR vaccinia strain, which has limited clinical testing as a non-vaccine strain, against the European smallpox vaccine strain, Lister; which has been used in millions of humans as part of the

smallpox vaccination program, but for which we have few data regarding its efficacy as an oncolytic virus.

1.7.2. Vaccinia virus structure

Poxviruses, including vaccinia, are brick-shaped particles (350nm in diameter) consisting of outer lipoprotein membranes surrounding a complex core structure (Figure 3.). [75] The genome contains double-stranded DNA with inverted terminal repeats and terminal hairpin loops; consisting of 191 636 bp encoding 2063 proteins. [86]

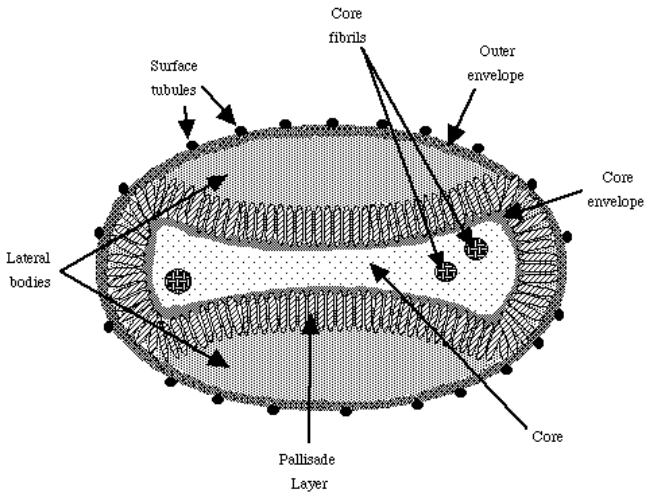

Figure 3. Vaccinia virus structure.

Vaccinia virus spends its life cycle in the host cell cytoplasm and does not integrate into the host genome (Figure 4.). There are four forms of the virus (Figure 4.): the intracellular mature virion (IMV), intracellular enveloped virus (IEV), cell associated enveloped virus (CEV), and the extracellular enveloped virion (EEV); which differ in structure by the number and origin of their lipid membrane. The IMV form is the initial viral particle produced by the cytoplasmic viral factories. It is surrounded by a single lipoprotein layer and is released when infected cells are lysed. The IEV form is triple lipoprotein-enveloped and is produced after fusion with the trans-Golgi network or early endosomes. The CEV form is a result of the fusion of the IEV form with the cell surface membrane. The EEV form is a double lipoprotein-enveloped virus and is released from the cell by membrane fusion; it is this form that is responsible for cell to cell spread. It has host-derived complement control proteins in the outer envelope, making it more resistant to antibody neutralisation than the IMV form.[87] However the EEV form is too

fragile to survive the purification process during its manufacture; [88] as a result the form of the virus made for experimental use is the more immunogenic IMV form.

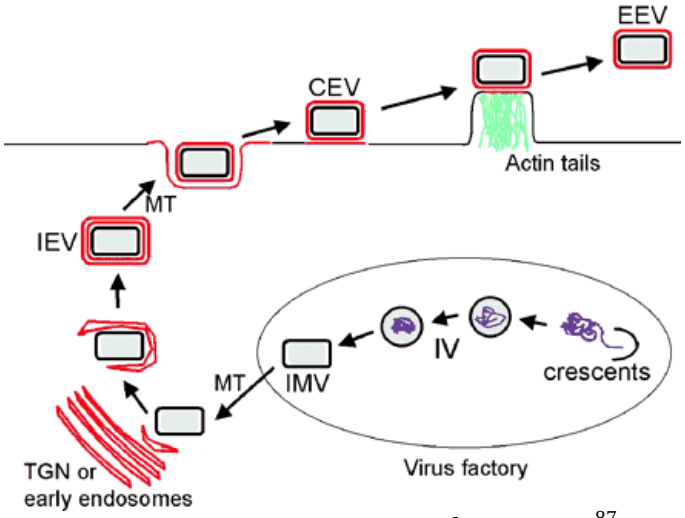

Figure 4. Vaccinia virus morphogenesis. [87]

Vaccinia virus has a wide tropism and can enter most mammalian cell lines. [89] Although no specific vaccinia virus receptor has been identified for cellular entry, several outer membrane proteins, including A27L, A28L and D8L, are thought to facilitate the process. [78,90-94] These proteins bind to heparan sulphate and chondroitin sulphate on the host cell surface. [91,92] The mechanism of vaccinia virus cell entry is dependent on the infectious form with IMV forms entering by plasma membrane fusion and EEV forms entering by endocytosis. [78]

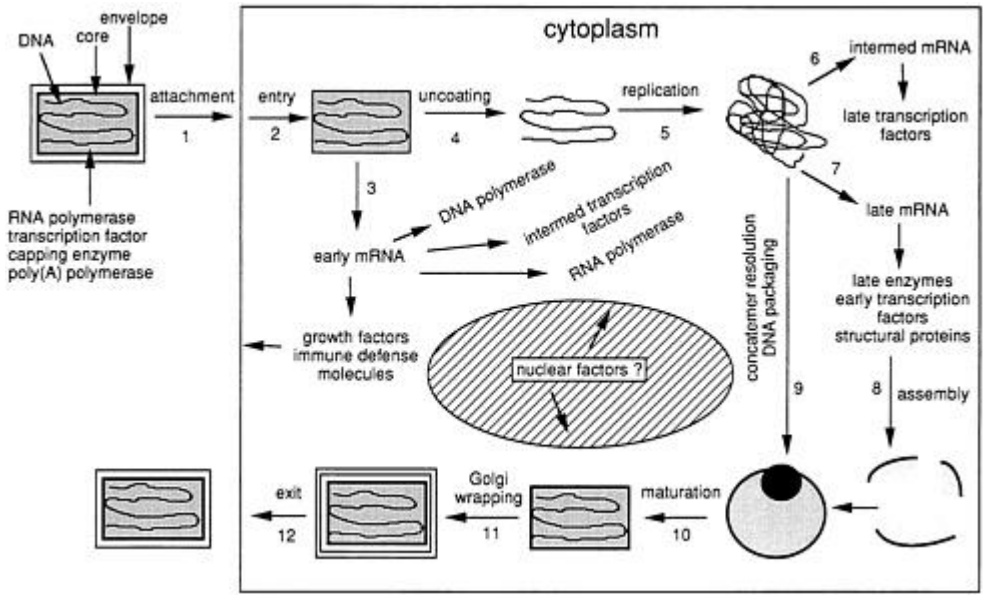

Figure 5. Vaccinia virus life cycle. [90]

Viral entry into the cell is rapidly followed by release of viral transcription enzymes that transcribe early viral mRNA, which encodes proteins involved in uncoating viral DNA and transcribing intermediate mRNA (Figure 5.). Intermediate mRNA encodes late transcription factors leading to late mRNA synthesis, with late proteins including viral structural proteins and early transcriptional factors to be incorporated into the mature virion. DNA replication produces concatemers which are cut into individual genomes and assembled into mature virions. The mature virion contains three membranes, the outer membrane fuses with the host cell membrane, releasing a double-membrane EEV. The A34L vaccinia gene product keeps the EEV attached to the cell membrane, allowing the virus to spread to another cell without being released into the blood-stream. [95] This replication process is very efficient; within 4 – 6 hours host protein synthesis is shut down, within 8 hours the first viral particles are produced and the infected cell is destroyed after 12 hours. [60]

1.7.3. Tumour selectivity

Vaccinia has a natural tropism for tumours. Following IV administration of wild-type WR strain the highest viral titres are found in the tumour followed by the ovary, with intermediate titres in brain and bone marrow, and minimal virus in other tissues. [96] It has been postulated that this may be due to tumour capillaries lacking an intact basement membrane and having large gaps between endothelial cells, allowing the 350nm vaccinia virus to "leak" into the extravascular space. [97] This theory is supported by evidence of hypothermia improving vaccinia dissemination through induction of capillary dilatation. [98] Other factors that may explain VV cancer tropism include improved viral replication in cells with: activated epidermal growth factor receptor (EGFR) – Ras pathway (which is present in most human cancers), vascular endothelial growth factor (VEGF) expression (Hiley *et al*, unpublished work) and loss of host cancer cell immunological factors, including interferon gamma (IFNγ) anti-viral responses. [99]

However it has been possible to further improve tumour selectivity by deleting viral genes responsible for transforming a normal cell into an optimal state for viral replication. These genes often have an effect of inducing a malignant-like cellular phenotype of uncontrolled cell cycle and evasion of apoptotic pathways. [60] As the cancer cells are already in this state of unregulated growth, there is no requirement for

them to be virally induced, and can be safely deleted without detriment to viral replication in cancer cells.

One such deletion is the thymidine kinase (TK) gene, which when deleted renders the virus dependent on cellular thymidine kinase which is transiently expressed during S phase in normal cells, but constitutively expressed at high levels in cancer cells. [100] Vaccinia also expresses an EGF homologue (vaccinia growth factor; VGF) that binds EGFR. [101-103] VGF induces cell proliferation, but as many cancers already have an activated EGFR – Ras pathway, deletion of this gene does not interfere with viral replication in cancer cells. WR VV with deletions of TK and VGF, so-called double-deleted virus (vvDD or WRDD) shows markedly enhanced tumour specificity compared to wild-type and single-deletion mutants. [83] Another tumour-selective deletion is the gene encoding an IFNγ receptor homologue. Interferons are key components of the innate immune response to viruses. Normally the virus produces a decoy receptor to sequester extracellular IFN. [104,105] However viruses that are unable to produce this decoy receptor have replication limited to cells that have lost the ability to produce or respond to IFN, and in particular cancer cells. [106] Other strategies include deleting serpins (SPI-1 and SPI-2) which inhibit apoptosis, [107,108] and an inhibitor of cytochrome c release. [109]

1.7.4. Immune evasion of vaccinia virus

The oncolytic efficiency of vaccinia virus is critically dependent on its clearance by the host immune system. A too vigorous immune response will remove the virus prematurely and result in a weak anti-tumour response. Conversely, a powerful immune response can be triggered by vaccinia virus against both virally infected and uninfected tumour cells, resulting in robust anti-tumour potency. [110] The host immune response to viral infections is biphasic, comprising the immediate, non-specific and amnesic innate immune system, followed by the delayed onset, specific and memory-inducing adaptive immune responses, sub-divided into the humoural and cellular systems (the latter seems to be the more crucial for viral clearance). [79]

1.7.5. Host anti-viral innate immune response

The innate response is the immediate immune response and relies on critical effectors, such as interferons (IFNs), natural killer (NK) cells, macrophages and neutrophils. IFNs are a group of secreted proteins produced in response to viral infections. There are two

types of IFNs: type 1 IFNs include IFNα and IFNβ, and are secreted by leukocytes and fibroblasts. They offer resistance to virus infection, stimulate MHC class 1 expression and inhibit cellular proliferation. [111] Type 2 IFN (IFNγ) is secreted by NK cells and T cells. IFNγ recruits leukocytes to the site of the infection, stimulates the bactericidal activity of macrophages and regulates the Th2 response. [112] Both types of interferon have demonstrated a key role in limiting poxvirus infections; with mice deficient in IFN receptors abnormally susceptible to vaccinia infections. [113]

Macrophages phagocytose opsonised virus, but also have an important function as antigen presenting cells (APC) for the activation of T cells and initiation of a specific immune response. Mice depleted of macrophages are unable to control vaccinia infections due to impaired viral clearance and antigen presentation. [114] NK cells are attracted to the site of infection and kill virus-infected cells, especially those with reduced levels of MHC class 1 expression. [115] NK cells have a direct cytotoxic effect on vaccinia-infected cells *in vitro*. [116] NK cell depletion has also been associated with enhanced vaccinia virulence *in vivo*. [117]

The innate immune system also includes the complement system of proteins in the plasma that are able to destroy enveloped virions or infected cells via the formation of membrane attack complexes (MAC); through either the classic (antibody-dependent) or alternative (antibody-independent) pathways. Additional functions of the complement system include opsonisation, mediated by C3b, and attracting macrophages and neutrophils, via the C3a and C5a fragments.

1.7.6. Host anti-viral cellular immune response

The T cell response is the most important adaptive immune response against vaccinia infection. In mouse models, the absence of a functional T cell population allowed vaccinia to express genes within tumour cells for greater durations than in an immunocompetent model. [118] Also progressive vaccinia infection (vaccinia necrosum) is known to correlate with defects in cell-mediated immunity. [119] Furthermore it has been demonstrated that vaccinia infection is capable of raising a cytotoxic T lymphocyte (CTL) or CD8+ T cell response not only against virus, but also against virally infected tumour cells. [120]

CD4+ T helper cells may have a greater role in the immune response against vaccinia than CD8+ T cells. Depletion of T helper cells has been shown to cause viral persistence, whereas CTL depletion fails to demonstrate a similar effect. [114] Moreover, most of the immunomodulatory proteins expressed by vaccinia virus also target the T helper cell induced immune response. [121]

1.7.7. Host anti-viral humoural immune response

The smallpox vaccination programme has resulted in the majority of older patients being immunised to vaccinia, with patients born after the 1970s free from immunity. The presence of circulating antibodies against vaccinia has the potential to diminish the anti-tumour potency of vaccinia virus. However this appears not to be significant, with no effect on anti-tumour potency demonstrated in a recent clinical trial following IT vaccinia delivery. [122] Additionally, it is known that systemic spread occurs 1-2 weeks post-infection in humans despite rising antibody levels, and that re-infection is still possible. [123] The EEV form of vaccinia virus is resistant to antibody neutralisation and, as this form is responsible for the majority of long-range spread of vaccinia, represents a significant advantage to vaccinia use as a gene therapy vector and/or oncolytic virus. [124] Mutations in vaccinia virus that increase the proportion of EEV released compared to CEV have been shown to increase viral spread through tumours, and to distant tumour sites in the face of neutralising antibodies.[125]

1.7.8. Vaccinia virus immunomodulatory proteins

Vaccinia virus has evolved a number of strategies to evade the host immune response that shall be considered in turn below.

Firstly, as previously stated, the EEV form of vaccinia virus is resistant to antibody neutralisation, in contradistinction to the IMV forms. [88,113,126] The EEV form mediates distant spread of vaccinia following inoculation and therefore represents a promising systemic treatment for metastatic cancer.

The vaccinia genome encodes a number of immunomodulatory proteins that block the innate and cellular immune systems, through inhibition of cytokines (Interferons, TNF, Interleukins), chemokines, complement and Toll-like receptors. [127]

Interferons are important mediators of the host anti-viral response and vaccinia produces interferon decoy receptors (B8R, B18R) [128,129] and also blocks interferon-induced apoptosis (E3L), [130] and protein translation shut-down (K3L). [131] TNF are critical cytokines in the early defence against viruses, and vaccinia genes A53R and B28R encode TNF decoy receptors preventing TNF action. [132]

Toll-like receptors (TLR) are pattern recognition receptors (PRR) that recognise pathogen-associated molecular patterns (PAMPs) and form an important sentinel function of the innate immune system. A52R and A46R vaccinia genes encode inhibitors TLR signalling, [133] thereby impairing the innate immune response to the invading virus.

Nuclear factor kappa-light-chain-enhancer of activated B cells (NF-kB) is a transcription factor that regulates innate immune responses to cellular stresses including viral infection. N1L vaccinia protein has an immunomodulator action by blocking NF-kB signalling pathways. [134]

Chemokines are small cytokines that direct chemotaxis during the immune response. B29R and A41L vaccinia genes have been identified as inhibiting chemokine activity. [127,135] More recently a 35kDa viral CC chemokine inhibitor (vCCI) has been identified as expressed by several strains of vaccinia, excluding WR strain. [136] Vaccinia genes B13R, B15R and C12L block IL-1β and IL18 proinflammatory cytokine function. [127]

Furthermore, vaccinia expresses several genes that inhibit serpins, [137] cytochrome c release, [109] and complement activation, [138] enhancing the persistence of the virus in the face of the host immune response.

Other studies have examined the role of certain cytokines in changing the balance of Th1 (IFNγ, IL12) and Th2 (IL4, IL10) immune responses. Viral replication was enhanced in IL12 and IFNγ knockout mice, whereas IL4 and IL10 knockout mice exhibited increased viral clearance. [139] This suggests that the Th1 response is most important in vaccinia virus clearance.

1.7.9. Development of vaccinia virus as an oncolytic agent

Preclinical evidence suggests that wild-type vaccinia virus strains are naturally tumour-targeting following systemic delivery.[140] Several trials in the 1970s and 1990s using wild-type viruses, mainly in melanoma patients intratumourally, have demonstrated only mild, transient, flu-like symptoms with objective tumour regression rates (>50% reduction in volume) in over 50% of cases; and complete regression in 25% of cases. [123,141-143] A further phase I/II trial, evaluating intravesical instillation of virus in bladder cancer patients showed the treatment was again well tolerated, and evidence of intratumoural viral replication and tumour destruction was recorded. [144] Despite these promising early results research over the intervening years has focused on improving tumour targeting, raising the possibility of a systemically delivered therapy that could treat both primary and metastatic disease, and enhancing anti-tumour potency of the wild-type virus through genetic modification.

1. Tumour targeting

Viruses endeavour to induce a cellular state in their host cell very much like the cellular state of cancer cells. They express a number of genes that result in the host cells inability to arrest cell cycle and enter apoptosis, and consequently undergo uncontrolled proliferation. This cellular state is often present in cancer cells and therefore preferentially supports viral replication compared to non-cancer cells. Specifically for vaccinia virus, cells with activation of the epidermal growth factor receptor (EGFR) – Ras signalling pathway support vaccinia replication and spread. [145] Activation of this pathway is seen in most cancers; [7] suggesting vaccinia has a broad tropism for tumours. Therefore when viruses infect cancer cells the viral genes that are required to induce the optimal cellular state for viral replication in non-cancer cells are not needed. Deleting these genes from the viral genome consequently restricts viral replication to cancer cells.

The most successful gene deletions to restrict viral replication to cancer cells are thymidine kinase (TK) and vaccinia growth factor (VGF). TK insertional inactivation leads to viral dependence on host cell sources of TK; [146] which are only transient in normal cells, but constitutively high in the majority of cancer cells. [100] It has been shown in biodistribution experiments that viral replication of TK-deleted vaccinia virus

is much higher in tumours compared to other organs. [118] Most cancer gene therapy trials have used TK-deleted viruses. [79]

Vaccinia also expresses an EGF homologue (vaccinia growth factor; VGF) that binds EGFR, [101-103] and induces a proliferative state optimal for viral replication. Double deleted virus has demonstrated tumour-restricted replication and tumour regression *in vivo*.[83] Further cancer selectivity deletions include anti-apoptotic serpin genes SP-1/SP-2, [147] and IFNγ receptor homologues. [148]

2. Arming vaccinia virus

Insertion of foreign genes into the vaccinia backbone has been attempted to further improve anti-tumour efficacy of the recombinant virus. Vaccinia represents a good virus for transgene expression given its large cloning capacity (25kbp) and promoters that direct high-level late gene expression. [149] Ideal transgenes should not have a direct anti-viral action, which would limit the viral anti-tumour efficacy, and should achieve a bystander effect, whereby non-virally infected cells are also influenced. Transgenes can the categorised into: immunomodulatory, anti-angiogenic, pro-drug converting enzymes, and imaging mediators.

Researched immunomodulatory transgenes include co-stimulatory molecules to increase the immune response against tumour cells, which themselves attempt to reduce their immunogenicity to evade the host immune system. Recombinant vaccinia virus expressing polymorphic epithelial mucin (MUC-1) and IL2 has been used in breast and prostate cancer. [150,151] Another vaccinia virus construct expressing carcinoembryonic antigen (CEA), and a triad of co-stimulatory molecules (TRICOM; B7.1, intracellular adhesion molecule-1 (ICAM-1), leukocyte function associated molecule-3 (LFA-3)) has been trialled in melanoma patients. [152]

Inflammatory mediating cytokines can be used as transgenes causing local expression in the tumour milieu to modulate the immune response against the cancer and infecting virus. The Th1 T cell mediated immune response is thought to be the most important in clearing vaccinia virus by the host, principally mediated by IFNγ, TNFβ, and IL12 cytokines; [139] as well as the most critical in the host immune response to cancer. [153] Promotion of the Th2 response, mediated by IL10 and IL4 cytokines, is therefore thought to be anti-inflammatory and virus promoting. The most successful cytokine

researched so far is using granulocyte-macrophage-colony-stimulating-factor (GM-CSF); which acts as a growth factor for white blood cells including neutrophils, macrophages and dendritic cells. This construct has demonstrated clinical anti-tumour efficacy in patients with recurrent and/or refractory melanoma, [123] and refractory primary or metastatic liver cancer following IT delivery. [122] IL2 is classically associated with the Th1 response and vaccinia-expressed IL2 has been assessed in the patients in patients with refractory malignant pleural mesothelioma. [154] Vaccinia-mediated IFNβ and IL2 expression have also shown promising results in pre-clinical testing. [106,155] A converse approach is to promote an anti-inflammatory response through the transgene expression of Th2 cytokines to reduce viral clearance. There is pre-clinical evidence of anti-tumour efficacy of recombinant vaccinia-mediated IL4 expression. [156] IL10 transgene expression has also been shown to reduce peritoneal growth of MKN45 gastric cancer in a mouse model following intraperitoneal injection. [157] Such strategies to reduce viral clearance by the immune system do, however, pose safety concerns, in that treatment may cause overwhelming viral infection that cannot be controlled by the host immune system. [79]

Another approach is to use a toxic or pro-drug converting enzyme to improve therapeutic efficacy. Gene-directed enzyme pro-drug therapy (GDEPT) involves cloning an enzyme into a virus that is able to convert a systemically administered non-toxic pro-drug into a cytotoxic drug within the tumour microenvironment. The gene encoding cytosine deaminase (CD) has been the most extensively investigated. [158] It converts 5-fluorocytosine (5-FC) into the toxic metabolite 5-fluorouracil (5-FU). Improved animal survival and tumour responses were demonstrated in mice treated with 5-FC and low dose vaccinia virus compared to virus alone. [158]

Finally, transgenes can be used to mediate tracking of the virus following administration in conjunction with imaging technology. This is useful to both monitor the biodistribution of viruses as well as their therapeutic action. Genes employed include human somatostatin receptor type 2 (SSTR2) in conjunction with a radiolabelled long-acting somatostatin analogue, [159] luciferase and/or fluorescent proteins, [140] and transferrin receptors which can be detected on MRI. [160]

1.7.10. Current State of Oncolytic Vaccinia Virus Clinical Trials

The first use of vaccinia as an oncolytic virus was based on the administration of IT wild-type virus in patients with malignant melanoma in the 1960s and 1970s. These studies showed reasonable responses and lack of adverse side effects. [141,142] A subsequent clinical trial again investigated patients with melanoma, but this time used a recombinant vaccinia virus expressing granulocyte macrophage-colony stimulating factor (GM-CSF). [123] Of the seven patients, four had partial responses and one had a complete response. More recently, a Wyeth GM-CSF expressing and TK deleted virus - JX-594, was investigated by IT delivery to 22 patients with primary or metastatic liver tumours refractory to conventional treatment. [122] Three partial responses, six stable disease, and one progressive disease were demonstrated based on Response Evaluation Criteria in Solid Tumours (RECIST). Interestingly, responsive patients included those who had anti-vaccinia antibodies following previous smallpox vaccination. Also virus was found replicating in distant (non-injected) tumour sites with resultant reduction in tumour volume. Further phase I trials are investigating JX-594 in application to refractory melanoma, non-small cell lung cancer, renal cell carcinoma, head and neck squamous cell carcinoma, colorectal cancer and a selection of paediatric cancers. A phase II dose-finding trial of JX-594 in 30 patients with advanced hepatocellular carcinoma has recently demonstrated radiological and survival advantages at the higher 10^9 PFU virus dose. [161]

GL-ONC1/GLV-1h68 is a Lister strain-based virus with insertional mutations of TK and A56R haemagglutinin loci with three reporter genes including a renilla luciferase-green fluorescent protein (Ruc-GFP) allowing, in addition to oncolysis, diagnosis of metastatic disease and monitoring of treatment. [162] A phase I trial in patients with a heterogeneous group of advanced solid organ tumours has very recently completed; with the results of primary outcome analysis, as yet, unpublished.

1.8. IL10 and cancer

1.8.1. IL10

Interleukin-10 (IL10) was first described as a cytokine synthesis inhibitor factor secreted by murine T-helper 2 (Th2) cells, which suppressed cytokine production by T-helper 1 (Th1) cells. [163] IL10 has broad anti-inflammatory properties through suppression of the antigen-presenting cell function and pro-inflammatory cytokine production of macrophages and dendritic cells. [164] This anti-inflammatory action has led to research to investigate the use of IL10 in the treatment of chronic inflammatory diseases, such as Crohn's disease, rheumatoid arthritis and psoriasis. More recently a role for IL10 in cancer treatment has been researched with evidence of anti-tumour efficacy, [157] and suppression of angiogenesis. [165-167] This study will establish the effect of an IL10-expressing recombinant Lister strain vaccinia virus on a number of types of cancer *in vitro* and *in vivo*; and investigate the hypothesis that IL10 suppresses viral host clearance, thus enhancing anti-tumour potency.

1.8.2. IL10 and IL10 receptor gene and protein structure

The human IL10 gene is located on chromosome 1, encoding for 5 exons (5.1kb). [168] Human IL10 is a homodimer, with each monomer consisting of 160 amino acids with a molecular mass of 18.5kDa [169]. Murine and human IL10 exhibit 80% homology; and there are several viral homologues, with the EBV-derived BCRF1 being the most extensively studied. Additionally five human structurally related molecules have been discovered and are considered to belong to the IL10 family: IL19, IL20, IL22, IL24 (mda-7) and IL26 (AK155). The elucidation of the function of these accessory IL10 family members is incomplete. The x-ray crystal structure of IL10 (Figure 6.) shows two intertwining polypeptide chains, each consisting of six helices, arranged in a V-shaped structure. [168,170]

IL10 production has been demonstrated in various cell types including Th2 cells, monoctyes, B cells, eosinophils, mast cells and dendritic cells; however the major source appears to be macrophages. [168]

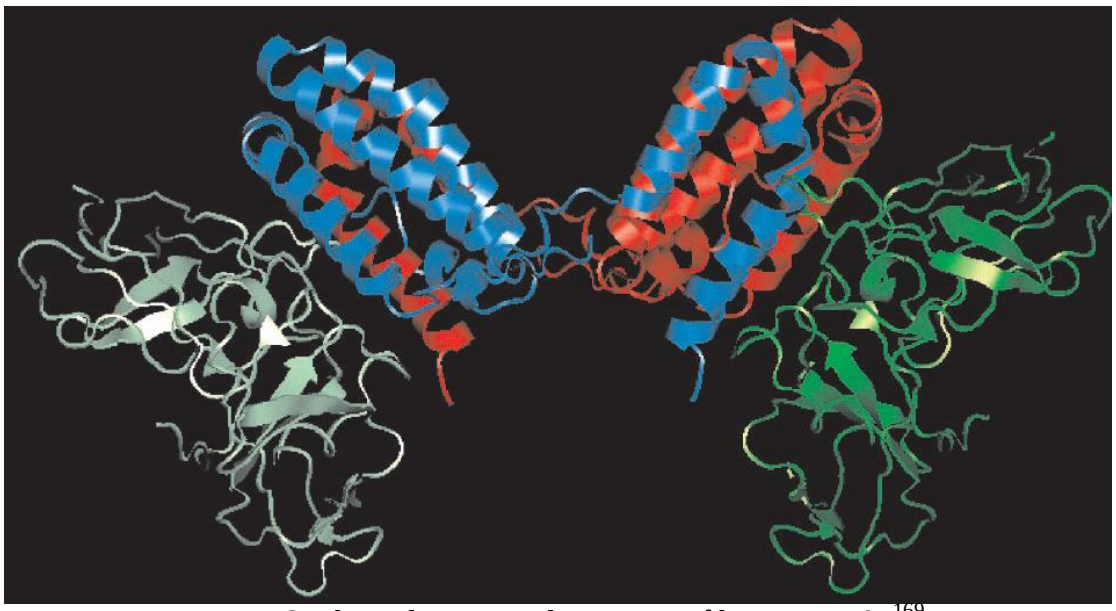

Figure 6. Three-dimensional structure of human IL10. [169]

1.8.3. IL10 secretion, receptor and signalling

The IL10 promoter is highly polymorphic and contains several transcription factor-responsive elements, [171] that are stimulated by several endogenous and exogenous factors such as endotoxin (via Toll-like receptor 4, NF-κB-dependent), tumour necrosis factor (TNF)-α (via TNF receptor p55, NF-κB-dependent), catecholamines and cAMP-elevating drugs. [172-177] Of particular significance is the role of the stress axis in affecting IL10 expression. [169]

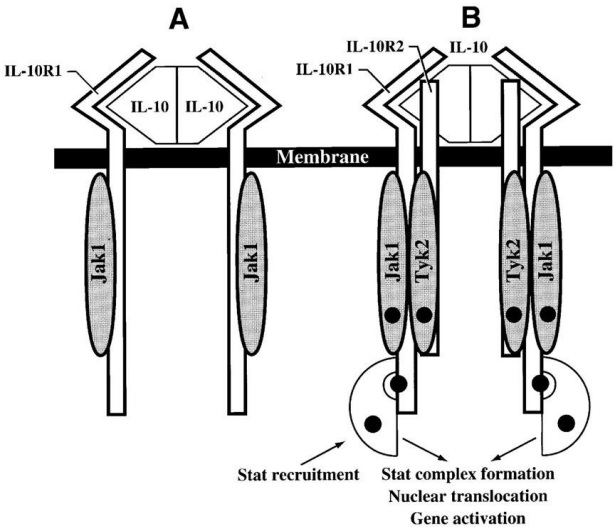

Figure 7. IL10 receptor and signalling. [178]

IL10 activity is mediated through binding to a specific cell surface receptor (IL10R) which is expressed predominantly in immune cells (Figure 7.). IL10R expression has been shown to be increased by endotoxin, [179] and decreased by T cell stimulation,

glucocorticoids, vitamin D3 and calcipotriol. [180,181] IL10R is composed of α chain (or IL10R1) [182] and β chain (CRFB4 or IL10R2); [178] and is a member of the class II cytokine receptor (CRF2) family. CRF2 are transmembrane glycoproteins, with extracellular domains consisting of 210 amino acids with several conserved areas important for secondary structure. [169] IL10 and IL10R1/2 interaction causes transcription of hundreds of genes through activation of tyrosine kinases Jak1 and Tyk2, [170] and subsequent stimulation of STAT 1,3 and 5 transcription factors. [183]

1.8.4. IL10 function and immunology

The human IL10 gene was first cloned from a T-cell clone that secreted IL10 and IFNγ amongst other cytokines. [184] Further research has demonstrated IL10 production by Th1 cells in human and murine systems, [164] and has been shown to be required for murine immune regulation against Toxoplasma gondii and Leishmania major infections. [185,186] This is suggestive of a regulatory role for IL10 and IFNγ in the equilibrium between pathogen clearance and persistence,[187,188] – resulting in either chronic infection or immunopathology. In this immuno-regulatory role, IL10's actions are generally considered immunosuppressive; with inhibition of macrophage and dendritic cell function, including production of pro-inflammatory cytokines, expression of co-stimulators and major histocompatibility complex (MHC) class II molecules. [164] This immunosuppressive function is supported by evidence from IL10-deficient mice, which develop colitis in the absence of a pathogenic stimulus,[189,190] and sometimes fatal immunopathology in the presence of pathogens. [164] Therefore, IL10 acts to protect the host from an unrestrained immune system, but at high levels can prevent adequate pathogen clearance leading to chronic infection. Conversely it has also been demonstrated that IL10 can exert a pro-inflammatory role by activating humoural immune responses by promoting MHC class II B cell expression and inducing immunoglobulin production. [182,191-194] Additionally IL10 has been show to activate mast cells,[195,196] CD8+ and NK cell action. [197-200] Intracellularly, IL10 inhibition of immune function is thought to be mediated through blocking nuclear factor kappa-light-chain-enhancer of activated B cells (NFκB); which is a key regulator of the immune response to infection and is implicated in autoimmune/inflammatory diseases and cancer. [201] Other anti-inflammatory mechanisms of IL10 include inhibition of interferon-induced gene transcription, [170,202,203] induction of the suppressor of cytokine synthesis (SOCS) – 3, [202] and heme oxygenase-1 (HO-1). [204]

1.8.5. IL10 applications to inflammatory diseases

Given the anti-inflammatory actions of IL10, a number of studies have examined the effect of IL10 on the treatment of immune-mediated inflammatory diseases such as psoriasis, Crohn's disease (CD) or rheumatoid arthritis (RA). Phase I and II trials have demonstrated efficacy of systemically administered recombinant IL10 in patients with psoriasis and CD; the results in RA were less convincing. [205,206] Later studies in larger blinded studies showed only limited beneficial effects. [169]

IL10 has also been investigated for its effects of CNS autoimmune inflammatory disease using an animal model of human multiple sclerosis - experimental autoimmune encephalomyelitis (EAE). It has been demonstrated that IL10 null mice are unable to recover from acute CNS inflammation, [207-209] and intracerebral administration of an IL10-expressing replication-deficient adenovirus (rAdV) rendered mice EAE-resistant. [210]

1.8.6. IL10 applications to cancer

Growth of cancer cells depends on an appropriately tolerant tumour microenvironment, where the tumour escapes the host immune system. This achieved through a number of immunosuppressive mechanisms that subvert tumour recognition and rejection. Anti-tumour responses depend on activation of cytotoxic CD8+ T cells, macrophages, NK cells and Th1-derived cytokines. [211-213] Moreover a number of tumours have demonstrated pronounced Th2 responses and suppressed CTL responses. A pro-tumour environment is further supported by Th2 cytokine driven macrophages. [214,215] IL10 is an important Th2 cytokine that inhibits macrophage antigen presenting capabilities and encourages tumour tolerance. [170] Furthermore, as a rationale for an immunosuppressive strategy to enhance viral oncolysis, the use of systemic immunosuppressive agents, such as cyclophosphamide, has been shown to enhance viral replication and hence anti-tumour potency. [216]

IL10 has been found to be expressed by a variety of malignant tumour cell types, including breast, colorectal and lung, [164] and is correlated with poor prognosis. It has also been shown that IL10 contributes to tumour survival by generating a microenvironment conducive to tumour growth and metastasis. [217-220] The majority of tumour-associated macrophages (TAMs) in solid tumours express higher levels of IL10 and lower levels of IL12 and TNFα; [221-224] resulting in suppression of anti-tumour T cell responses. In addition to TAMs, DC are critical to the host cellular anti-tumour response. Increased numbers of IL10 producing DC and Tregs have been demonstrated within many human cancers. [225-230] IL10-producing Tregs suppress CD8+ T cells and DC maturation.

Further evidence for the role of IL10 in tumour-associated immunosuppression comes from research using IL10 transgenics, IL10 knockouts and IL10 transfectants. For example, IL10 knockout mice are resistant to UV-induced skin cancer, which has been related to a potent Th1 response; not seen in wild-type mice. [231] However the effects of IL10 on tumour growth *in vivo* are conflicting in the literature; with some studies showing increased tumour growth, consistent with tumour immuno-tolerance; whilst some other studies show decreased tumour growth, suggesting immune system activation and tumour rejection. [164] A possible explanation for these contradictory findings relates to the actual level of IL10 expression; with the suggestion that low level IL10 expression causing immunosuppression and tumour progression, and high levels resulting in tumour regression. [164] Evidence for high-dose IL10 anti-tumour efficacy is far from unequivocal at this stage; however recombinant IL10 anti-tumour efficacy has been demonstrated in some animal models of immune-sensitive tumours.[232-234]

The anti-tumour function of IL10 may also be dependent on non-immune mechanisms, such as inhibition of angiogenesis and elevation of levels of nitric oxide. IL10 has been shown to inhibit angiogenesis in various cancers, including melanoma, Burkitt's lymphoma, prostate and ovarian cancer. [165-167] In prostate cancer cells this effect has be demonstrated to be mediated by the stimulation of tissue inhibitors of metalloproteases and inhibition of matrix metalloproteases. [235] Another anti-tumour mechanism of IL10 is mediated through nitric oxide. Nitric oxide is known to have potent anti-tumour activity, [169] and IL10 gene transfer in murine mammary tumour cells was associated with increased expression and activity of the inducible isoform of nitric-oxide synthase (iNOS), resulting in elevated levels of nitric oxide in transfected cancer cells. [236]

1.8.7. IL10 application to viral gene therapy

The anti-tumour effects of IL10 are thought to be mediated through the cells of the immune system, angiogenesis and nitric oxide. However, an indirect effect of IL10 on cancer, in the context of viral gene therapy, relates to the effect of IL10 on the virus, either as a vector delivering therapeutic transgenes or as an inherently cancer-killing (oncolytic) virus. Again the T cell response is vital to clearing viruses, as it is for mounting a powerful anti-tumour response. Evidence from IL10-knockout mice infected with mutants of lymphocytic choriomeningitis virus (LCMV) demonstrated more rapid virus elimination and development of anti-viral memory T cells. [237] Additionally administration of IL10 antibody in mice with wild-type IL10 gene restored T cell function and allowed virus elimination. [237] However, there is some conflicting evidence in the literature where IL10 was given after non-replicating vaccinia virus administration to mice bearing CT26 pulmonary metastases. [59] Although a reduction in pulmonary metastases was observed in mice receiving adjuvant IL10 12 hours after the virus was administered. An immunosuppressive mechanism was not seen with enhanced cytotoxic lymphocyte activity and lower viral titres from the lungs in the IL10 group compared to the no-IL10 groups, and higher titres from ovaries in the no-IL10 group. [59] Further research using more sensitive techniques is required to definitively establish the effect of IL10 on viral persistence within the tumour.

1.9. Aims of this study

1. To compare the anti-tumour potency and viral replication of Lister and WR strain tumour selective mutants *in vitro*.
2. To assess the relative tumour selectivity of viral replication in cancer and normal cells of the Lister and WR strain vaccinia viruses *in vitro*.
3. To establish the *in vivo* anti-tumour efficacy in nude and immunocompetent models of murine and human cancer.
4. To determine the biodistribution of Lister and WR strain vaccinia viruses in nude and immunocompetent mouse models of murine and human cancer.
5. To assess the effect of IL10 transgene expression on *in vitro* anti-tumour potency, viral replication, *in vivo* anti-tumour potency and biodistribution.
6. To investigate mechanisms of action of IL10 for cancer treatment by examining changes in cytokine profiles.

2. Materials and Methods

2.1. Cell lines

All cell lines were maintained in their respective media at 37°C in air supplemented with 5% carbon dioxide (CO_2). Repeated experiments were performed using cells of similar passage. All cells were grown in media containing 0.06μg/l penicillin and 0.1μg/l streptomycin obtained from Cancer Research UK Central Cell Services (CRUK CCS, Clare Hall, Hertfordshire, UK) unless otherwise stated and were regularly tested for mycoplasma.

2.1.1. Human cell lines

2.1.1.1. HNSCC

The HNSCC cell lines SCC4 (tongue) and SCC25 (tongue) were obtained from the CRUK CCS and were maintained in 1:1 Dulbecco's modified Eagle's medium (DMEM) and Ham's F12 supplemented with 10% heat-inactivated foetal calf serum (FCS) and 400ng/ml hydrocortisone (Sigma-Aldrich, MO, USA). The HNSCC cell lines TR126 (tongue) and TR138 (larynx) were obtained from the CRUK CCS and were maintained in DMEM and Ham's F12 respectively, each with 10% FCS. FaDu was obtained from American Type Culture Collection (ATCC; VA, USA) and maintained in Earle's minimal essential medium (EMEM) with 10% FCS.

2.1.1.2. Pancreatic carcinoma

The pancreatic carcinoma cell lines SUIT2, MiaPaCa2, PANC1, PT45 and Capan2 were obtained from CRUK CCS and maintained in DMEM with 10% FCS.

2.1.1.3. Colorectal carcinoma

The colorectal carcinoma cell lines HT29, HCT116, and SW620 were obtained from ATCC and maintained in DMEM with 10% FCS.

2.1.1.4. Gastric carcinoma

MKN45 gastric adenocarcinomas cell line was kindly provided by Professor Stephen Mather (Barts Cancer Institute, Queen Mary University of London, UK) and maintained in DMEM with 10% FCS.

2.1.1.5. Ovarian carcinoma

The ovarian carcinoma cell line A2780 was kindly provided by Professor I. McNeish (Barts Cancer Institute, Queen Mary University of London, UK) and maintained in DMEM with 10% FCS.

2.1.1.6. Primary cell line

Normal human bronchial epithelial cells (NHBE) were obtained from Cambrex (Cambridge, UK) and maintained in Bronchial Epithelial Growth Medium (BEGM) (Cambrex). Cambrex obtained these cells from their patient donation programme following the acquisition of informed consent for use of cells in research.

2.1.2. Murine cell lines

The HNSCC cell line SCCVII was kindly provided by Dr. Osam Mazda (Department of Microbiology, Kyoto Prefectural University of Medicine, Japan) and maintained in DMEM supplemented with 10% FCS. The pancreatic carcinoma cell line PANC02 was obtained from the ATCC and maintained in DMEM with 10% FCS. The colorectal carcinoma cell lines CT26 and CMT93 was obtained from CRUK CSS and maintained in DMEM supplemented with 10% FCS. MOSEC ovarian carcinoma cell line was kindly provided by Professor I. McNeish (Barts Cancer Institute, Queen Mary University of London, UK) and maintained in DMEM with 1% Insulin-Transferrin-Selenium supplement-G (GIBCO, Invitrogen) and 3% FCS.

2.1.3. Monkey cell line

CV1, the immortalised non-transformed African Green Monkey kidney cell line was obtained from ATCC and cultured in DMEM with 10% FCS.

2.2. Viruses

2.2.1. Vaccinia viruses

The highly attenuated Lister vaccine strain of vaccinia virus (VVLister) and all recombinant vaccinia viruses (VVIL10 and VVL15) were constructed and kindly provided by Professor Istvan Fodor (Loma Linda University Campus, CA, USA).

2.2.2. Recombinant vaccinia virus construction

Istvan Fodor used the highly attenuated Lister vaccine strain of vaccinia virus (VVLister) as the backbone for production of other engineered viruses. Vaccinia vector construction was performed by Istvan Fodor using an *in vitro* intracellular recombination technique previously described. [238]

VVL15 was constructed by the insertion of the lacZ reporter and the firefly luciferase genes into the TK region of VVLister under the control of the synthetic early/late and p7.5 promoters respectively. [239] Expression of firefly luciferase enables real-time luminescence imaging of viral location *in vivo* following the addition of the substrate D-Luciferin.

VVIL10 was constructed by the insertion of the LacZ reporter and murine IL10 genes into the TK region of VVLister under the control of the p7.5 and synthetic early/late promoters respectively. [240]

WR, TK deletion, and WRDD, double deletion (TK and VGF) viruses, were kindly provided by Dr Steve Thorne (University of Pittsburgh, Pittsburgh, USA) and Dr A. McCart (University of Toronto, Toronto, Canada) respectively. [83,241]

2.2.3. Vaccinia virus mass production

CV1 cells were cultured until 90% confluent and infected with 20µl of purified virus to produce a primary expansion. This was harvested when significant cytopathic effect (CPE) was observed by cell detachment at 48-72 hours. A CF10 viral production factory (Nunc, NY, USA) was seeded with four 175cm^2 flasks of CV1 cells at 90% confluence. After 72 hours, this was infected with the primary expansion in DMEM with 2% FCS until significant CPE was observed a further 72-96 hours later.

Cells harvested from the CF-10 were centrifuged in Sorvall centrifuge bottles (Sorvall, MA, USA) at 3,500 revolutions per minute (rpm) for 15 minutes at 4°C. The cell pellet in each bottle was re-suspended in 30ml phosphate-buffered saline (PBS), transferred to a 50ml tube and centrifuged in the same manner. The supernatant was again discarded and each pellet of cells re-suspended in 7ml of 10mM Tris-HCl pH 9.0, then combined. Cell membranes were disrupted by 3 cycles of freezing in liquid nitrogen and thawing in a 37°C water bath, prior to homogenisation by 60 strokes with a Dounce homogeniser.

Cells were centrifuged at 900 rpm for 5 minutes at 4°C and the supernatant removed and saved. The cell pellet was re-suspended in 3ml of 10mM Tris-HCl pH 9.0 prior to a second centrifugation. Both supernatants were combined and the pellet discarded. This was sonicated in an ultrasound ice bath for 20 seconds (Grant Instruments, Hertfordshire, England) and diluted to 30ml with 10mM Tris-HCl pH 9.0. 7.5ml was carefully layered onto 17ml of 36% sucrose (w/v) 10mM Tris-HCl pH 9.0 in each of four SW17 Beckman ultracentrifuge tubes (Beckman Coulter UK Ltd, Bucks, UK). After careful balancing by weight, these tubes were centrifuged at 13,500 rpm for 80 minutes at 4°C.

Each supernatant was discarded and purified viral pellets re-suspended in 1ml of 1mM Tris-HCl pH 9.0 prior to combination and storage at -80°C. The viral titre was determined by $TCID_{50}$ plaque assay (See 2.4.2)

2.3. Cell proliferation MTS assay of vaccinia virus in tumour cell lines.

The potency of all viruses against a panel of cell lines was determined by CellTiter 96® AQ_{ueous} Non-Radioactive Cell Proliferation (MTS) assay. Cells were infected with 9 serial dilutions of virus in 96 well plates and the proportion of cells alive after 6 days at each viral concentration compared to a non-infected control following the addition of MTS reagents. The assay measures cell survival by dehydrogenase enzyme activity found in metabolically active cells, which reduces MTS into formazan in proportion to the number of living cells present.

Cells were cultured in 90µl of media with 5% FCS in 96-well plates at a density of between $1x10^3$ and $1x10^4$ cells per well, depending on the rate of cell growth, to ensure that mock-infected wells were nearly confluent 6 days after infection. Plates were incubated at 37°C and 16-18 hours later, infected in sextuplicate with 10µl of 9 serial dilutions of viruses (range optimised for each cell line; typically MOI 100 or 1000 PFU/ml) diluted in media with 5% FCS or mock-infected with media with 5% FCS alone. Six days following infection, MTS (3-(4,5-dimethylthiazol-2-yl)-5-(3-carboxymethoxyphenyl)-2-(4-sulfophenyl)-2H tetrazolium) was added to PMS (phenazine methosulfate; Promega, WI, USA) according to the manufacturer's instructions in a ratio of 20MTS: 1PMS. 20µl was added to each well and plates incubated for 1 to 3 hours. Cell viability was determined by measuring the absorbance or optical density (OD) at 490nm using an Opsys MR 96-well plate absorbance reader (Dynex, VA, USA). Cell viability was determined in infected cells in comparison to mock-infected cells (positive control) after correction for absorbance due to the media alone (negative control). All OD values in positive controls were greater than 1. The concentration of virus required to kill 50% of cells (half maximal effective concentration or EC_{50}) was then calculated for each cell line (Section 2.15.1) and a dose-response curve created by non-linear regression using Prism® (GraphPad Software, CA, USA). Experiments were repeated in sextuplicate.

2.4. Viral replication of vaccinia virus in tumour and normal human bronchial epithelial cell lines.

2.4.1. Viral Infection

Cells were seeded in 3 wells of a 6-well plate in 2ml of media with 10% FCS at a density of between 2 and $4x10^5$ cells per well depending on the rate of cell growth. One plate was seeded for each virus at each time point (24, 48, 72 and 96 hours) with a further control plate. All plates were incubated overnight at 37°C in air supplemented with 5% CO_2.

16 to 18 hours later, cells from the control plate were harvested, counted and the mean number of cells per well used to determine the amount of virus required to infect the other plates. Plates were infected by 2ml of media with 2% FCS containing vaccinia virus at a multiplicity of infection (MOI) of 1 PFU/cell. Cells and supernatant were

harvested together by scraping from each individual well to give samples in triplicate at every time point. Cell lysates were created by three cycles of freezing samples in liquid nitrogen and thawing in a 37°C water bath.

2.4.2. $TCID_{50}$ viral titration assay

The titres of purified viruses and the replication of viruses in cell lines were determined by measuring the 50% tissue culture infective dose ($TCID_{50}$) of samples titrated onto indicator cells.

$1x10^4$ CV1 cells were seeded in 200µl of DMEM with 10% FCS into 96 well plates and incubated at 37°C in air supplemented with 5%CO_2. 16 to 18 hours later, plates were infected with purified virus or viral burst assay sample lysates diluted to $1x10^{-5}$ or $1x10^{-3}$ respectively in DMEM supplemented with 10% FCS. 20µl was added with a multi-tip pipette to all 12 wells of the top row and mixed. Following a change of pipette tips, serial 1:10 dilutions were made to the next 7 consecutive rows of CV1 cells up to a dilution of $1x10^{-11}$ for purified virus or $1x10^{-9}$ for burst assay sample lysates. Row H was left uninfected as a negative control.

The CPE of viruses on CV1 cells were determined by light microscopy 10 days after infection. Each well was scored 0 (no CPE) or 1 (any CPE) to make a score for each row out of 12. These were used to calculate the $TCID_{50}$ using the established Reed-Muench accumulate method (Section 2.15.2). $TCID_{50}$ plates were performed in duplicate for each sample, with three samples at each time-point. Purified viral titres were converted to PFU/ml and viral burst titres to PFU/cell based on the number of cells present at viral infection.

2.5. Anti-tumour efficacy of vaccinia virus *in vivo*.

In vivo studies of viral efficacy in mouse tumour models were all designed by JH and performed at the Biological Services Unit at Clare Hall laboratories (Hertfordshire, UK) with the assistance of Gary Martin and Sandra Peak, and at the Sino-British Research Centre, Zhengzhou University, China with the assistance of Jiwei Wang, Donling Gao and Penju Wang, and the Biological Services Unit at The Barts Cancer Institute (London, UK). Mice at Clare Hall and The Barts Cancer Institute were kept in accordance with the UK co-ordinating committee on cancer research guidelines and the

Animals (Scientific Procedures) Act 1986 (Home Office, London). Mice at the Chinese Academy of Sciences were kept in accordance with the Regulations on the Management of Experimental Animals (Government of People's Republic of China) and purchased from approved suppliers. The general health of mice was assessed daily and animals killed if judged to be terminally sick, tumour size reached 1.44cm^2 or had been present for 3 months (See 2.5.3). Tumour volumes were estimated using (volume = (width x length^2 x π)/6) twice weekly from the start of treatment until the sacrifice or death of the first mouse in each treatment group**.**

Anti-tumour efficacy was measured by the changes in tumour volumes over time until the death or sacrifice of the first mouse in each group, and the length of survival of each mouse until the tumour volume reached 1.44cm^2 or tumour ulceration occurred. Kaplan-Meier curves (indicating percentage of animals without tumour progression) were created. Statistical analysis using log rank testing compared different viral treatments and PBS treated mice.

2.5.1. Efficacy of IT vaccinia virus mutants against FaDu human HNSCC cancer xenograft model in nude mice.

1x10^6 FaDu cells were implanted subcutaneously into the right flank of 30 BALB/c nu/nu female 4-5 week old mice (Harlan UK Ltd). When tumours reached 0.4-0.5cm in diameter, tumour volumes were measured and mice were regrouped into 10 mice per group to ensure even spread of tumour sizes. Each group received 50µl IT injections of 1x10^7 PFU VVL15, WRDD or PBS on days 1, 3 and 5. Tumours were measured twice a week from first appearance until the mice were sacrificed.

2.5.2. Efficacy of IT vaccinia virus mutants against PT45 human pancreatic cancer xenograft model in nude mice.

5x10^6 PT45 cells were implanted subcutaneously into the right flank of 40 BALB/c nu/nu female 4-5 week old mice (Harlan UK Ltd). When tumours reached 0.4-0.5cm in diameter, tumour volumes were measured and mice were regrouped into 10 mice per group to ensure even spread of tumour sizes. Each group received 50µl IT injections of 1x10^7 PFU VVL15, VVIL10, WRDD or PBS on days 1, 3 and 5. Tumours were measured twice a week from first appearance until the mice were sacrificed.

2.5.3. Efficacy of IT vaccinia virus mutants against CT26 murine tumour model in immunocompetent mice.

$1x10^6$ CT26 cells were implanted subcutaneously into the right flank of 40 BALB/c immunocompetent female 4-5 week old mice (Harlan UK Ltd). When tumours reached 0.4-0.5cm in diameter, mice were regrouped into 10 mice per group to ensure even spread of tumour sizes. Each group received 50µl IT injections of $1x10^8$ PFU VVL15, VVIL10, WRDD or PBS on days 1, 3 and 5. Tumours were measured twice a week from first appearance until the mice were sacrificed.

2.5.4. Efficacy of IT vaccinia virus mutants against CMT93 murine colorectal tumour model in nude mice.

$5x10^6$ CMT93 cells were implanted subcutaneously into the right flank of 40 ICRF nu/nu female 4-5 week old mice (Harlan UK Ltd). When tumours reached 0.4-0.5cm in diameter, tumour volumes were measured and mice were regrouped into 10 mice per group to ensure even spread of tumour sizes. Each group received 50µl IT injections of $1x10^7$ PFU VVL15, VVIL10, WRDD or PBS on days 1, 3 and 5. Tumours were measured twice a week from first appearance until the mice were sacrificed.

2.5.5. Efficacy of IT vaccinia virus mutants (3 x injections) against CMT93 murine tumour model in immunocompetent mice.

$5x10^6$ CMT93 cells were implanted subcutaneously into the right flank of 40 C57BL/6 immunocompetent mice female 4-5 week old mice (Harlan UK Ltd). When tumours reached 0.4-0.5cm in diameter, tumour volumes were measured and mice were regrouped into 10 mice per group to ensure even spread of tumour sizes. Each group received 50µl IT injections of $1x10^8$ PFU VVL15, VVIL10, WRDD or PBS on days 1, 3 and 5. Tumours were measured twice a week from first appearance until the mice were sacrificed.

2.5.6. Efficacy of IT vaccinia virus mutants (5 x injections) against CMT93 murine tumour model in immunocompetent mice.

$5x10^6$ CMT93 cells were implanted subcutaneously into the right flank of 40 C57BL/6 immunocompetent mice female 4-5 week old mice (Harlan UK Ltd). When tumours

reached 0.4-0.5cm in diameter, tumour volumes were measured and mice were regrouped into 10 mice per group to ensure even spread of tumour sizes. Each group received 50µl IT injections of $1x10^8$ PFU VVL15, VVIL10, WRDD or PBS on days 1, 2, 3, 4, 5. Tumours were measured twice a week from first appearance until the mice were sacrificed.

2.6. Expression of IL10 *in vitro* by ELISA.

2×10^5 CMT93/ PT45 and 1×10^5 SCC7 cells were seeded in 3 wells of a 6-well plate with 2ml of 10% DMEM. One plate was seeded for each virus (VVL15, WRDD, VVIL10) at each time point (6 and 24 hours) with 2 control plates representing mock infections at the same time points. All plates were incubated overnight at 37°C in air supplemented with 5%CO_2.

16 to 18 hours later, cells from the control plate were harvested, counted and the mean number of cells per well used to determine the amount of virus required to infect the other plates. Plates were infected by 2ml of DMEM with 2% FCS containing vaccinia virus at a multiplicity of infection (MOI) of 5 PFU/cell. Cells and supernatant were harvested together by scraping from each individual well to give samples in triplicate at every time point. Cell lysates were created by three cycles of freezing samples in liquid nitrogen and thawing in a 37°C water bath.

IL10 concentration in the lysates was determined using the Quantikine Mouse IL10 kit (R&D Systems, Abingdon, UK) according to the manufacturer's instructions. Cell lysate samples were prepared into undiluted, ½ diluted, 1/5 diluted, 1/10 and 1/20 diluted triplicates with the provided calibrator diluents.

The OD of each well was determined using a microplate reader at 450 nm and OD values at 540 nm subtracted to correct for optical plate imperfections. Mean OD values were used to create a standard curve, which was used to obtain IL10 levels for each sample.

2.7. Biodistribution of vaccinia virus in ICRF nude mice bearing murine CMT93 flank tumours.

5 x 10^6 CMT93 cells were implanted subcutaneously into the right flank of 60 ICRF nude female 4-5 week old mice (Harlan UK Ltd). When tumours reached 0.4-0.5cm in diameter, mice were regrouped into 12 mice per group to ensure even spread of tumour sizes. Each group received a single 100µl IV tail vein injections of $1x10^7$ PFU VVL15, WRDD, or PBS. On days 2, 6, 8 and 12 four mice were sacrificed from each group and the tumours and other tissues (ovary, bone marrow, liver, lungs, brain and spleen) were harvested and snap frozen in liquid nitrogen for further processing.

2.8. Biodistribution of vaccinia virus in C57BL/6 immunocompetent mice bearing murine CMT93 flank tumours.

5 x 10^6 CMT93 cells were implanted subcutaneously into the right flank of 36 C57BL/6 female 4-5 week old mice (Harlan UK Ltd). When tumours reached 0.4-0.5cm in diameter, mice were regrouped into 9 mice per group to ensure even spread of tumour sizes. Each group received 100µl IV tail vein injections of $2x10^8$ PFU VVL15, VVIL10, WRDD or PBS. On days 4, 8 and 12 three mice were sacrificed from each group and the tumours and other tissues (ovary, bone marrow, liver, lungs, brain, blood and spleen) were harvested and snap-frozen in liquid nitrogen for further processing. Blood collected in serum separator tubes, allowed to stand for 10 minutes to clot, then centrifuged at 1100rpm and the serum pipetted off and snap frozen in liquid nitrogen for further processing.

2.9. Biological time-points of vaccinia virus in C57BL/6 immunocompetent mice bearing murine CMT93 flank tumours.

5 x 10^6 CMT93 cells were implanted subcutaneously into the right flank of 48 C57BL/6 female 4-5 week old mice (Harlan UK Ltd). When tumours reached 0.4-0.5cm in diameter, mice were regrouped into 12 mice per group to ensure even spread of tumour sizes. Each group received 50µl IT injections of $1x10^8$ PFU VVL15, VVIL10, WRDD or PBS on days 1, 3, 5. On days 5, 10, 15 and 20 three mice were sacrificed from each

group, and the tumours and ovaries were harvested and snap-frozen in liquid nitrogen for further processing. Blood samples were collected in heparinised tubes prior to freezing.

2.10. Biodistribution of vaccinia virus in ICRF nude mice bearing human PT45 flank tumours.

5 x 10^6 PT45 cells were implanted subcutaneously into the right flank of 36 ICRF nude female 4-5 week old mice (Harlan UK Ltd). When tumours reached 0.4-0.5cm in diameter, mice were regrouped into 9 mice per group to ensure even spread of tumour sizes. Each group received a single 100µl IV tail vein injections of 1x10^7 PFU WRDD, VVL15, VVIL10 or PBS. On days 8, 12 and 18 four mice were sacrificed from each group, and the tumours were harvested and snap-frozen in liquid nitrogen for further processing. Blood samples were collected in heparinised tubes prior to freezing.

2.11. Biological time-points of vaccinia virus mutants in ICRF nude mice bearing human PT45 flank tumours.

5 x 10^6 PT45 cells were implanted subcutaneously into the right flank of 36 ICRF nude female 4-5 week old mice (Harlan UK Ltd). When tumours reached 0.4-0.5cm in diameter, mice were regrouped into 9 mice per group to ensure even spread of tumour sizes. Each group received 50µl IT injections of 1x10^7 PFU VVL15, VVIL10, WRDD or PBS on days 1, 3, 5. On days 7, 12 and 20 four mice were sacrificed from each group, and the tumours were harvested and snap frozen in liquid nitrogen for further processing. Blood samples were collected in heparinised tubes prior to freezing.

2.12. Histology and immunohistochemistry for vaccinia virus coat protein.

All histology and IHC was kindly performed by Mohammed Ikram and Keyur Trivedi (Pathology department, Barts Cancer Institute, Queen Mary University of London, UK) and all slides reviewed by JH and YW. The biodistribution of VVL15 and WRDD *in vivo* was determined by vaccinia coat protein staining of tumours and organs (optimised for frozen sections of tumours and paraffin sections of organs) of vaccinia-treated animals compared to PBS-treated controls.

2.12.1. Sample processing

4μm frozen sections were cut from blocks of tumours from all experiments using a Leica CM1900 cryostat (Leica Microsystems, Wetzlar, Germany). All other organs were fixed in 10% formaldehyde and then processed, paraffin embedded and cut into 4μm sections using Leica EG1160. Slides were stained with hematoxylin and eosin (H&E) according to standard protocols using a Leica autostainer XL. Further sections were cut for IHC, which was performed using the Ventana® Discovery staining module (Ventana, Tucson, USA). This system used biotin-free secondary antibodies, which were already conjugated to streptavidin-HRP. These were visualised with a hydrogen peroxide (H_2O_2) substrate and 3,3'-diaminobenzidine tetrahydrochloride (DAB) chromogen, which produced a dark brown substrate on light microscopy.

2.12.2. Optimisation of IHC in frozen sections

Optimisation of vaccinia coat protein primary antibody (MorphoSys UK Ltd, Bath, UK) for use in frozen sections was performed by IHC on positive controls at a range of antibody dilutions. Primary antibody was applied to slides for 1 hour and then washed before Omnimap anti-rabbit secondary antibodies were applied to the slides for 16 minutes. Slides were washed, visualised with DAB and H_2O_2 and reviewed by JH and YW. Primary antibody dilutions that produced strong signals and weak background were chosen and validated on negative and positive controls for use on all further slides (1:2000).

2.12.3. Optimisation of IHC in paraffin embedded sections

Optimisation of vaccinia coat protein IHC in paraffin sections was performed in stages. Slides were deparaffinised using EZ Prep™ (Ventana) at 75°C for 8 minutes. A range of reagents were tried in order to break the covalent bonds between the aldehyde and amino groups that form when tissues are formalin-fixed. Trypsin resulted in high background activity; therefore slides were heated to 95°C for 8 minutes in the presence of conditioning solution 1 (CC1; Tris-EDTA based buffer), CC2 (citrate based buffer) or protease 1 (All Ventana). CC1 resulted in the least background. Various dilutions of the primary antibody were tried with Omnimap anti-Rabbit HRP secondary antibody. The least background was seen after a 1:200 dilution of primary antibody. The protocol was finalised with washes after every stage:

1. Deparaffinisation with EZ Prep™ at 75°C for 8 minutes

2. CC1 at 95°C for 8 minutes
3. 1:200 anti-vaccinia virus antibody for 60 minutes at 37°C
4. Omnimap anti-Rabbit HRP for 16 minutes
5. DAB and H_2O_2 for 8 minutes
6. Haematoxylin (nucleus) counterstain for 2 minutes
7. Bluing agent (counterstaining background) for 2 minutes

2.13. Homogenisation of animal tissues for *in vitro* studies.

Mouse tissues from *in vivo* experiments for use in viral titre determination (qRT-PCR and $TCID_{50}$) and ELISA were processed according to the following protocol. Mouse tissue was weighed and any hair was removed from the sample using a scalpel under sterile conditions. The tissue was homogenised using an Omni TissueMaster hand-held homogeniser to a total volume of 2 ml in DMEM, then frozen and thawed three times in liquid nitrogen and in a water bath at 37 ºC. 100 µl of the resultant lysate was used for DNA extraction using the DNeasy 96 blood and tissue kit (QIAGEN, Hilden, Germany) according to the manufacturer's instructions, and eluted in 100 µl of Buffer AE. DNA concentration was determined using the NanoDrop ND-1000 Spectrophotometer (Nanodrop Technologies, Delaware, USA) and a fixed amount of DNA was used for quantitative real-time polymerase chain reaction (qRT-PCR) (see 2.14). DNA was accepted as adequately pure where the ratio of absorbance at 260 and 280nm was ~1.8. DNA copies were against total DNA and the results are displayed as arbitrary units. The results are displayed as PFU/ml/g, normalised against the weight of the tissue sample.

2.14. Vaccinia virus DNA quantification in mouse tissues by qRT-PCR.

2.14.1 Primers and probes

Primers and probes for VVLister were designed manually by James Tysome using Primer Express® v3.0 software (Applied Biosystems, New Jersey, USA) and constructed by Sigma-Aldrich and Applied Biosystems respectively. Briefly, the vaccinia genome was imported from NCRI Corenucleotide database and the vaccinia late gene transcription factor-1 [242] (VLTF-1) sequences identified from their open reading frames as List107 (103385 to 105298bp) and List082 (77898 to 78680bp) [243]. Primers and probes (Table 1.) were chosen for optimum PCR efficiency with minimal

secondary structures with probe length 17-20bp, Tm (Melting temperature) 68-70°C, GC content 40-60% with repeats minimised. Primers were chosen to be 20-26bp in length either side of the probe with Tm 58-60°C and GC content 40-60%.

Table 1. Primers and probes used for qRT-PCR.

S = sense; AS = antisense

Gene	**Primer or Probe**	**Sequence**
VVLister VLTF-1	Probe	ATTTTAGAACAGAAATACCC
	Primers	S 5'-AACCATAGAAGCCAACGAATCC AS 5'-TGAGACATACAAGGGTGGTGAAGT

2.14.2. Quantitative Real-Time PCR (qRT-PCR)

Samples, control (RNAse free water) and nine 10-fold serial dilutions of standards ($5x10^8$ to 5 viral genome copies diluted in 5µl RNAse free water) were tested in triplicate in each plate by quantitative real-time polymerase chain reaction (qRT-PCR). A 25µl reaction volume consisted of 5µl sample or standard and 20µl of Master mix (0.9µM forward primer, 0.9µM reverse primer, 0.2µM probe in TaqMan® Universal PCR Master Mix). Reactions were performed in MicroAmp™ optical 96-well reaction plates sealed with optical adhesive covers and amplified using the 7500 Real-time PCR System (1 cycle of 48°C for 30min, 95°C for 10min then 40 cycles of 95°C for 15s, 60°C for 1min). Cycle thresholds (C_T) were determined using 7500 System SBS software (All Applied Biosystems, New Jersey, USA).

Standard and sample triplicates were accepted for analysis where their standard deviation was <0.3. Standard curves were created using mean cycle thresholds in Prism® and sample genome copy number determined accordingly. Standard curves were accepted as valid where $R^2 \geq 0.99$ with a slope of –3.30 to-3.32. Results were corrected for weight for harvested tumours and organs, and expressed in arbitrary units.

2.15. Quantification of vaccinia virus in tumour and organ homogenates using $TCID_{50}$ (see 2.4.2 $TCID_{50}$ viral titration assay).

Vaccinia virus titration of *in vivo* homogenised mouse tumour and organ samples using a $TCID_{50}$ technique as previously described (see 2.4.2 $TCID_{50}$ viral titration assay). As with the *in vitro* samples, 20µl of homogenised tissue was added to the first row of seeded CV1 cells and following a change of pipette tips, serial 1:10 dilutions were made to the next 7 consecutive rows. Viral titres were corrected for the initial weight of the sample.

2.16. Effect of Recombinant IL10 alone, and in conjunction with VVL15 compared to VVIL10 on cell proliferation as measured by MTS assay.

The effect of recombinant murine unconjugated IL10 (R&D Systems, Abingdon, UK) on tissue culture cell proliferation was investigated. Firstly recombinant IL10 was applied on its own to CMT93 cells and a cytopathic response was investigated. As per previous MTS cell proliferation protocol (2.3 Cell proliferation (MTS) assay) 5000 CMT93 cells were seeded in 90µl of media with 5% FCS in 96-well plates. The 10µl aliquot of 9 serial dilutions in media with 5% FCS recombinant IL10 ($1x10^6$pg/ml) was applied; resulting in a maximum initial concentration of $1x10^5$pg/ml. Following three days of incubation under standard conditions, the plates were read as previously described.

To assess the effect of recombinant IL10 on VVL15 *in vitro* cytotoxicity, the previously described cell proliferation (MTS) assay was further adjusted. CMT93 cells were seeded in 90µl of media with 5% FCS in 96-well plates at a density of 5000 cells per well. 16-18 hours later the cells were infected with VVL15 and VVIL10 viruses (MOI=1000 PFU/ml). Immediately prior to the virus application 10µl of media was removed from half the VVL15 infected plates and replaced with 10µl of recombinant IL10 ($1x10^6$pg/ml) in 5% FCS media (i.e. no recombinant IL10 serial dilution). 10µl of serially diluted viruses were applied as previously described; yielding the following

experimental combinations: VVL15 alone, VVIL10 alone, and VVL15 + recombinant IL10. The plates were read as previously described at 3 days post-infection.

2.17. Assessment of pro-inflammatory cytokines in CMT93 tissue culture supernatants following infection with different vaccinia virus mutants.

CMT93 cells were seeded and infected with vaccinia virus as previously described (see 2.4. Viral replication of vaccinia virus mutants in solid tumour and normal human bronchial epithelial cell lines). Cytokine concentration was determined for several pro-inflammatory cytokines using a Meso Scale Discovery multi-spot assay system mouse pro-inflammatory 7-plex ultra-sensitive kit (MSD Gaithersburg, Maryland, USA). The manufacturer's instructions were followed and a series 1:5 dilutions were used, with samples tested in triplicate.

Further testing of selected cytokines (IL10, IL12 and IFNγ) was conducted using Quantikine Mouse IL10/IL12/IFNγ kits (R&D Systems, Abingdon, UK) according to the manufacturer's instructions. Undiluted, 1:5 and 1:20 dilutions were used. Experiments were repeated twice in triplicate.

2.18. Assessment of pro-inflammatory cytokines in immunocompetent mouse CMT93 flank tumours and serum following IT treatment with different vaccinia virus mutants.

Tumour and serum samples were generated and processed as previously described (see 2.9 Biological time points of Vaccinia virus mutants in C57BL/6 immunocompetent mice bearing murine CMT93 flank tumours; 2.10. Homogenisation of animal tissues for *in vitro* studies). Cytokine concentration was determined for several pro-inflammatory cytokines using a Meso Scale Discovery multi-spot assay system mouse pro-inflammatory 7-plex ultra-sensitive kit (MSD Gaithersburg, Maryland, USA). The manufacturer's instructions were followed and 1:2 dilutions were used, with samples tested in triplicate.

Further testing of selected cytokines (IL10, IL12 and IFNγ) was conducted using Quantikine Mouse IL10/IL12/IFNγ kits (R&D Systems, Abingdon, UK) according to

the manufacturer's instructions. Undiluted, 1:5 and 1:20 dilutions were used. Experiments were repeated twice in triplicate.

2.19. Analysis of tumour homogenate and serum IL10 concentrations in nude mice bearing PT45 flank tumours following IT vaccinia virus treatment.

Biological specimens were generated and processed as previously described (see 2.11. Biological time points of Vaccinia virus mutants in ICRF nude mice bearing human PT45 flank tumours; 2.10. Homogenisation of animal tissues for *in vitro* studies). IL10 concentrations were determined using a Quantikine Mouse IL10 kit (R&D Systems, Abingdon, UK) according to the manufacturer's instructions. Samples were diluted 1:2 and 1:20. Experiments were repeated twice in triplicate.

2.20. Data handling and statistical analysis

2.20.1. EC_{50} and variable slope non-linear regression

EC_{50} = ((X where Y=top) – (X where Y= bottom))*0.5

$$Y = \text{Bottom} + \frac{(\text{Top-Bottom})}{(1+10^{((\text{LogEC50-X})*\text{HillSlope})})}$$

X = log[virus] ;Y = %cells alive; Hillslope = steepness of curve

Top/Bottom = Maximum/Minimum Y value (or cell death)

2.20.2. $TCID_{50}$

The Reed-Muench method of $TCID_{50}$ calculation is based on the adding the proportionate distance between CPE scores of rows above and below 6 out of 12 to the log of the viral dilution where CPE is 6 or less. Viral dilutions range from 10^{-5} to 10^{-11} for purified virus and 10^{-3} to 10^{-9} for viral replication samples.

$$\log TCID_{50} = \frac{\log(\text{viral dilu}^{n} \text{ at row above 50\% CPE}) - (\text{\% CPE next above 50\%}) - 50\%}{(\text{\% CPE next above 50\%}) - (\text{\% CPE next below or equal to 50\%})}$$

This is converted to PFU/ml for purified viral titres:

Since volume of sample inoculated into the first row = 0.02ml

$TCID_{50}$/ml = (1/ $TCID_{50}$)*(1/0.02)

$TCID_{50}$ PFU/ml = $TCID_{50}$/ml*0.69

This is then converted into PFU/cell for viral replication titres.

$$TCID_{50}\ (PFU/cell) = \frac{TCID_{50}\ PFU/ml}{\text{number of cells at infection}}$$

2.20.3. Statistical analysis

Unpaired t-tests were used to compare peak viral replication *in vitro* and tumour sizes *in vivo*.

Log rank testing was used to compare the percentage of animals free of tumour progression *in vivo.*

3. Results: Comparison of the anti-tumour potency of vaccinia virus mutants *in vitro* and *in vivo*.

Wild-type Western Reserve (WR) vaccinia virus has been reported to have superior anti-tumour potency compared to other wild-type strains of vaccinia virus. [82] However, the WR strain is a laboratory, non-vaccine strain and there are very limited data on its behaviour in humans. Also the experiments demonstrating this superior potency used only two human cancer cell lines (A2780 and HCT116) *in vitro* to make this assertion. Furthermore, we know from early Phase I/II trials in the 1970s and 1990s that wild-type vaccinia viruses demonstrate limited anti-tumour potency. [141-143,244] Tumour-selective viruses have been developed since that time to improve tumour targeting and reduce side-effects. Despite these shortcomings, a double-deleted mutant (TK-, VGF-) of the WR strain (WRDD) shows great promise as an anti-cancer therapeutic with marked tumour selectivity and anti-tumour potency. [83] Single deleted WR strain (TK-, WRLuc) shows less favourable tumour selectivity compared to WRDD, with significant titres of virus recovered from brain, testicular and bone marrow tissue in mice following intraperitoneal injection; and was included initially in this study as a control. [83]

An alternative vaccinia strain, Lister, is a European vaccine strain and has been used in millions of humans safely. A Lister strain TK-deleted virus, VVL15, has recently been shown to have favourable anti-tumour potency compared to adenovirus, with cytotoxicity even demonstrated against adenovirus insensitive cancer cell lines. [245] These initial experiments will compare the in anti-tumour potency of tumour-selective WR and Lister vaccinia viruses in several cancer cell lines from multiple organs *in vitro* and *in vivo*.

3.1. Anti-tumour potency of Lister and Western Reserve strain vaccinia virus mutants in a panel of murine and human cancer cell lines *in vitro*.

The hypothesis that Lister strain vaccinia virus is a better alternative to Western Reserve as an oncolytic virus shall be investigated by comparing the potency of TK-deleted

Lister strain (VVL15) to TK-deleted WR strain (WRLuc), and TK and VGF double-deleted WR strain (WRDD) in a panel of solid tumour cell lines from multiple anatomical sites, including head and neck, pancreatic, gastrointestinal and ovarian, using the MTS cell proliferation assay.

Tumour type	**Cell line**	**VVL15**		**WRLuc**		**WRDD**	
		Mean EC_{50} (PFU/cell)	**SEM**	**Mean EC_{50} (PFU/cell)**	**SEM**	**Mean EC_{50} (PFU/cell)**	**SEM**
HNSCC	FaDu	**0.056**	0.0022	0.16	0.011	0.66	0.089
	SCC4	**0.00081**	6.38×10^{-5}	0.0026	4.87×10^{-4}	0.0035	2.78×10^{-4}
	SCC25	0.003	0.00063	**0.0013**	3.54×10^{-4}	0.014	0.0029
	TR138	0.015	0.00208	**0.0061**	0.00079	0.029	0.0018
	SCCVII	81.16	12.16	**3.06**	0.72	**6.35**	1.31
Pancreatic	PANC1	**0.26**	0.034	**0.25**	0.0108	0.98	0.070
	Capan2	0.0091	0.00084	**0.0062**	0.00058	0.023	0.0023
	PT45	**5.53**	1.39	11.37	0.919	18.42	1.88
	SUIT2	**2.63**	0.499	10.65	1.58	11.85	1.84
	MiaPaCa2	**9.79**	1.047	19.51	1.25	27.03	2.74
	Panc02	842.9	45.9	481.5	22.37	**50.58**	5.80
Gastro intestinal	HCT116	9.42	1.124	**2.16**	0.262	**2.78**	0.148
	HT29	**0.408**	0.051	**0.443**	0.027	1.195	0.113
	SW620	6.37	0.592	**2.83**	0.138	9.14	0.4004
	MKN45	2.62	0.114	**1.61**	0.129	2.42	0.145
	CMT93	25.17	1.575	**0.048**	0.013	0.189	0.0322
	CT26	1.70	0.148	**0.046**	0.0054	**0.065**	0.0114
Ovary	A2780	0.412	0.103	**0.035**	0.0069	0.0602	0.0092
	MOSEC	0.121	0.014	**0.0137**	0.0011	0.049	0.0015

Table 2. Potency of the Lister and Western Reserve strain of vaccinia virus in a panel of human and murine tumour cell lines. Comparison of mean EC_{50} values ± SEM generated from sextuplicate MTS cell proliferation assays 6 days after infection; 1000 cells per well were infected with different VV at a series of MOI (highest MOI of 1000 PFU/cell). Statistical analysis was performed using the unpaired T-test. Grey shaded cells are murine cell lines; white cells are human cell lines. Bold figures

represent the most potent virus overall; underlined figures represent the most potent virus comparing VVL15 and WRDD. Where two viruses are highlighted, they are jointly most potent statistically (i.e. no statistically significant difference).

Therefore when comparing the mean EC_{50} values from sextuplicate MTS assays VVL15 showed greater cytotoxicity compared to WRDD in 11 of the 14 human cancer cell lines tested. MKN45 human gastric cancer cell line showed equivalent EC_{50} values for VVL15 and WRDD treated cells. Two human cancer cell lines, A2780 and HCT116, demonstrated greater anti-tumour potency with WRDD compared to VVL15. All five of the murine cancer cell lines showed greater cytotoxicity with WRDD compared to VVL15 treatment.

WRLuc showed a more mixed picture compared to WRDD, with superior potency (compared to VVL15 and WRDD) in two mouse cancer cell lines and six out of the 14 human cancer cell lines.

3.2. Viral replication of Lister and Western Reserve strain vaccinia virus mutants in a panel of murine and human cancer cell lines *in vitro*.

A number of cell lines used in the cell proliferation studies (MTS assay) were selected for further investigation to determine the ability of Lister and WR strain vaccinia virus mutants to replicate in these cell lines using a viral burst assay technique. These experiments were designed to provide corroborating evidence to the MTS data in assessing *in vitro* anti-tumour potency of the respective viruses.

Tumour type	Cell line	VVL15		WRLuc		WRDD	
		Viral Replication (PFU/cell)	SEM	Viral Replication (PFU/cell)	SEM	Viral Replication (PFU/cell)	SEM
HNSCC	FaDu	**17.15**	0.70	9.17	2.54	8.45	2.29
	SCCVII	28.81	4.67	**634.48**	47.11	392.94	5.57
Pancreatic	PANC1	**133.89**	24.74	**140.68**	0.001	56.75	5.00
	PT45	**25.16**	5.01	**19.40**	0.65	7.29	0.42
	SUIT2	**121.08**	8.67	52.43	7.73	56.01	4.16
	MiaPaCa2	**127.20**	17.00	38.35	3.50	19.59	0.034
	Panc02	51.04	2.66	**2861.96**	132.03	1711.86	413.96
Gastro intestinal	CMT93	142.41	31.56	**1627.42**	309.48	618.91	225.25
	CT26	147.75	34.17	1057.85	77.28	**2534.72**	388.33

Table 3. Viral Replication of the Lister and Western Reserve strain of vaccinia virus in a panel of human and murine tumour cell lines. Burst assays were infected with 1 PFU/cell of virus ($2x10^5$ cells per well). Cell lysates were harvested at 24 hour intervals typically up to 96 hours. Mean viral replication at 72 hours ± SEM was determined by TCID50 assay on CV1 cells are tabulated. Statistical analysis was performed using the unpaired T-test. Grey shaded cells are murine cell lines; white cells are human cell lines. Bold figures represent the most potent virus overall; underlined figures represent the most potent virus comparing VVL15 and WRDD. Where two viruses are highlighted, they are jointly most potent statistically (i.e. no statistically significant difference).

All cancer cell lines supported replication of Lister and WR strain viruses. The Lister strain virus demonstrated inferior replication in murine cancer cell lines (CMT93, CT26, SCCVII and Panc02) compared to WR strain; in keeping with the MTS cell proliferation study findings. VVL15 replication was superior to WRDD in human cell lines (PT45, SUIT2, PANC1, MiaPaCa2, FaDu); again in congruence with the cell proliferation studies.

3.3. Tumour selectivity of viral replication of Lister and Western Reserve strain vaccinia virus mutants.

To assess the tumour selectivity of Lister and WR strain viruses *in vitro*, viral replication was determined in non-malignant Normal Human Bronchial Epithelial cells (NHBE). Ratios for viral replication in cancer cells over normal cells were then calculated.

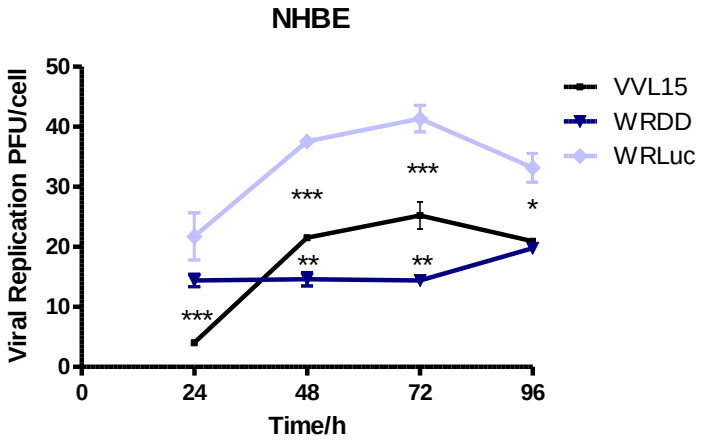

Figure 8. Replication of Lister and WR vaccinia virus mutants in Normal Human Bronchial Epithelial cells. Burst assays were infected with 1 PFU/cell of virus ($2x10^5$ cells per well). Cell lysates were harvested at 24 hour intervals typically up to 96 hours. Mean viral replication ± SEM was determined by $TCID_{50}$ assay on CV1 cells. Statistical analysis was performed using the unpaired T-test with * representing statistical significance at $p<0.05$, ** representing statistical significance at $p<0.01$, *** representing statistical significance at $p<0.001$ and ns indicating no statistical significance.

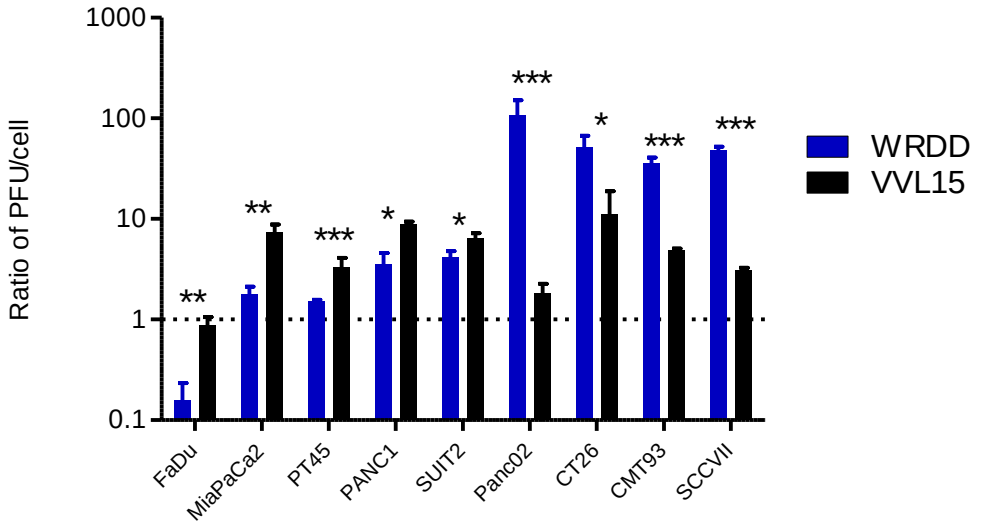

Figure 9. Relative replication of WR and Lister strain viruses in cancer cells compared to normal human cells (NHBE). Viral titres were compared at 96 hours post-infection. Mean viral replication ± SEM was determined by $TCID_{50}$ assay on CV1 cells. A ratio greater than 1 indicates superior viral replication in the respective cancer cells compared to non-malignant cells (NHBE). Statistical analysis was performed using the unpaired T-test with * representing statistical significance at $p<0.05$, ** representing statistical significance at $p<0.01$, *** representing statistical significance at $p<0.001$ and ns indicating no statistical significance.

Both WR and Lister strain vaccinia viruses showed higher replication in all cancer cells compared to non-malignant cells, except FaDu. Interestingly WRDD replicated better in NHBE cells compared to FaDu. This perhaps relates to the slow doubling time of the FaDu tumour cells *in vitro*. Again a distinction between human and murine cancer cells is apparent. VVL15 demonstrates higher ratios compared to WRDD in human cancer cell lines (FaDu, MiaPaCa2, PT45, PANC1, SUIT2) suggesting greater tumour selectivity for human tumours. Whereas the pattern was reversed in murine cancer cells; with WRDD showing higher ratios compared to VVL15.

To further investigate the relative potency of Lister and WR strain vaccinia viruses, experimentation *in vivo* using nude and immunocompetent mouse models of solid tumours was performed. Based upon the above *in vitro* results and findings from the literature, VVL15 and WRDD were selected for investigation of *in vivo* efficacy in a number of nude and immunocompetent mouse models. WRLuc has been shown to demonstrate poor tumour-selectivity in biodistribution experiments in C57BL/6

immunocompetent mice bearing MC38 tumours compared to WRDD. [83] Furthermore marked cytotoxicity following intra-peritoneal injection into nude and immunocompetent C57BL/6 mice (non-tumour bearing) at 1 x10^8 and 1x10^9 PFU was shown. [83] Experience in our laboratory has demonstrated significant *in vivo* cytotoxicity demonstrated in nude mice bearing CMT93 flank tumours following 3 x 1x10^7 PFU intra-tumoural injection.

3.4. Anti-tumour efficacy of Lister and Western Reserve vaccinia virus mutants in a human HNSCC (FaDu) nude mouse (BALB/c) model.

Having established a general pattern of superior anti-tumour potency, viral replication and tumour selectivity for the Lister vaccinia virus strain over the WR in human cancer cell lines *in vitro*; the potency *in vivo* was investigated. The effect on tumour growth and the percentage of animals without tumour progression was examined following repeated IT viral treatments.

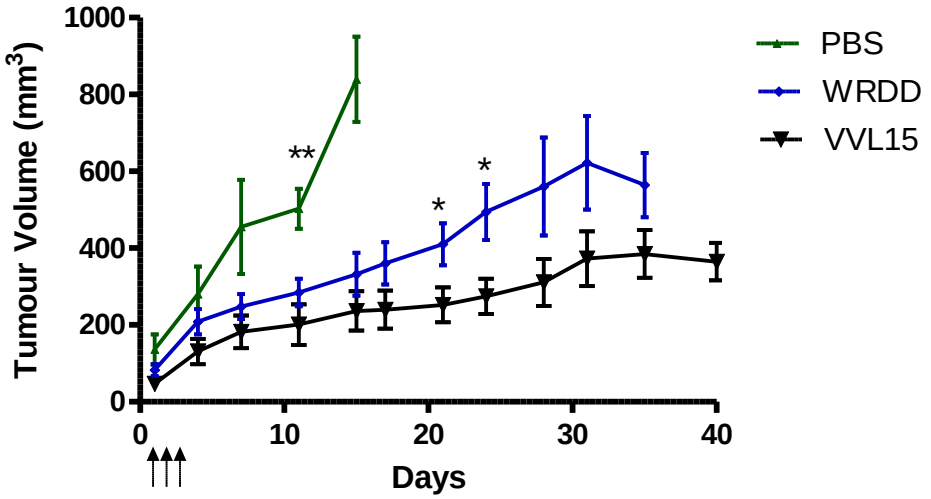

Figure 10a. Growth of established human HNSCC tumours in nude mice after treatment with different vaccinia virus mutants. 1x10^6 FaDu cells were seeded by subcutaneous injection into the right flank of 30 BALB/c nude mice. When tumours reached 4-5mm in diameter, 10 mice each received IT injections of PBS, WRDD or

VVL15 on days 1,3,5 (3 x $1x10^7$ PFU). Tumours were measured twice weekly. Mean tumour sizes ± SEM are displayed.

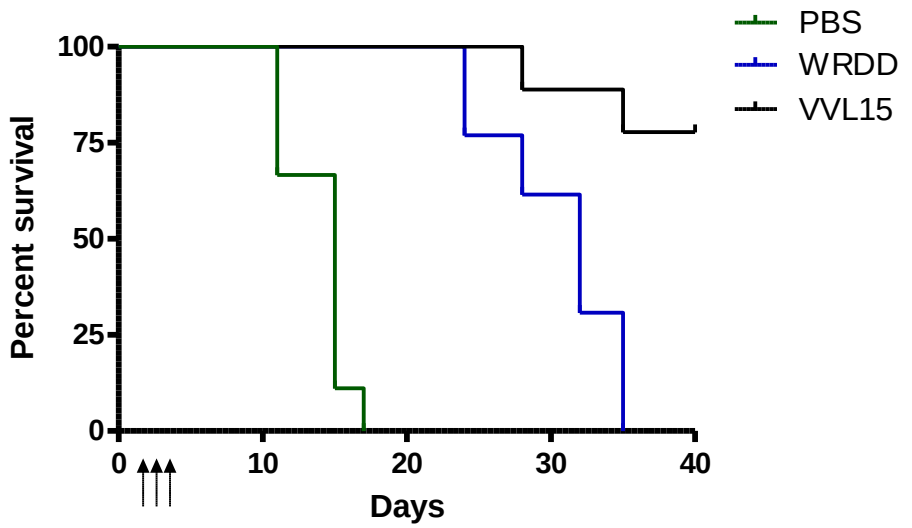

Figure 10b. Animal survival of nude mice bearing established human HNSCC tumours after treatment with different vaccinia virus mutants. $1x10^6$ FaDu cells were seeded by subcutaneous injection into the right flank of 30 BALB/c nude mice. When tumours reached 4-5mm in diameter, 10 mice each received IT injections of PBS, WRDD or VVL15 on days 1,3,5 (3 x $1x10^7$ PFU). Kaplan-Meier curves are shown. Log-rank test statistical analysis showed significant differences at the 0.1% level between PBS and WRDD data sets, and at the 1% level between VVL15 and WRDD data sets.

Reduced tumour growth was demonstrated in the treatment group receiving VVL15 compared to WRDD and PBS. This result is in keeping with *in vitro* data, which showed better viral replication and cytotoxicity with VVL15 in the FaDu human cancer cell line.

3.5. Anti-tumour potency of Lister and Western Reserve vaccinia virus mutants in a human pancreatic carcinoma (PT45) nude mouse model (ICRF nu/nu).

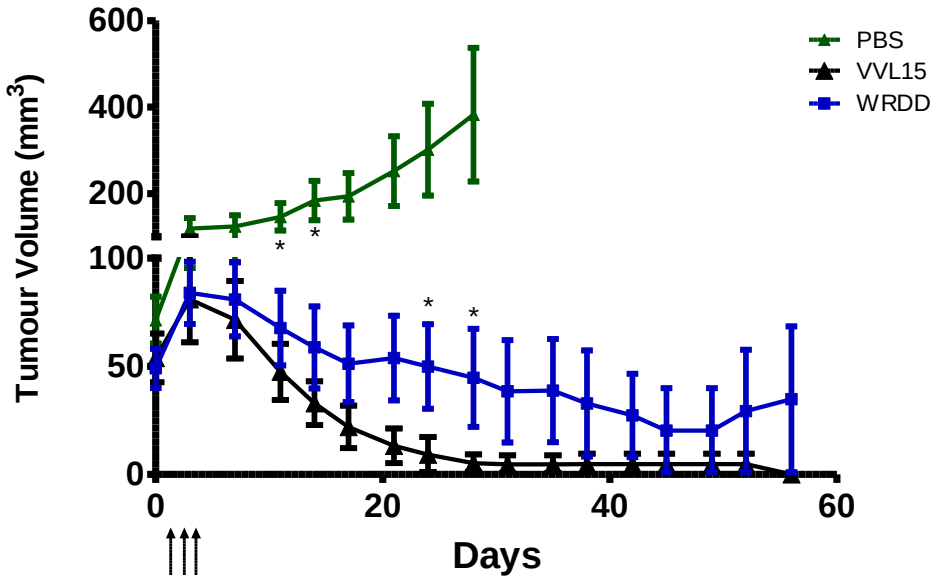

Figure 11a. Growth of established human pancreatic tumours in nude mice after treatment with different vaccinia virus mutants. $5x10^6$ PT45 cells were seeded by subcutaneous injection into the right flank of 30 ICRF nude mice. When tumours reached 4-5mm in diameter, 10 mice each received IT injections of PBS, WRDD or VVL15 on days 1,3,5 (3 x $1x10^7$ PFU). Tumours were measured twice weekly. Mean tumour sizes ± SEM are displayed. Statistical analysis of tumour sizes at stated time-points was performed using the unpaired T-test with * representing statistical significance at $p<0.05$, ** representing statistical significance at $p<0.01$, *** representing statistical significance at $p<0.001$ and ns indicating no statistical significance.

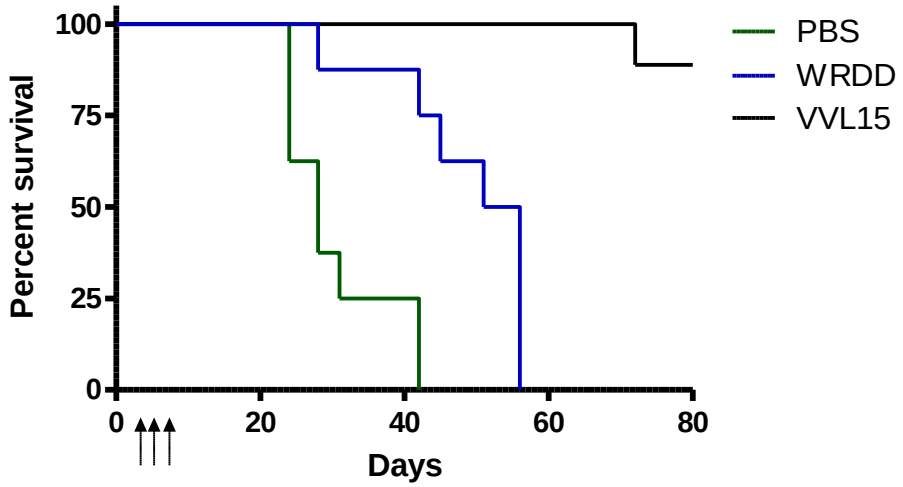

Figure 11b. Animal survival of nude mice bearing established human pancreatic tumours after treatment with different vaccinia virus mutants. $5x10^6$ PT45 cells were seeded by subcutaneous injection into the right flank of 30 ICRF nude mice. When tumours reached 4-5mm in diameter, 10 mice each received IT injections of PBS, WRDD or VVL15 on days 1,3,5 (3 x $1x10^7$ PFU). Kaplan-Meier curves are shown. Log-rank test statistical analysis showed significant differences at the 0.1% level between PBS and VVL15 & WRDD data sets.

Significant tumour regression was demonstrated in the treatment group receiving VVL15 compared to WRDD and PBS. This result is in keeping with *in vitro* data, which showed better viral replication and cytotoxicity with VVL15 in the PT45 human cancer cell line.

3.6. Anti-tumour potency of Lister and Western Reserve vaccinia virus mutants in a mouse colorectal carcinoma (CMT93) nude mouse model (ICRF nu/nu).

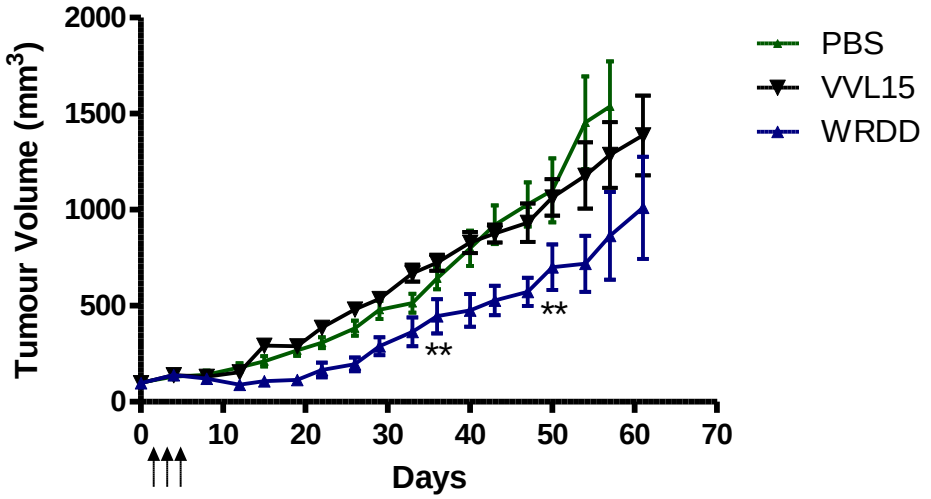

Figure 12a. Growth of established murine colorectal tumours in nude mice after treatment with different vaccinia virus mutants. $5x10^6$ CMT93 cells were seeded by subcutaneous injection into the right flank of 30 ICRF nu/nu mice. When tumours reached 4-5mm in diameter, 10 mice each received IT injections of PBS, WRDD or VVL15 on days 1,3,5 (3 x $1x10^7$ PFU). Tumours were measured twice weekly. Mean tumour sizes ± SEM are displayed. Statistical analysis of tumour sizes at stated time-points was performed using the unpaired T-test with * representing statistical significance at $p<0.05$, ** representing statistical significance at $p<0.01$, *** representing statistical significance at $p<0.001$ and ns indicating no statistical significance.

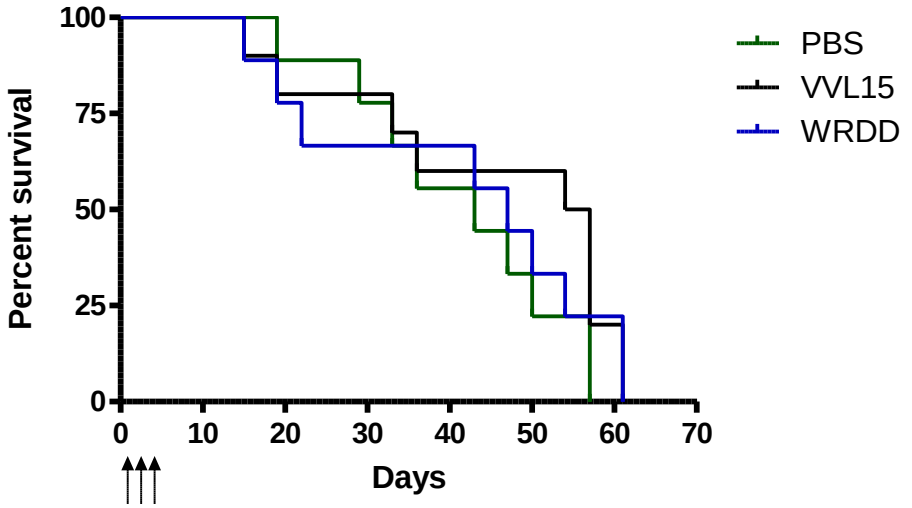

Figure 12b. Animal survival of nude mice bearing established murine colorectal tumours after treatment with different vaccinia virus mutants. $5x10^6$ CMT93 cells were seeded by subcutaneous injection into the right flank of 30 ICRF nu/nu mice. When tumours reached 4-5mm in diameter, 10 mice each received IT injections of PBS, WRDD or VVL15 on days 1,3,5 (3 x $1x10^7$ PFU). Kaplan-Meier curves are shown. Log-rank test statistical analysis showed no significant difference between the treatment groups.

Reduced tumour progression was demonstrated in the treatment group receiving WRDD compared to VVL15 and PBS. This result is in keeping with *in vitro* data, which showed better viral replication and cytotoxicity with WRDD in the CMT93 murine cancer cell line. Interestingly there was no statistical difference in tumour growth between PBS and VVL15 treatment. The EC_{50} value for VVL15 was 133x that of WRDD and the viral replication of WRDD was four times the VVL15 value. The only cell lines with two orders of magnitude difference in EC_{50} between VVL15 and WRDD was the murine colorectal cell lines CMT93 and CT26. Clearly the CMT93 cell line is relatively insensitive to VVL15 *in vitro* and in a nude *in vivo* model.

3.7. Anti-tumour potency of Lister and Western Reserve vaccinia virus mutants in a mouse colorectal carcinoma (CMT93) immunocompetent mouse model (C57BL/6).

To assess the anti-tumour potency efficacy studies were performed using a C57BL/6 immunocompetent mouse model. This immunocompetent model would allow assessment of the behaviour of the different vaccinia virus strain mutants in the presence of an intact host immune system. CMT93 flank tumours were grown and IT viruses administered at $1x10^8$ PFU on a three-day (days 1,3,5) and five-day (1,2,3,4,5) injections regime. Our hypothesis was that the anti-tumour effect of the viruses in an immunocompetent model may be different to the *in vitro* and nude *in vivo* models; and that any effect would be enhanced with a five day injection regime, whilst maintaining safety.

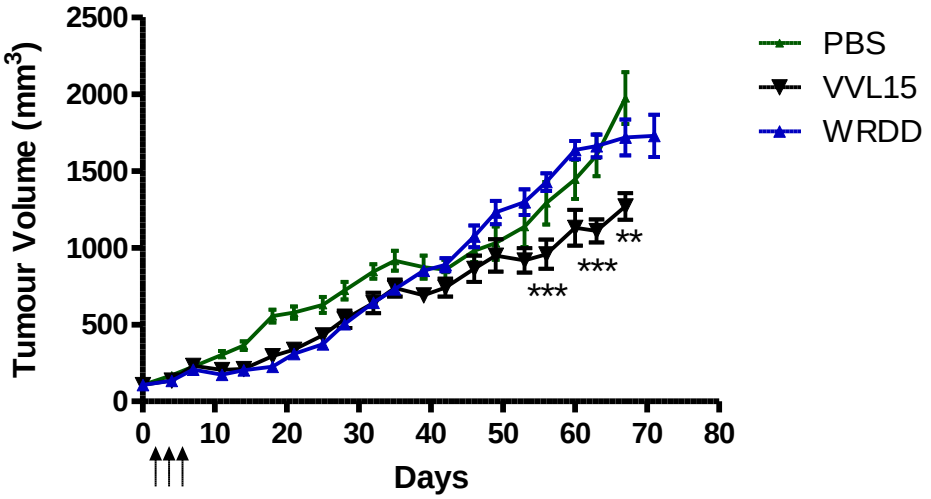

Figure 13a. Growth of established murine colorectal tumours in immunocompetent mice after treatment with different vaccinia virus mutants. $5x10^6$ CMT93 cells were seeded by subcutaneous injection into the right flank of 30 C57BL/6 mice. When tumours reached 4-5mm in diameter, 10 mice each received IT injections of PBS, WRDD or VVL15 (3 x $1x10^8$ PFU) on days 1,3,5. Tumours were measured twice weekly. Mean tumour sizes ± SEM are displayed. Statistical analysis of tumour sizes at stated time-points was performed using the unpaired T-test with * representing statistical significance at $p<0.05$, ** representing statistical significance at $p<0.01$, *** representing statistical significance at $p<0.001$ and ns indicating no statistical significance.

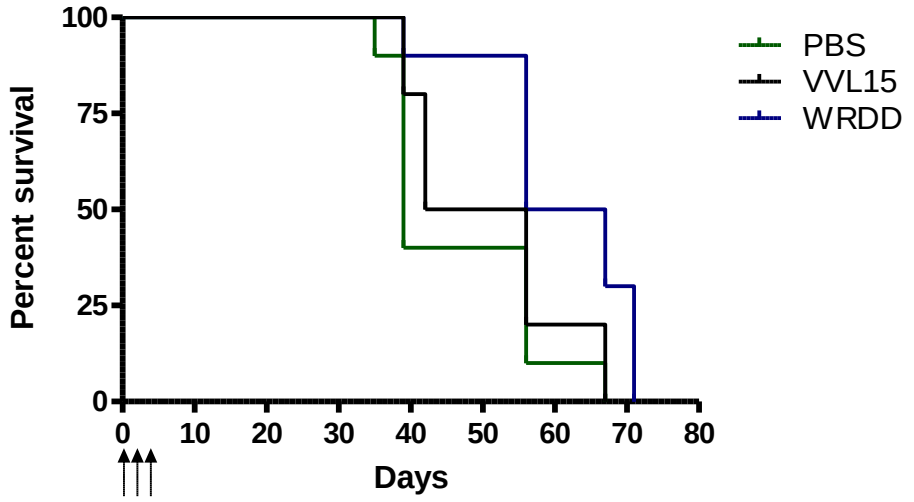

Figure 13b. Animal survival of immunocompetent mice bearing established murine colorectal tumours after treatment with different vaccinia virus mutants. $5x10^6$ CMT93 cells were seeded by subcutaneous injection into the right flank of 30 C57BL/6 mice. When tumours reached 4-5mm in diameter, 10 mice each received IT injections of PBS, WRDD or VVL15 (3 x $1x10^8$ PFU) on days 1,3,5. Kaplan-Meier survival curves are shown. Log-rank test survival curve statistical analysis showed no significance between all 3 data sets.

Interestingly in the immunocompetent model the pattern is reversed compared to the nude CMT93 murine cancer model. Here tumour progression is slower in the VVL15-treated mice compared to WRDD. The presence of an intact host immune system completely reverses the potency of the viruses against CMT93 tumours.

The experiment was then repeated using a five-day regime of IT injections (5 x $1x10^8$ PFU) to determine if the anti-tumour effect could be enhanced without compromising the side-effects profile.

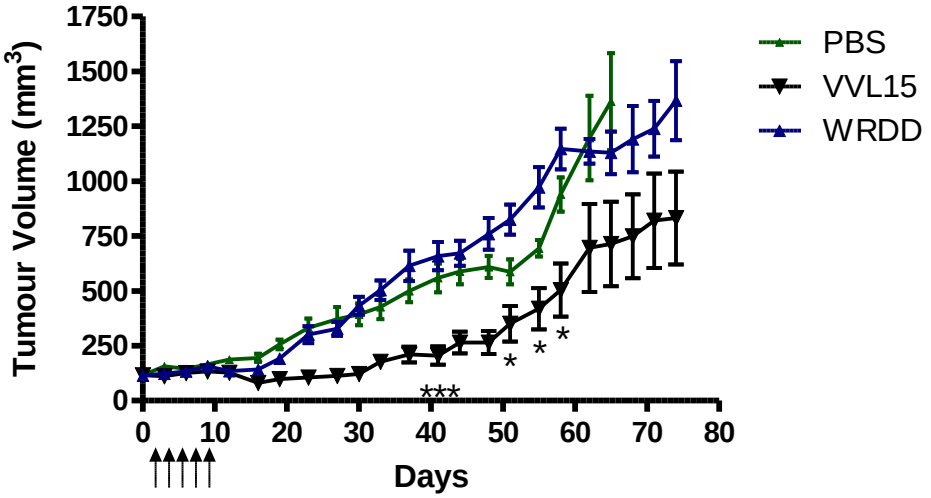

Figure 14a. Growth of established murine colorectal tumours in immunocompetent mice after treatment with different vaccinia virus mutants. $5x10^6$ CMT93 cells were seeded by subcutaneous injection into the right flank of 30 C57BL/6 mice. When tumours reached 4-5mm in diameter, 10 mice each received IT injections of PBS, WRDD or VVL15 (5 x $1x10^8$ PFU) on days 1,2,3,4,5. Tumours were measured twice weekly. Mean tumour sizes ± SEM are displayed. Statistical analysis of tumour sizes at stated time-points was performed using the unpaired T-test with * representing statistical significance at $p<0.05$, ** representing statistical significance at $p<0.01$, *** representing statistical significance at $p<0.001$ and ns indicating no statistical significance.

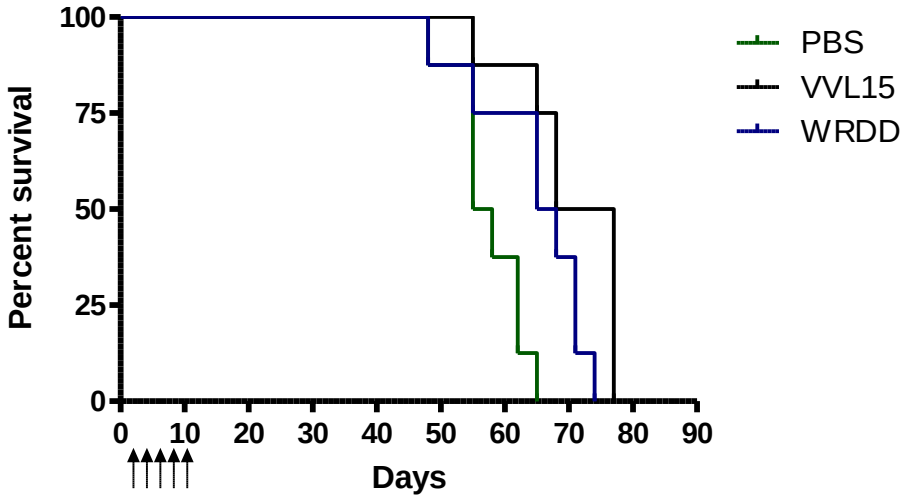

Figure 14b. Animal survival of immunocompetent mice bearing established murine colorectal tumours after treatment with different vaccinia virus mutants.

$5x10^6$ CMT93 cells were seeded by subcutaneous injection into the right flank of 30 C57BL/6 mice. When tumours reached 4-5mm in diameter, 10 mice each received IT injections of PBS, WRDD or VVL15 (5 x $1x10^8$ PFU) on days 1,2,3,4,5. Tumours were measured twice weekly. Kaplan-Meier survival curves are shown. Log-rank test survival curve statistical analysis showed no significance between all 3 data sets.

The reduced tumour progression with VVL15 compared to WRDD was enhanced when the virus was administered for five days rather than three days. The five-day viral injection regime was well tolerated by the mice. No difference was found between the groups in animal survival.

3.8. Anti-tumour potency of Lister and Western Reserve vaccinia virus mutants in a mouse colorectal carcinoma (CT26) immunocompetent mouse model (BALB/c).

Having demonstrated reduced tumour progression with VVL15-treated mice in the nude FaDu, nude PT45, and immunocompetent CMT93 models compared to WRDD, vaccinia virus behaviour in a further immunocompetent model was investigated. CT26 cell line, like CMT93, demonstrated relatively poor sensitivity to VVL15 (EC_{50} 26x) and significantly reduced viral replication (17x less). Given the reversal of potency of the two viruses in the CMT93 immunocompetent model, corroborating evidence of VVL15's superior anti-tumour potency in mice with intact immune systems was sort.

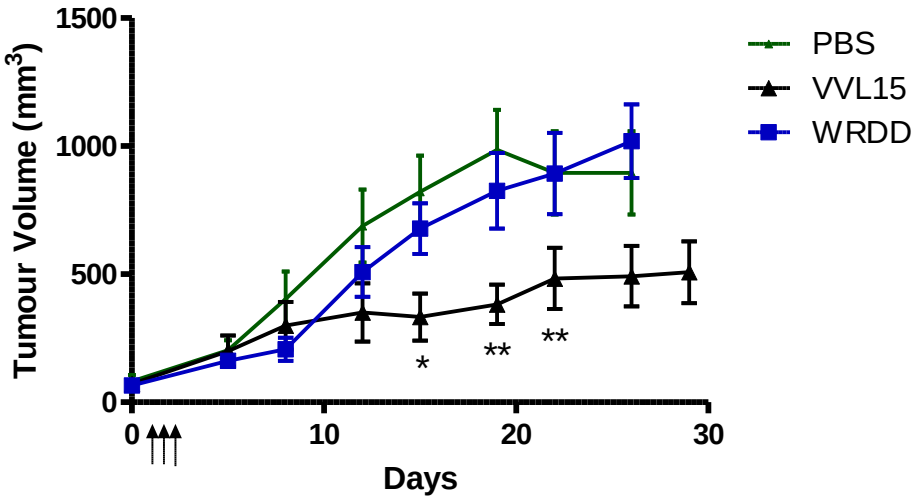

Figure 15a. Growth of established murine colorectal tumours in immunocompetent mice after treatment with different vaccinia virus mutants.

$1x10^6$ CT26 cells were seeded by subcutaneous injection into the right flank of 30 BALB/c immunocompetent mice. When tumours reached 4-5mm in diameter, 10 mice each received IT injections of PBS, WRDD or VVL15 on days 1,3,5 (3 x $1x10^8$ PFU). Tumours were measured twice weekly. Mean tumour sizes ± SEM are displayed. Statistical analysis of tumour sizes at stated time-points was performed using the unpaired T-test with * representing statistical significance at $p<0.05$, ** representing statistical significance at $p<0.01$, *** representing statistical significance at $p<0.001$ and ns indicating no statistical significance.

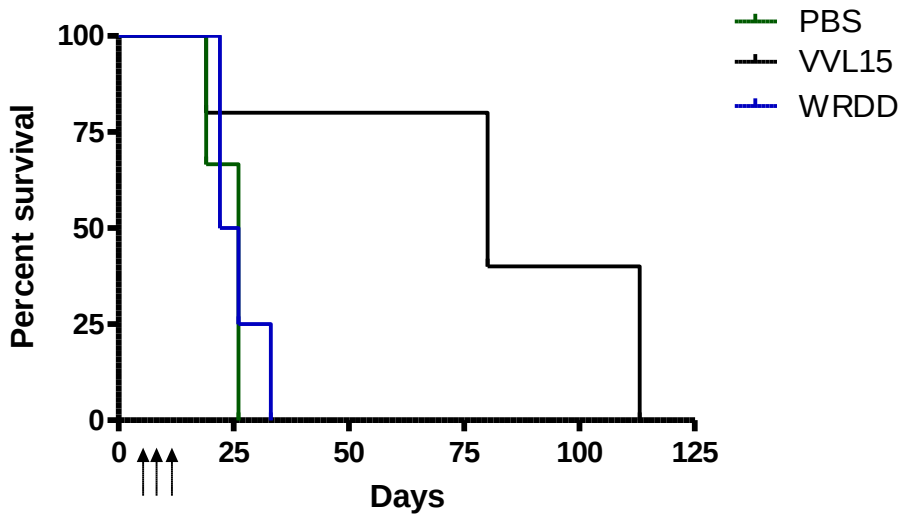

Figure 15b. Animal survival of immunocompetent mice bearing established murine colorectal tumours after treatment with different vaccinia virus mutants. $1x10^6$ CT26 cells were seeded by subcutaneous injection into the right flank of 30 BALB/c immunocompetent mice. When tumours reached 4-5mm in diameter, 10 mice each received IT injections of PBS, WRDD or VVL15 on days 1,3,5 (3 x $1x10^8$ PFU). Kaplan-Meier survival curves are show. Log-rank test survival curve statistical analysis showed significance at the 0.1% level between VVL15 and WRDD treated mice, and at the 5% level between VVL15 and PBS.

Reduced tumour progression was demonstrated in the treatment group receiving VVL15 compared to WRDD. Statistically significant differences were demonstrated in the animal survival between the WRDD- and VVL15-treated mice. Interestingly in both of these immunocompetent murine colorectal models there is no significant difference between the PBS- and WRDD –treated mice, in terms of tumour growth and animal

survival. The host immune system is able to overcome the anti-tumour potency demonstrated *in vitro* and in the nude cancer models.

To explain why Lister and WR demonstrated different anti-tumour potencies in different cell lines, investigation was made into the genetic changes of the different cell lines used. A distinction between the sensitivities of murine and human origin cell lines was apparent and is possibly explained by the development of the WR parent strain, Wyeth, by repeated passage in mice brains. [246]

Differences in status of tumour suppressor genes and oncogenes in the cell lines used in my experiments were established through a literature search and presented in Table 4.

Sensitivities of cell lines to radiotherapy and/or chemotherapy dependent of p53 and other genetic changes has been investigated elsewhere, with wild-type status conferring greater sensitivity to treatments. [247,248] Furthermore adenovirus-mediated restoration of p53 function to p53-deficient tumours was a key cancer gene therapy strategy. [4]

However differences in cell line sensitivities to different vaccinia viruses dependent on their p53 and other tumour suppressor or oncogene status has not been reported. It is impossible to conclude definitively relationships between genetic changes of the infected cell line and WRDD vs VVL15 sensitivity. However there is a suggestion that WR strain may be more potent in cell lines with wild-type p53; as is the case with SCCVII, Capan2, Panc02, HCT116, MKN45 and CMT93 (but not SW620 and SCC25). VVL15 appears to be more potent in the cell lines with mutated p53, such as FaDu, SCC4, PT45, SUIT2, MiaPaCa. This suggestion requires further investigation to demonstrate that virus sensitivity can be reversed in individual cell lines with wild-type and mutated p53 function.

Tumour type	Cell line (Human/**Murine**)	K-ras	p53	p16/ CDKN2A	DPC4 smad4	BRAF	PIK3CA	PTEN
HNSCC	FaDu [249]		Mut (pm)	Mut (pm)				
	SCC4 [249]		Mut (pm)	Mut (pm)				
	SCC25 [249]		Mut (pm)	Mut (pm)	Mut (pm)			
	TR138	No data found						
	SCCVII [250]			**Mut (pm)**				
Pancreatic	PANC1 [251]	Mut (pm)	Mut (pm)	Mut (hd)	WT			
	Capan2 [251]	Mut (pm)	WT	Mut (ins)	low protein expression			
	PT45 [251]	Mut (pm)	Mut (pm)	Mut (hd)	WT			
	SUIT2 [252]	Mut (pm)	Mut (pm)	Mut (pm)	WT			
	MiaPaCa2[251]	Mut (pm)	Mut (pm)	Mut (hd)	WT			
	Panc02 [253]	SNP	WT	WT	Mut (pm)			
Gastro intestinal	HCT116 [254]	Mut (pm)	WT			WT	Mut (pm)	WT
	HT29 [254]	WT	WT	WT	WT	Mut	Mut	WT
	SW620 [249]	Mut (pm)	Mut (pm)			WT	WT	WT
	MKN45 [255,256]		WT	Mut	Mut			
	CMT93 [257]	WT	WT			WT	Mut	
	CT26 [258]	Mut						
Ovary	A2780 [259]	WT					WT	Mut
	MOSEC	No data found						

Table 4. Genetic profile of cancer cell lines and sensitivity to different Vaccinia virus strains. Dark grey = VVL15 most potent; dark blue = WR most potent; light blue = WRLuc most potent; white = WR = VVL15. Mut = Mutation; WT = Wild Type; pm = point mutation; hd= homozygous deletion; SNP = Single-nucleotide polymorphism.

3.9 Chapter Conclusions

- VVL15 > WRDD 11/14 human cancer cell lines *in vitro*.
    - A2780 and HCT116 are outliers showing a reverse in sensitivity.
- WRDD > VVL15 5/5 murine cancer cell lines *in vitro*
- WRLuc (single deleted) more potent than WRDD (double deleted) except in Panc02.
- Viral replication studies supported cell proliferation study findings, with higher viral titres in cell lines with lowest EC_{50}.
- WR Luc toxic *in vivo*.
- Nude *in vivo* models of cancer evidenced superior anti-tumour potency of VVL15 in human (FaDu and PT45) cancer s; in keeping with *in vitro* data. A nude murine model of cancer (CMT93) demonstrated identical findings to *in vitro* data, with superior WRDD potency.
- Immunocompetent murine models of cancer (CMT93 and CT26) conversely showed superior anti-tumour of VVL15 compared to WRDD.

4. Results: Comparison of the biodistribution of vaccinia virus mutants in mouse models of solid tumours in nude and immunocompetent mice.

Investigation of the biodistribution of vaccinia virus mutants in nude and immunocompetent solid tumour mouse models following systemic (IV) delivery was carried out to establish relative *in vivo* tumour selectivity and viral clearance by the host immune system. Viruses were injected into the tail vein of mice bearing CMT93 flank tumours and then at set time-points the mice were sacrificed, and tumours and organs of interest were harvested for determination of viral titre by $TCID_{50}$, qRT-PCR and immunohistochemistry.

4.1 Biodistribution of vaccinia virus mutants in ICRF nu/nu mice bearing CMT93 flank tumours determined by $TCID_{50}$.

Tumour Site	**PBS**		**VVL15**		**WRDD**	
	Viral Recovery (PFU/ml/g)	**SEM**	**Viral Recovery** (PFU/ml/g)	**SEM**	**Viral Recovery** (PFU/ml/g)	**SEM**
Tumour	0	0	6235153.00	4116647.00	6.912245x 10^8	4.263284 x10^8
Ovary	0	0	95789.840	36684.390	4.716238 x10^8	3.072911 x10^8
Lung	0	0	21652.690	7162.151	81952.930	8212.015
Liver	0	0	13435.280	4988.430	61266.930	29240.290
Spleen	0	0	0	0	91273.190	26757.480
Brain	0	0	0	0	0	0
Bone Marrow	0	0	0	0	0	0

Table 5. Biodistribution of vaccinia virus mutants in ICRF nu/nu mice bearing CMT93 flank tumours determined by $TCID_{50}$. $5x10^6$ CMT93 cells were seeded by subcutaneous injection into the right flank of 36 ICRF nude mice. When tumours reached 4-5mm in diameter, 12 mice each received single IV injections of PBS, WRDD or VVL15 (1 x 1x107 PFU). On days 2, 6, 8 and 12 four mice from each group were

sacrificed and ovaries were harvested and frozen. Samples were then homogenised and repeatedly freeze-thawed. Mean viral recovery at 8 days post injection ± SEM was determined by $TCID_{50}$ assay on CV1 cells are tabulated.

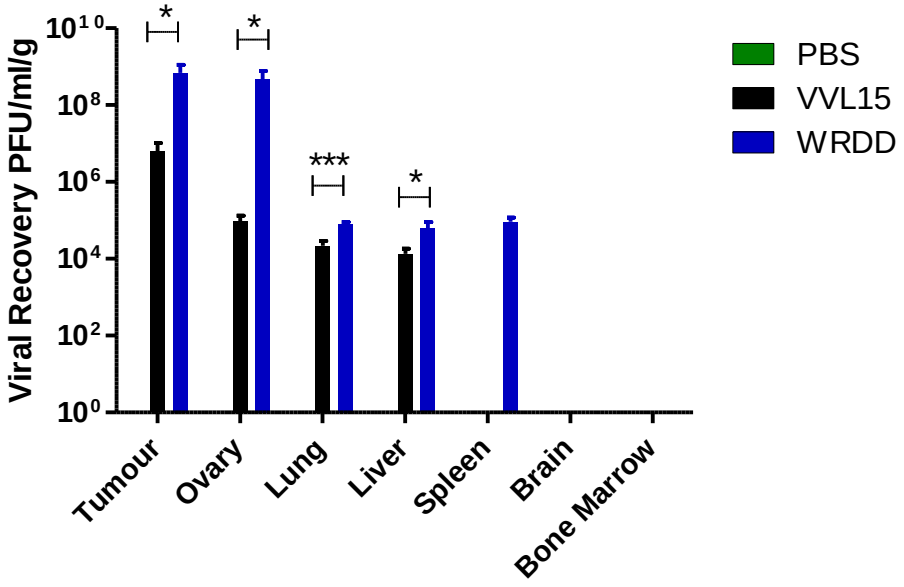

Figure 16. Biodistribution of vaccinia virus mutants in ICRF nu/nu mice bearing CMT93 flank tumours determined by $TCID_{50}$. Viral titre of harvested tumours and other organs in ICRF nu/nu mice bearing CMT93 flank tumours following IV vaccinia virus treatment. 5x106 CMT93 cells were seeded by subcutaneous injection into the right flank of 36 ICRF nude mice. When tumours reached 4-5mm in diameter, 12 mice each received single IV injections of PBS, WRDD or VVL15 (1 x 1x107 PFU). On days 2, 6, 8 and 12 four mice from each group were sacrificed and ovaries were harvested and frozen. Samples were then homogenised and repeatedly freeze-thawed. Mean viral recovery at 8 days post injection ± SEM was determined by TCID50 assay on CV1 cells are shown. Statistical analysis of tumour sizes at stated time-points was performed using the unpaired T-test with * representing statistical significance at $p<0.05$, ** representing statistical significance at $p<0.01$, *** representing statistical significance at $p<0.001$ and ns indicating no statistical significance.

WRDD vaccinia virus demonstrated higher viral titres from tumour, ovary, liver, and spleen samples compared to VVL15. There was no recoverable virus from splenic samples other than WRDD at 6 and 8 days. Therefore, although WRDD had higher viral titres in the tumour samples, there was less tumour selectivity with higher titres in other organs.

4.2. Biodistribution of vaccinia virus mutants in ICRF nu/nu mice bearing CMT93 flank tumours determined by qRT-PCR.

To confirm the $TCID_{50}$ findings, homogenised tumour and organ samples underwent DNA extraction, total DNA quantification and qRT-PCR of vaccinia genomes using vaccinia late primers to assess vaccinia genome copy number.

Tumour Site	**PBS**		**VVL15**		**WRDD**	
	Viral Recovery (PFU/ml/g)	**SEM**	**Viral Recovery** (PFU/ml/g)	**SEM**	**Viral Recovery** (PFU/ml/g)	**SEM**
Tumour	0	0	9289.081	2516.674	212877.500	97294.850
Ovary	0	0	188.7133	22.18592	103459.100	28499.390
Lung	0	0	93.55778	14.54905	189.7389	46.71809
Liver	0	0	31.515	5.440252	95.19625	32.46453
Spleen	0	0	83.18188	23.75478	247.6278	32.77229
Brain	0	0	28.61928	1.259999	244.9778	41.50741
Bone Marrow	0	0	233.1237	59.31355	774.6817	69.85658

Table 6. Biodistribution of vaccinia virus mutants in ICRF nu/nu mice bearing CMT93 flank tumours determined by qRT-PCR. $5x10^6$ CMT93 cells were seeded by subcutaneous injection into the right flank of 36 ICRF nude mice. When tumours reached 4-5mm in diameter, 12 mice each received single IV injections of PBS, WRDD or VVL15 (1 x $1x10^7$ PFU). On days 2, 6, 8 and 12 four mice from each group were sacrificed and ovaries were harvested and frozen. Samples were then homogenised and repeatedly freeze-thawed. Mean viral recovery at 8 days post injection ± SEM was determined by $TCID_{50}$ assay on CV1 cells are tabulated.

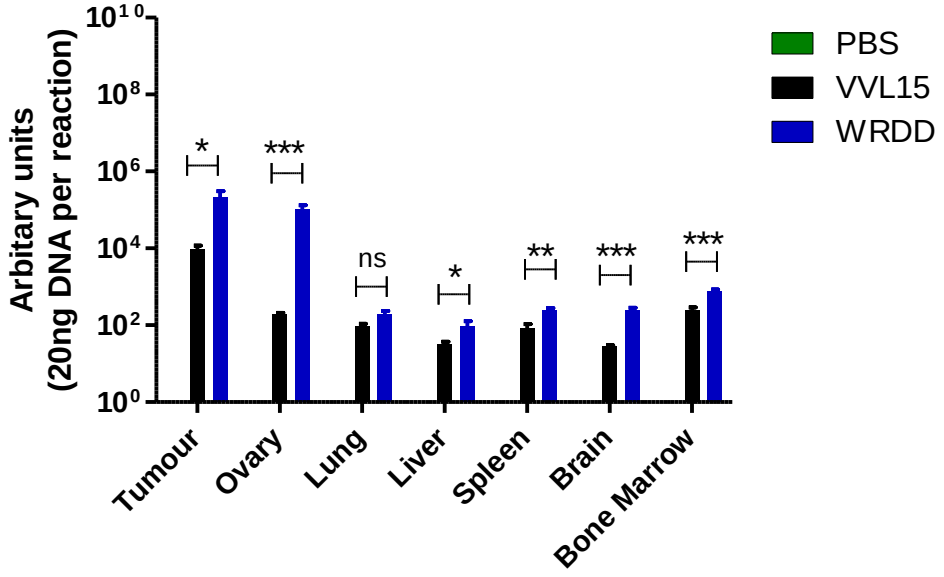

Figure 17. Biodistribution of vaccinia virus mutants in ICRF nu/nu mice bearing CMT93 flank tumours determined by qRT-PCR. $5x10^6$ CMT93 cells were seeded by subcutaneous injection into the right flank of 36 ICRF nude mice. When tumours reached 4-5mm in diameter, 12 mice each received single IV injections of PBS, WRDD or VVL15 (1 x 1x107 PFU). On days 2, 6, 8 and 12 four mice from each group were sacrificed and ovaries were harvested and frozen. Samples were then homogenised and repeatedly freeze-thawed. Mean viral recovery at 8 days post injection ± SEM was determined by TCID50 assay on CV1 cells are shown. Statistical analysis of tumour sizes at stated time-points was performed using the unpaired T-test with * representing statistical significance at $p<0.05$, ** representing statistical significance at $p<0.01$, *** representing statistical significance at $p<0.001$ and ns indicating no statistical significance.

qRT-PCR findings are similar to the $TCID_{50}$ findings. The increased sensitivity of qRT-PCR compared to $TCID_{50}$ allowed fuller assessment of splenic distribution, and an assessment of bone marrow and brain tissue. Again the pattern is confirmed with WRDD showing higher copy numbers in tumour and non-tumour tissues, especially ovary and bone marrow, compared to VVL15.

4.3. Biodistribution of vaccinia virus mutants in ICRF nu/nu mice bearing CMT93 flank tumours determined by immunohistochemistry.

To confirm the $TCID_{50}$ and qRT-PCR findings, the frozen sections of tumour and organ samples were stained with vaccinia coat protein antibody. Only tumour and ovary tissues stained positive.

4.3.1. Optimisation of anti vaccinia virus antibody for immunohistochemistry.

The anti-Lister vaccinia virus antibody was optimised for immunohistochemistry in frozens sections using several dilutions (Figure 18), with 1:2000 chosen since there was no background staining and clear positive staining of vaccinia virus infected tissue.

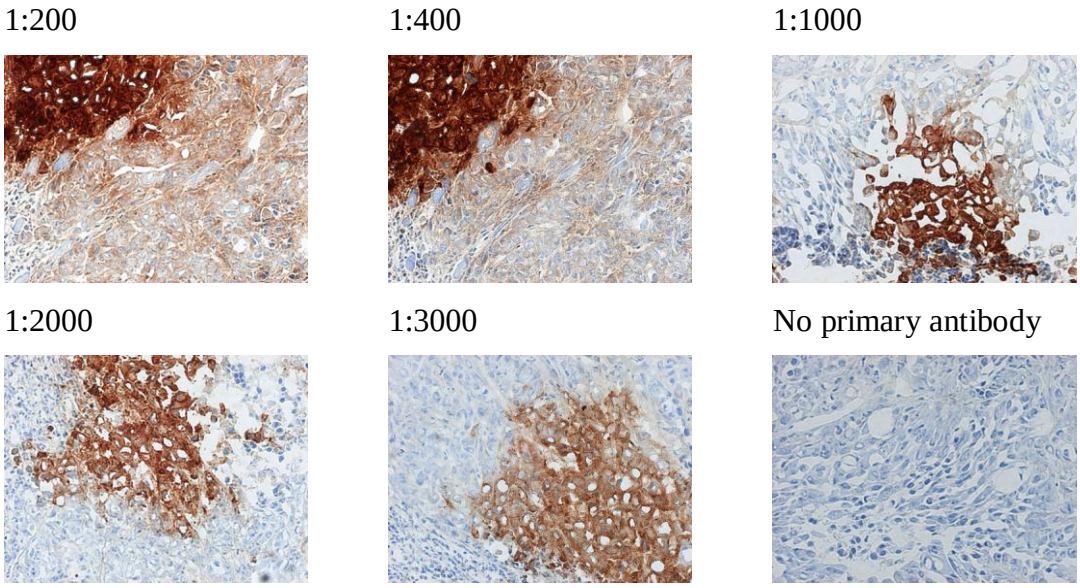

Figure 18. Optimisation of anti-Lister vaccinia virus coat protein antibody for immunohistochemistry in frozen sections. Immunohistochemistry was performed on frozen sections of CMT93 tumours infected IT with VVLister (+ve control) or PBS (-ve control) using different dilutions (1:200, 1:400, 1:1000, 1:2000, 1:3000 and no primary) of anti-Lister vaccinia virus coat protein antibody. Representative images are shown at x200 magnification.

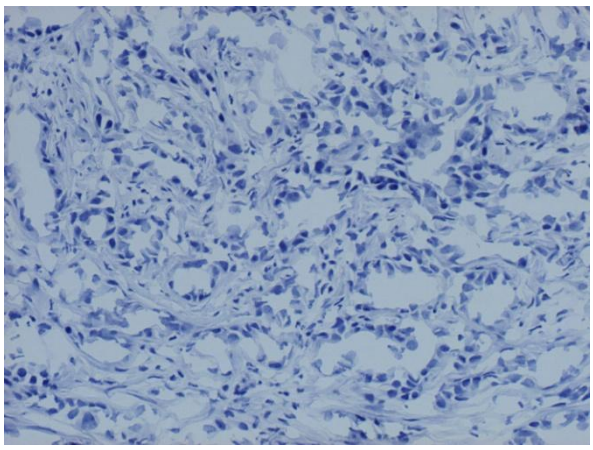

PBS 200x

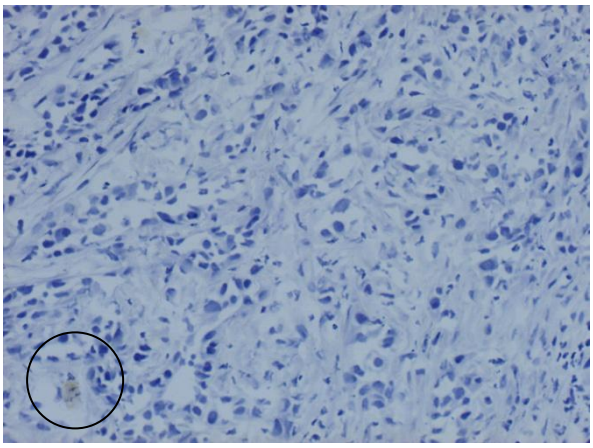

VVL15 200x

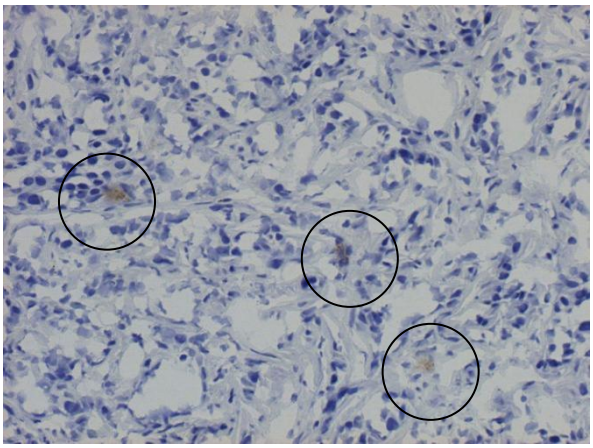

WRDD 200x (a)

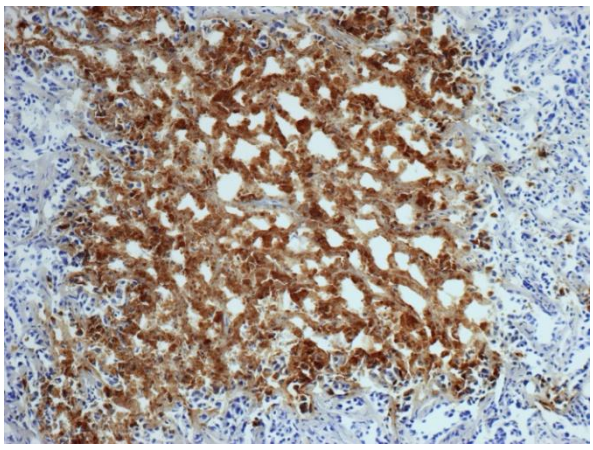

WRDD100x (b)

Figure 19. Biodistribution of vaccinia virus mutants in ICRF nu/nu mice bearing flank CMT93 tumours, as determined by immunohistochemistry of tumour samples. $5x10^6$ CMT93 cells were seeded by subcutaneous injection into the right flank of 36 ICRF nude mice. When tumours reached 4-5mm in diameter, 12 mice each received single IV injections of PBS, WRDD or VVL15 ($1 \times 1x10^7$ PFU). On days 2, 6, 8 and 12 four mice from each group were sacrificed and tumours were harvested and frozen. IHC for vaccinia coat protein was performed and representative images at day 8 are shown at 100-200x magnification; images were taken with a Zeiss Axioplan microscope fitted with a Zeiss AxioCam MRc camera.

WRDD-infected mice showed more VCP staining compared to VVL15. The WRDD tumour sections featured multiple necrotic centres (WRDD b). No necrotic centres were seen with VVL15 infected tumours nor PBS controls.

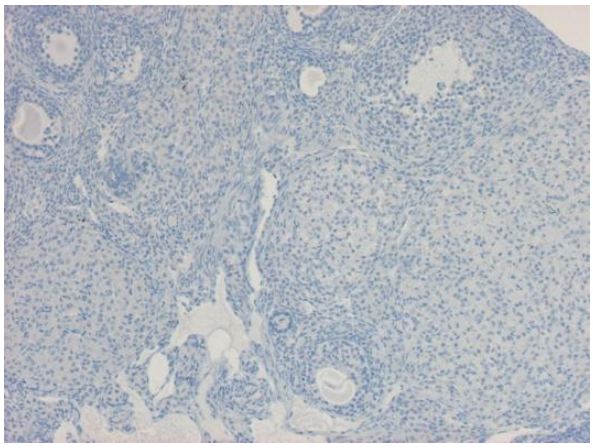

PBS 100x

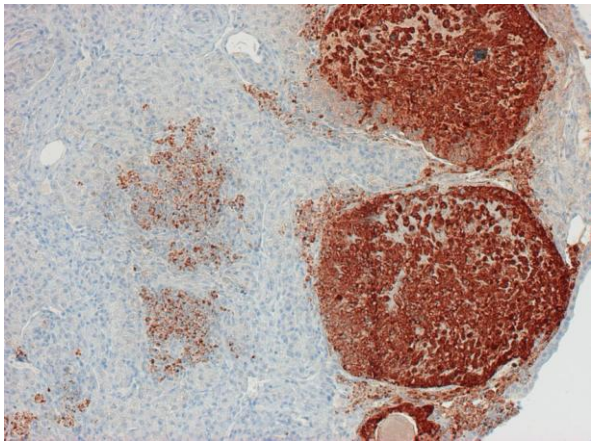

WRDD 100x

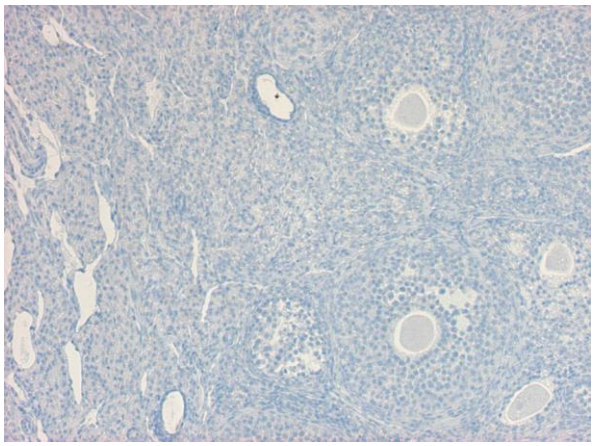

VVL15 100x

Figure 20. Biodistribution of vaccinia virus mutants in ICRF nu/nu mice bearing flank CMT93 tumours, as determined by immunohistochemistry of ovary samples. $5x10^6$ CMT93 cells were seeded by subcutaneous injection into the right flank of 60 ICRF nude mice. When tumours reached 4-5mm in diameter, 12 mice each received single IV injections of PBS, WRDD or VVL15 (1 x $1x10^7$ PFU). On days 2, 6, 8 and 12 four mice from each group were sacrificed and ovaries were harvested and frozen. IHC for vaccinia coat protein was performed and representative images at day 12 are shown at 200x magnification; images were taken with a Zeiss Axioplan microscope fitted with a Zeiss AxioCam MRc camera.

The immunoreactivity was more convincing in the ovary than in the tumour slides. Marked VCP staining was seen with the WRDD-infected ovarian tissue; with prominent necrotic follicles seen.

The immunohistochemistry staining evidenced similar patterns to the $TCID_{50}$ and qRT-PCR data, with greater WRDD replication in the tumours, but also the ovaries. Vaccinia coat staining was too weak to be visible in the other organs tested using $TCID_{50}$ and qRT-PCR virus quantification techniques, despite repeat optimisation of anti vaccinia virus antibody as outlined above.

4.4. Biodistribution of vaccinia virus mutants in C57BL/6 immunocompetent mice bearing CMT93 flank tumours determined by qRT-PCR.

To further assess the biodistribution of vaccinia virus mutants, systemic treatment of immunocompetent mice was investigated. This will evaluate the role of the host immune system in clearance of the viral oncolytic agents. The samples for this experiment were assessed using $TCID_{50}$ and qRT-PCR; however only qRT-PCR was sensitive enough to detect the virus. More DNA extraction lysate from the tissue homogenates had to be used for the PCR reaction (20ng DNA nude mice biodistribution versus 100ng DNA for immunocompetent mice biodistribution) to detect and quantify the virus.

Tumour Site	**PBS**		**VVL15**		**WRDD**	
	Viral Recovery (PFU/ml/g)	**SEM**	**Viral Recovery** (PFU/ml/g)	**SEM**	**Viral Recovery** (PFU/ml/g)	**SEM**
Tumour	0	0	23237.070	8439.108	358.8244	96.51902
Ovary	0	0	26.13517	2.398122	24654.400	10801.600
Lung	0	0	4292.671	691.9373	981.1987	175.5599
Liver	0	0	166.9944	34.23967	69.62366	17.23177
Spleen	0	0	78.040	18.0735	67.440	14.0419
Brain	0	0	0	0	0	0
Bone Marrow	0	0	130.9678	51.81752	173.180	55.06757

Table 7. Vaccinia virus genome copy number of harvested CMT93 tumours and other organs in immunocompetent C57BL/6 mice following IV vaccinia virus treatment. $5x10^6$ CMT93 cells were seeded by subcutaneous injection into the right flank of 36 C57BL/6 immunocompetent mice. When tumours reached 4-5mm in diameter, 12 mice each received single IV injections of PBS, WRDD or VVL15 (2 x $1x10^8$ PFU). On days 4, 8, and 12 four mice from each group were sacrificed and tumours were harvested and frozen. Samples were then homogenised and repeatedly freeze-thawed. Lysates underwent DNA extraction. Mean viral genome copy numbers ±

SEM at day 8 were determined by qRT-PCR using the vaccinia late gene (VLTF-1) and tabulated above.

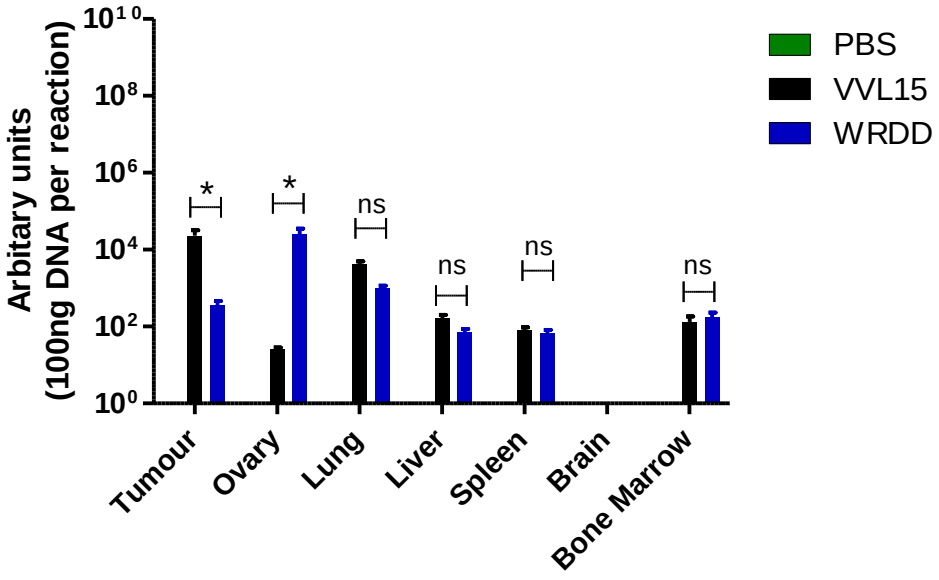

Figure 21. Vaccinia virus genome copy number of harvested CMT93 tumours and other organs in immunocompetent C57BL/6 mice following IV vaccinia virus treatment. $5x10^6$ CMT93 cells were seeded by subcutaneous injection into the right flank of 36 C57BL/6 immunocompetent mice. When tumours reached 4-5mm in diameter, 12 mice each received single IV injections of PBS, WRDD or VVL15 (2 x $1x10^8$ PFU). On days 4, 8, and 12 four mice from each group were sacrificed and tumours were harvested and frozen. Samples were then homogenised and repeatedly freeze-thawed. Lysates underwent DNA extraction. Mean viral genome copy numbers ± SEM at day 8 were determined by qRT-PCR using the vaccinia late gene (VLTF-1) and shown above. Statistical analysis of viral titres at stated time-points was performed using the unpaired T-test with * representing statistical significance at $p<0.05$, ** representing statistical significance at $p<0.01$, *** representing statistical significance at $p<0.001$ and ns indicating no statistical significance.

In the immunocompetent model VVL15 demonstrated higher tumour viral genome copy numbers compared to WRDD at the day 8 and 12 time-points. As before, the ovary viral genome copy number for WRDD was much higher than VVL15. For the liver, lungs and spleen samples there was no statistically significant difference between VVL15 and

WRDD copy numbers. The bone marrow data shows higher WRDD copy numbers at the late time point (day 12).

4.5. Biological time-points of vaccinia virus mutants in C57BL/6 immunocompetent mice bearing CMT93 flank tumours determined by qRT-PCR.

Following assessment of VVL15 and WRDD biodistribution in nude and immunocompetent murine tumour models, investigation into the behaviour of IT-delivered virus was undertaken.

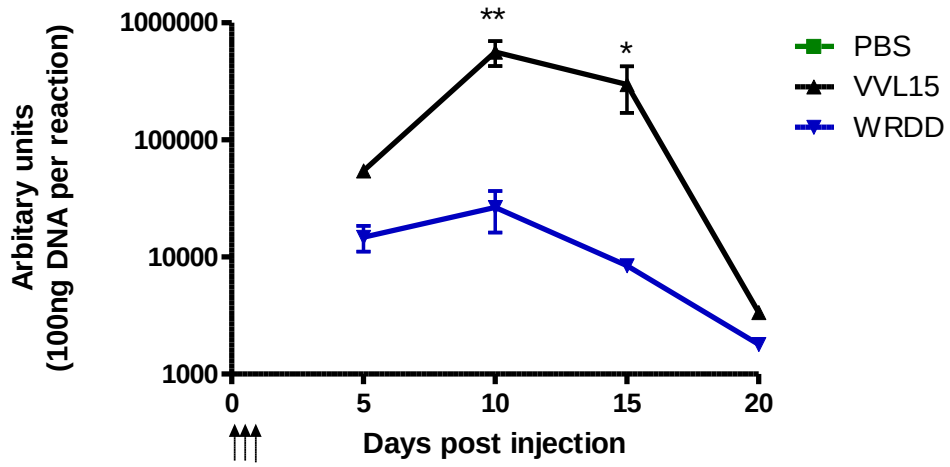

Figure 22. Vaccinia virus genome copy number of harvested tumours in C57BL/6 immunocompetent mice bearing CMT93 flank tumours following IT vaccinia virus treatment. $5x10^6$ CMT93 cells were seeded by subcutaneous injection into the right flank of 36 C57BL/6 immunocompetent mice. When tumours reached 4-5mm in diameter, 12 mice each received three IT injections of PBS, WRDD or VVL15 (3 x $1x10^8$ PFU). On days 5, 10, 15 and 20 three mice from each group were sacrificed and tumours were harvested and frozen. Samples were then homogenised and repeatedly freeze-thawed. Lysates underwent DNA extraction. Mean viral genome copy numbers ± SEM were determined by qRT-PCR using the vaccinia late gene (VLTF-1). Statistical analysis of viral titres at stated time-points was performed using the unpaired T-test with * representing statistical significance at $p<0.05$, ** representing statistical significance at $p<0.01$, *** representing statistical significance at $p<0.001$ and ns indicating no statistical significance.

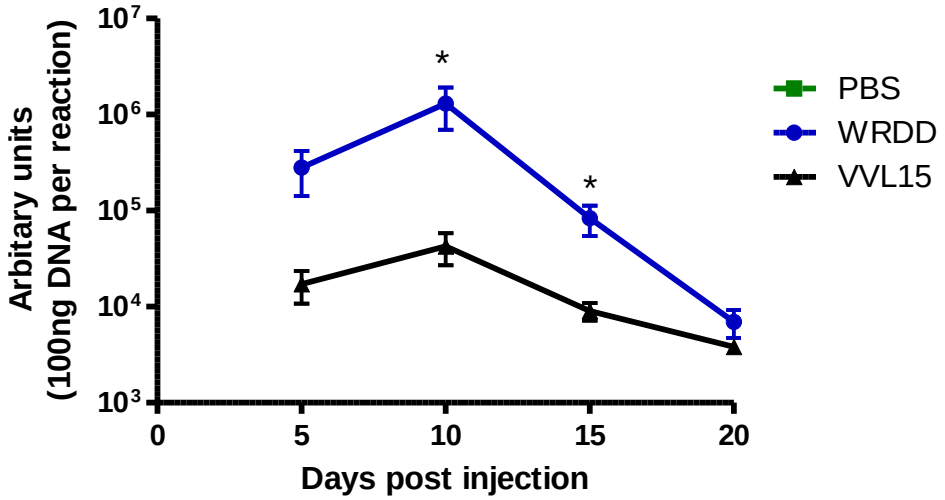

Figure 23. Vaccinia virus genome copy number of harvested ovaries in C57BL/6 immunocompetent mice bearing CMT93 flank tumours following IT vaccinia virus treatment. $5x10^6$ CMT93 cells were seeded by subcutaneous injection into the right flank of 36 C57BL/6 immunocompetent mice. When tumours reached 4-5mm in diameter, 12 mice each received three IT injections of PBS, WRDD or VVL15 (3 x $1x10^8$ PFU). On days 5, 10, 15 and 20 three mice from each group were sacrificed and ovaries were harvested and frozen. Samples were then homogenised and repeatedly freeze-thawed. Lysates underwent DNA extraction. Mean viral genome copy numbers ± SEM were determined by qRT-PCR using the vaccinia late gene (VLTF-1). Statistical analysis of viral titres at stated time-points was performed using the unpaired T-test with * representing statistical significance at $p<0.05$, ** representing statistical significance at $p<0.01$, *** representing statistical significance at $p<0.001$ and ns indicating no statistical significance.

Biological time-points studies showed that VVL15 delivered to IT replicated better in the immunocompetent model compared to WRDD. This would explain the better anti-tumour efficacy was demonstrated *in vivo*. WRDD virus delivered IT, and to a lesser extent VVL15, was able to spread to and replicate within the mouse ovaries.

4.6. Biodistribution of vaccinia virus mutants in ICRF nu/nu mice bearing PT45 flank tumours determined by qRT-PCR.

Following assessment of VVL15 and WRDD biodistribution in nude and immunocompetent murine tumour models, investigation into the biodistribution of the viruses in a model of human cancer was undertaken. The human pancreatic tumour PT45 was chosen and flank tumours in ICRF nu/nu mice were grown.

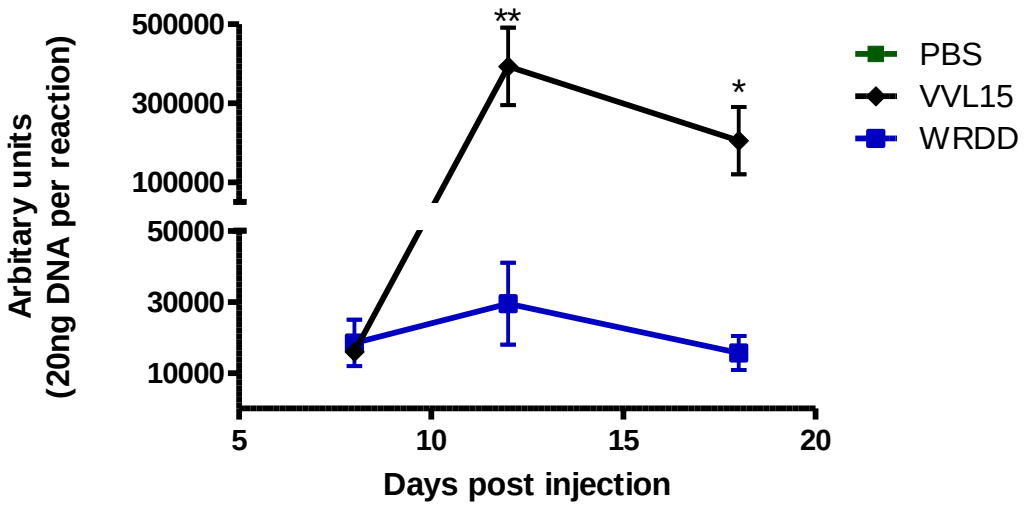

Figure 24. Vaccinia virus genome copy number in harvested tumours of ICRF nu/nu mice bearing PT45 flank tumours following IV vaccinia virus treatment. $5x10^6$ PT45 cells were seeded by subcutaneous injection into the right flank of 27 ICRF nu/nu mice. When tumours reached 4-5mm in diameter, 9 mice each received single IV injections of PBS, WRDD or VVL15 ($1x10^7$ PFU). On days 8, 12 and 18 three mice from each group were sacrificed and tumours were harvested and frozen. Samples were then homogenised and repeatedly freeze-thawed. Lysates underwent DNA extraction. Mean viral genome copy numbers ± SEM were determined by qRT-PCR using the vaccinia late gene (VLTF-1). Statistical analysis of viral titres at stated time-points was performed using the unpaired T-test with * representing statistical significance at $p<0.05$, ** representing statistical significance at $p<0.01$, *** representing statistical significance at $p<0.001$ and ns indicating no statistical significance.

The biodistribution results are in keeping with the PT45 *in vitro* cell proliferation and viral replication assays, which showed superior anti-tumour potency and viral replication of VVL15 over WRDD; and the PT45 *in vivo* efficacy studies, where

reduced tumour growth and disease progression was recorded in an ICRF nu/nu model. Good VVL15 replication was demonstrated with greater viral titres at two time-points, compared to WRDD which exhibited poor viral replication.

4.7. Biological time-points of vaccinia virus mutants in ICRF nu/nu mice bearing PT45 flank tumours determined by qRT-PCR.

Assessment of IT delivered viruses was also made in the mouse ICRF nu/nu PT45 human pancreatic cancer model.

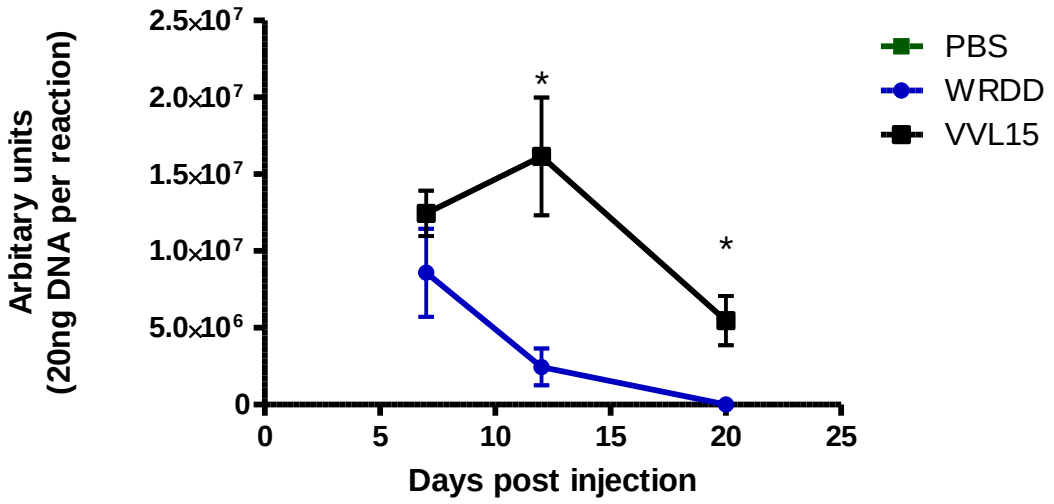

Figure 25. Vaccinia virus genome copy number in harvested tumours of ICRF nu/nu mice bearing PT45 flank tumours following IT vaccinia virus treatment. $5x10^6$ PT45 cells were seeded by subcutaneous injection into the right flank of 30 ICRF nu/nu mice. When tumours reached 4-5mm in diameter, 12 mice each received three IT injections of PBS, WRDD or VVL15 (3 x $1x10^7$ PFU). On days 7, 12 and 20 three mice from each group were sacrificed and tumours were harvested and frozen. Samples were then homogenised and repeatedly freeze-thawed. Lysates underwent DNA extraction. Mean viral genome copy numbers ± SEM were determined by qRT-PCR using the vaccinia late gene (VLTF-1). Statistical analysis of viral titres at stated time-points was performed using the unpaired T-test with * representing statistical significance at $p<0.05$, ** representing statistical significance at $p<0.01$, *** representing statistical significance at $p<0.001$ and ns indicating no statistical significance.

Higher viral titres for VVL15 were recovered following IT delivery compared to WRDD; indicating that VVL15 is better able to replicate in cancer cells *in vivo*. These results are in keeping with the *in vitro* cytotoxicity and viral replication studies; and additionally congruent with the *in vivo* PT45 efficacy study.

4.8 Chapter Conclusions

- WRDD demonstrates higher tumour viral titres compared to VVL15 following systemic delivery in a nude CMT93 biodistribution model, however the virus demonstrated less tumour selectivity with higher levels of WRDD found in off-target sites, including ovary, lung, liver, spleen, brain and bone marrow.
- Corroboration of qRT-PCR findings with $TCID_{50}$; with the former proving to be a more sensitive technique.
- Immunohistochemistry demonstrated superior vaccinia coat protein staining of tumour and ovarian tissues following systemic virus delivery of WRDD compared to VVL15.
- VVL15 demonstrated higher copy numbers compared to WRDD in a systemically delivered CMT93 immunocompetent model with a similar off target profile between the two viruses, except for the ovary tissue which showed high WRDD virus copy numbers.
- VVL15 when delivered IT to CMT93 flank tumours in nude mice achieved higher copy numbers than WRDD.
- Higher VVL15 copy numbers were achieved following systemic and IT virus delivery to nude mice bearing flank tumours compared to WRDD.

5. Results: Investigation into the host immune response to Western Reserve and Lister strain viruses

The reduced tumour viral clearance and superior anti-tumour potency of the Lister strain virus, VVL15, compared to the Western Reserve strain virus, WRDD, in immunocompetent, but not nude, models is suggestive of immunologically related differences between the two virus strain mutants. To characterise these potential differences I performed an investigation into the profile of multiple cytokines in serum and tumour murine samples (following IT delivery of virus to CMT93 flank tumours in C57BL/6 immunocompetent mice), as well as *in vitro* infection of CMT93 cells. Our hypothesis was that superior anti-tumour potency was related to reduced viral clearance; and that differences in the pro-inflammatory cytokine profile might exist following Lister infection, compared to WR.

5.1. Analysis of multiple pro-inflammatory cytokines in serum of C57BL/6 immunocompetent mice bearing CMT93 flank tumours following intratumoural viral injection.

To assess the differences in pro-inflammatory cytokines in the serum of C57BL/6 immunocompetent mice bearing CMT93 flank tumours, serum was sampled at various time-points following different IT viral treatments. Serum samples were subjected to cytokine quantification using a mouse pro-inflammatory ultra-sensitive kit for the Meso Scale Discovery multi-spot assay system.

Cytokine	PBS		VVL15		WRDD	
	Cytokine concentration (pg/ml)	**SEM**	**Cytokine concentration** (pg/ml)	**SEM**	**Cytokine concentration** (pg/ml)	**SEM**
IL1β	0.000	0.000	0.0415	0.0415	0.666	0.0451
TNFα	0.000	0.000	1.0058	0.355	0.915	0.471
IFNγ	1.409	0.090	2.39	0.324	12.0186	1.449
IL10	14.97	1.881	84.6	5.74	29.25	6.017
IL12	0.000	0.000	0.000	0.000	19.55	3.077
IL6	11.387	1.228	29.93	4.157	53.34	2.409
IL8	189.83	6.495	204.74	11.96	462.68	28.696

Table 8. Concentration of multiple pro-inflammatory cytokines in the serum of C57BL/6 immunocompetent mice bearing CMT93 flank tumours following intratumoural viral injection. $5x10^6$ CMT93 cells were seeded by subcutaneous injection into the right flank of 36 C57BL/6 mice. When tumours reached 4-5mm in diameter, 9 mice each received IT injections of PBS, WRDD or VVL15 on days 1,3,5 (3 x $1x10^8$ PFU). At days 5, 10 and 15 (day 5 samples not analysed here), 3 animals from each group were sacrificed and the serum was sampled. The cytokine concentration was quantified using a mouse pro-inflammatory 7-plex ultra-sensitive kit for the Meso Scale Discovery multi-spot assay system (2 animals per group in sample duplicate). Mean serum cytokine concentrations at day 10 ± SEM are shown.

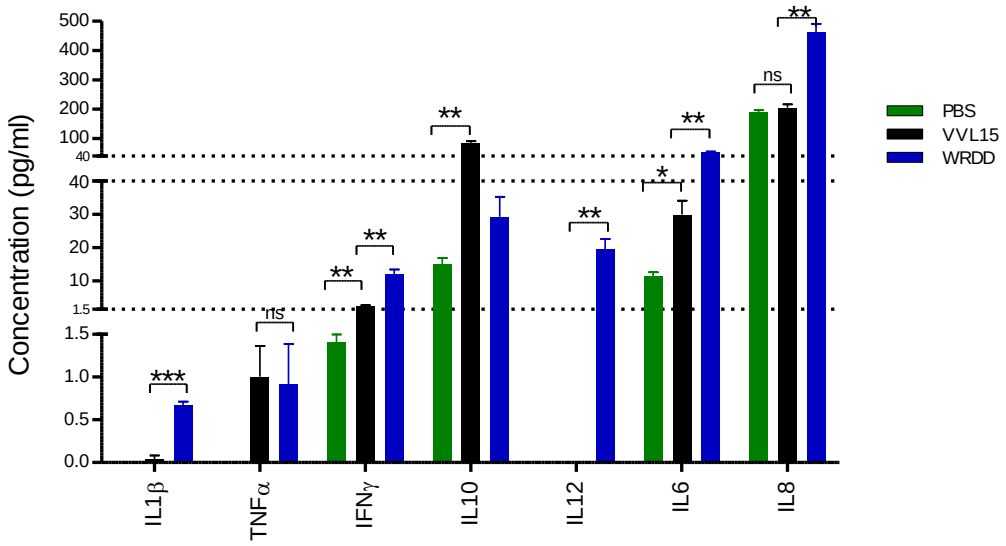

Figure 26. Concentration of multiple pro-inflammatory cytokines in the serum of C57BL/6 immunocompetent mice bearing CMT93 flank tumours following intratumoural viral injection. $5x10^6$ CMT93 cells were seeded by subcutaneous injection into the right flank of 36 C57BL/6 mice. When tumours reached 4-5mm in diameter, 9 mice each received IT injections of PBS, WRDD or VVL15 on days 1,3,5 (3 x $1x10^8$ PFU). At days 5, 10 and 15 (day 5 samples not analysed here), 3 animals from each group were sacrificed and the serum was sampled. The cytokine concentration was quantified using a mouse pro-inflammatory 7-plex ultra-sensitive kit for the Meso Scale Discovery multi-spot assay system (2 animals per group in sample duplicate). Mean serum cytokine concentrations at day 10 ± SEM are shown. Statistical analysis was performed using the unpaired T-test with * representing statistical significance at $p<0.05$, ** representing statistical significance at $p<0.01$, *** representing statistical significance at $p<0.001$ and ns indicating no statistical significance.

The results revealed higher levels of pro-inflammatory in animals treated with WRDD compared to VVL15; with the exception of IL10, which is considered an anti-inflammatory cytokine. This is highly suggestive of WR infections inducing a more potent host anti-viral immune response, with resultant enhanced viral clearance and, hence reduced anti-tumour potency in immunocompetent *in vivo* models of cancer. There is also evidence of cytokine production in response to what appears to be PBS

treatment. However this represents cytokines released into the tumour microenvironment by the tumour cells and the host immune cells in a battle of survival of the host and cancer cells.[260]

5.2. Analysis of multiple pro-inflammatory cytokines in tumour homogenates of C57BL/6 immunocompetent mice bearing CMT93 flank tumours following intratumoural viral injection.

To assess the differences in pro-inflammatory cytokines in the tumour microenvironment CMT93 flank tumours were grown in C57BL/6 immunocompetent mice and different viral treatments were applied intratumourally. Tumours harvested from sacrificed mice were weighed, homogenised and subjected to cytokine quantification using a mouse pro-inflammatory ultra-sensitive kit for the Meso Scale Discovery multi-spot assay system.

Cytokine	**PBS**		**VVL15**		**WRDD**	
	Cytokine concentration (pg/ml/g)	**SEM**	**Cytokine concentration** (pg/ml/g)	**SEM**	**Cytokine concentration** (pg/ml/g)	**SEM**
IL1β	374.89	41.03	2105.35	347.6	442.02	27.08
TNFα	8.359	0.8107	15.344	1.407	25.99	2.340
IFNγ	37.730	5.974	76.372	9.292	102.66	22.943
IL10	60.25	10.931	132.54	13.59	20.75	5.132
IL12	4.574	0.380	59.294	16.04	26.597	8.855
IL6	360.82	8.625	370.64	66.40	699.40	27.55
IL8	83.357	9.717	1509.981	261.9	8396.20	397.24

Table 9. Concentration of multiple pro-inflammatory cytokines in CMT93 flank tumour samples following IT viral infection of C57BL/6 immunocompetent mice. $5x10^6$ CMT93 cells were seeded by subcutaneous injection into the right flank of 36 C57BL/6 mice. When tumours reached 4-5mm in diameter, 9 mice each received IT injections of PBS, WRDD or VVL15 on days 1,3,5 (3 x $1x10^8$ PFU). At days 5, 10 and 15 (day 15 samples not analysed here), 3 animals from each group were sacrificed and the tumours were harvested. The tumours were weighed, homogenised and subjected to cytokine quantification using a mouse pro-inflammatory ultra-sensitive kit for the Meso Scale Discovery multi-spot assay system (2 animals per group in sample duplicate).

Mean serum concentrations at day 10 ± SEM are shown. Cytokine concentration was corrected for tumour weight.

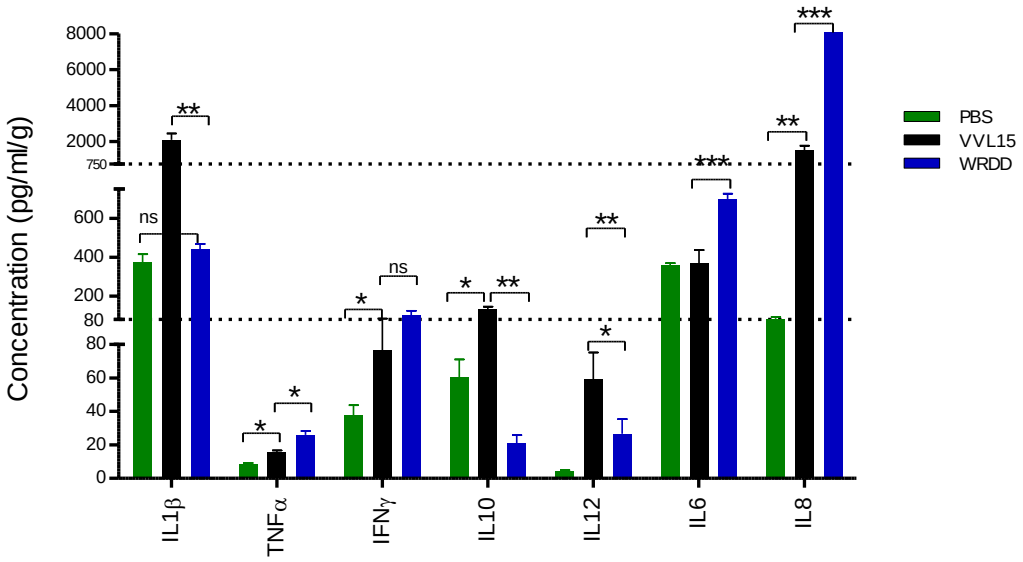

Figure 27. Concentration of multiple pro-inflammatory cytokines in CMT93 flank tumour samples following IT viral infection of C57BL/6 immunocompetent mice. $5x10^6$ CMT93 cells were seeded by subcutaneous injection into the right flank of 36 C57BL/6 mice. When tumours reached 4-5mm in diameter, 9 mice each received IT injections of PBS, WRDD or VVL15 on days 1,3,5 (3 x $1x10^8$ PFU). At days 5, 10 and 15 (day 15 samples not analysed here), 3 animals from each group were sacrificed and the tumours were harvested. The tumours were weighed, homogenised and subjected to cytokine quantification using a mouse pro-inflammatory ultra-sensitive kit for the Meso Scale Discovery multi-spot assay system (2 animals per group in sample duplicate). Mean cytokine concentration at day 10 ± SEM are shown. Cytokine concentration was corrected for tumour weight. Statistical analysis was performed using the unpaired T-test with * representing statistical significance at $p<0.05$, ** representing statistical significance at $p<0.01$, *** representing statistical significance at $p<0.001$ and ns indicating no statistical significance.

When considering the cytokine levels found within tumours the cytokine profile is more complicated with a less apparent overall pattern. WRDD infection resulted in higher

levels of TNFα, IL8 and IL6; but lower IL12, and IL1β and IL10 samples (differences in IFNγ levels were not significant). In contrast to the ideal host response in the serum, where a limited inflammatory response is favourable for the persistence and efficacy of oncolytic virotherapy, in the tumour a pro-inflammatory response can be beneficial in tumour lysis. However as I have demonstrated greater viral persistence together with superior *in vivo* anti-tumour potency with IT-delivered VVL15 compared to WRDD, a reduced host intra-tumoural anti-viral inflammatory response following VVL15 treatment is the most likely overall effect of this cytokine profile. Although the elevation of some pro-inflammatory cytokines (IL12 in particular) may contribute to the superior anti-tumour potency of VVL15 independent of this viral persistence mechanism.

5.3. Analysis of multiple pro-inflammatory cytokines of CMT93 tissue culture samples following viral infection.

To investigate further the observed differences in anti-tumour potency between VVL15 and WRDD an analysis of multiple pro-inflammatory cytokines was performed using a mouse pro-inflammatory ultra-sensitive kit for the Meso Scale Discovery multi-spot assay system. Samples were analysed from tissue culture supernatants of CMT93 cells infected with viruses.

Cytokine	**PBS**		**VVL15**		**WRDD**	
	Cytokine concentration (pg/ml)	**SEM**	**Cytokine concentration** (pg/ml)	**SEM**	**Cytokine concentration** (pg/ml)	**SEM**
IL1β	0.000	0.000	5.081	0.0940	4.1803	0.272
TNFα	0.000	0.000	0.000	0.000	1.677	0.194
IFNγ	0.000	0.000	0.000	0.000	4.242	0.187
IL10	4.795	4.795	337.72	32.75	4.494	3.882
IL12	11.270	5.687	48.633	4.555	121.9	9.310
IL6	14.355	2.346	0.000	0.000	40.132	3.217
IL8	55.253	7.221	266.48	9.017	398.15	32.64

Table 10. Concentration of multiple pro-inflammatory cytokines in CMT93 tissue culture samples following viral infection *in vitro*. $2x10^5$ cells per well were infected

with 1 PFU/cell of virus. Cell lysates were harvested at 6 and 24 hour intervals. Cytokine concentrations were quantified in triplicate using a mouse pro-inflammatory ultra-sensitive kit for the Meso Scale Discovery multi-spot assay system. Mean cytokine concentrations at 24 hours ± SEM are shown.

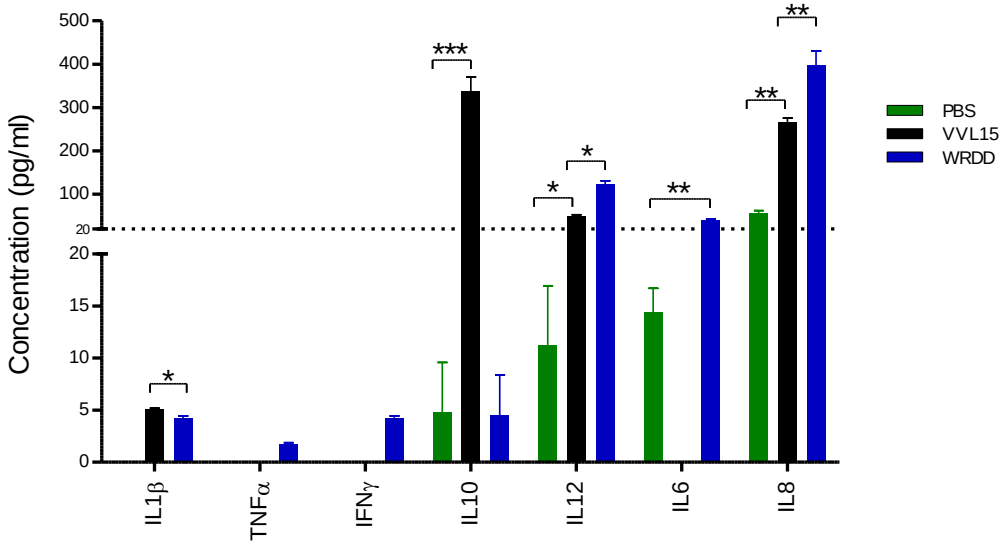

Figure 28. Concentration of multiple pro-inflammatory cytokines in CMT93 tissue culture samples following viral infection *in vitro*. $2x10^5$ cells per well were infected with 1 PFU/cell of virus. Cell lysates were harvested at 6 and 24 hour intervals. Cytokine concentrations were quantified in triplicate using a mouse pro-inflammatory ultra-sensitive kit for the Meso Scale Discovery multi-spot assay system. Mean cytokine concentrations at 24 hours ± SEM are shown. Statistical analysis was performed using the unpaired T-test with * representing statistical significance at $p<0.05$, ** representing statistical significance at $p<0.01$, *** representing statistical significance at $p<0.001$ and ns indicating no statistical significance.

The tissue culture cytokine profiles for VVL15 and WRDD show a similar pattern to those found in the serum samples, with elevated pro-inflammatory cytokines IFNγ, IL12, IL6, IL8 and TNFα; IL1β levels were not significantly different between the two groups. As before, IL10 was elevated in the VVL15-infected cells compared to WRDD.

Having reviewed the different cytokines and virus combinations, the cytokines that showed most promise as to explain the different anti-tumour potencies *in vitro* and *in vivo* were IL10, IL12 and IFN γ. More samples from an additional time-point and in sample triplicate were analysed.

5.4. Analysis of IL10, IL12 and Interferon γ cytokine concentrations in serum of C57BL/6 immunocompetent mice bearing CMT93 flank tumours following intratumoural viral injection.

IL10, IL12 and IFNγ cytokine concentrations in the serum of C57BL/6 immunocompetent mice bearing CMT93 flank tumours was quantified at various time-points following different IT viral treatments using R&D Systems Quantikine Mouse ELISA kits.

Cytokine	Day	PBS		VVL15		WRDD	
		Cytokine concentration (pg/ml)	SEM	Cytokine concentration (pg/ml)	SEM	Cytokine concentration (pg/ml)	SEM
IL12	5	0.000	0.000	0.000	0.000	1.859	0.1034
	10	0.622	0.073	0.000	0.000	1.745	0.1369
	15	0.897	0.103	0.129	0.0451	5.148	0.3509
IFNγ	5	0.337	0.023	0.518	0.0235	3.271	0.2001
	10	0.354	0.016	0.576	0.0429	3.037	0.2653
	15	0.906	0.035	0.425	0.0263	3.152	0.4395
IL10	5	0.099	0.062	23.74	2.882	3.607	0.344
	10	0.000	0.000	10.09	0.8861	1.535	0.1887
	15	0.000	0.000	3.002	0.395	0.502	0.1525

Table 11. Concentration of multiple pro-inflammatory cytokines in the serum of C57BL/6 immunocompetent mice bearing CMT93 flank tumours following intratumoural viral injection. $5x10^6$ CMT93 cells were seeded by subcutaneous injection into the right flank of 27 C57BL/6 mice. When tumours reached 4-5mm in diameter, 9 mice each received IT injections of PBS, WRDD or VVL15 on days 1,3,5 (3 x $1x10^8$ PFU). At days 5, 10 and 15, 3 animals from each group were sacrificed and the serum was sampled. The cytokine concentration was quantified using R&D Systems Quantikine Mouse IL10, IL12 and Interferon γ ELISA kits (3 animals per group in sample duplicate). Mean cytokine concentrations ± SEM are shown. Statistical analysis

was performed using the unpaired T-test with * representing statistical significance at $p<0.05$, ** representing statistical significance at $p<0.01$, *** representing statistical significance at $p<0.001$ and ns indicating no statistical significance.

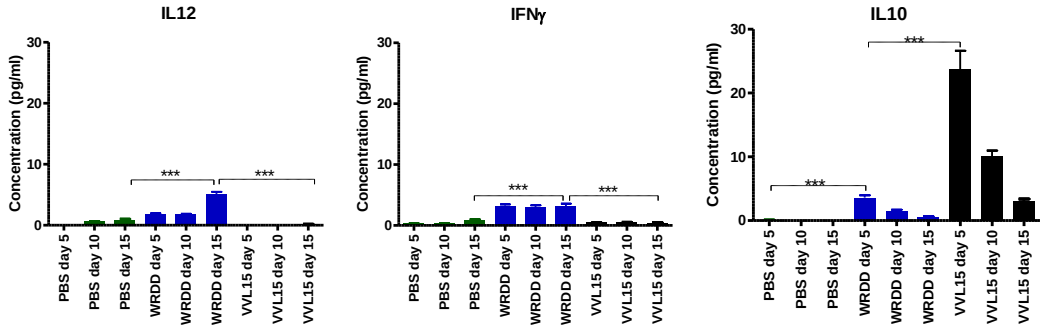

Figure 29. Concentration of multiple pro-inflammatory cytokines in the serum of C57BL/6 immunocompetent mice bearing CMT93 flank tumours following intratumoural viral injection. $5x10^6$ CMT93 cells were seeded by subcutaneous injection into the right flank of 27 C57BL/6 mice. When tumours reached 4-5mm in diameter, 9 mice each received IT injections of PBS, WRDD or VVL15 on days 1,3,5 (3 x $1x10^8$ PFU). At days 5, 10 and 15, 3 animals from each group were sacrificed and the serum was sampled. The cytokine concentration was quantified using R&D Systems Quantikine Mouse IL10, IL12 and Interferon γ ELISA kits (3 animals per group in sample duplicate). Mean cytokine concentrations ± SEM are shown. Statistical analysis was performed using the unpaired T-test with * representing statistical significance at $p<0.05$, ** representing statistical significance at $p<0.01$, *** representing statistical significance at $p<0.001$ and ns indicating no statistical significance.

These data over three time-points confirm the previous findings over two time-points using the Meso Scale Discovery multi-spot assay system. The pro-inflammatory cytokines were raised following WRDD IT treatment of mice bearing CMT93 flank tumours, whereas the anti-inflammatory cytokine IL10 was reduced compared to VVL15.

5.5. Analysis of IL10, IL12 and Interferon γ cytokine concentrations in CMT93 flank tumour homogenates following intratumoural viral injection of C57BL/6 immunocompetent mice.

In order to assess IL10, IL12 and Interferon γ cytokine concentrations in the tumour microenvironment, CMT93 flank tumours were grown in C57BL/6 immunocompetent mice and different viral treatments were applied intratumourally. Harvested tumours from sacrificed mice were weighed, homogenised and subjected to cytokine quantification using R&D Systems Quantikine Mouse IL10, IL12 and IFN γ ELISA kits.

Cytokine	Day	PBS		VVL15		WRDD	
		Cytokine concentration (pg/ml/g)	**SEM**	**Cytokine concentration** (pg/ml/g)	**SEM**	**Cytokine concentration** (pg/ml/g)	**SEM**
IL12	5	0.922	0.070	18.070	2.640	0.223	0.111
	10	1.169	0.055	19.830	2.552	6.43	0.837
	15	0.892	0.114	20.33	1.963	7.818	0.805
IFNγ	5	14.419	0.700	30.88	2.092	55.27	6.079
	10	10.487	0.960	19.10	1.329	25.60	2.898
	15	14.249	0.599	15.942	0.713	29.72	4.894
IL10	5	11.737	1.611	82.545	7.448	17.015	1.933
	10	12.44	1.40	43.028	3.14	5.087	0.498
	15	9.081	0.778	47.060	4.460	5.098	0.767

Table 12. Concentration of multiple pro-inflammatory cytokines in harvested and homogenised CMT93 flank tumour samples following IT viral infection of C57BL/6 immunocompetent mice. $5x10^6$ CMT93 cells were seeded by subcutaneous injection into the right flank of 27 C57BL/6 mice. When tumours reached 4-5mm in diameter, 9 mice each received IT injections of PBS, WRDD or VVL15 on days 1,3,5 (3 x $1x10^8$ PFU). At days 5, 10 and 15, 3 animals from each group were sacrificed and the tumours were harvested. The tumours were weighed, homogenised and subjected to cytokine quantification using R&D Systems Quantikine Mouse IL10, IL12 and Interferon γ ELISA kits (3 animals per group in sample duplicate). Mean cytokine concentrations ± SEM are shown. Cytokine concentration was corrected for tumour weight.

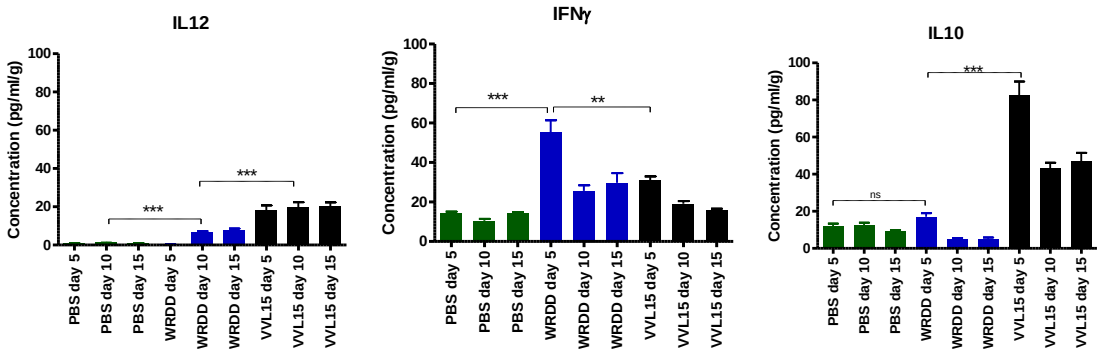

Figure 30. Concentration of multiple pro-inflammatory cytokines in harvested and homogenised CMT93 flank tumour samples following IT viral infection of C57BL/6 immunocompetent mice. $5x10^6$ CMT93 cells were seeded by subcutaneous injection into the right flank of 27 C57BL/6 mice. When tumours reached 4-5mm in diameter, 9 mice each received IT injections of PBS, WRDD or VVL15 on days 1,3,5 (3 x $1x10^8$ PFU). At days 5, 10 and 15, 3 animals from each group were sacrificed and the tumours were harvested. The tumours were weighed, homogenised and subjected to cytokine quantification using R&D Systems Quantikine Mouse IL10, IL12 and Interferon γ ELISA kits (3 animals per group in sample duplicate). Mean cytokine concentrations ± SEM are shown. Cytokine concentration was corrected for tumour weight. Statistical analysis was performed using the unpaired T-test with * representing statistical significance at $p<0.05$, ** representing statistical significance at $p<0.01$, *** representing statistical significance at $p<0.001$ and ns indicating no statistical significance.

These data over three-time points are similar to the previous findings over two time-points using the Meso Scale Discovery multi-spot assay system. However now there are significant differences in IFNγ levels whereas previously no significant differences were found between the two virus-treated groups. Again this is suggestive of a more powerful inflammatory reaction elicited locally in response to the WRDD virus, resulting in accelerated viral clearance and reduced anti-tumour potency *in vivo.*

5.6. Analysis of IL10, IL12 and Interferon γ cytokine concentration of CMT93 tissue culture samples following viral infection.

IL10, IL12 and Interferon γ cytokine concentrations of CMT93 tissue culture supernatants at 6, 24 and 48 hours following WRDD, VVL15 and mock infection were quantified using R&D Systems Quantikine Mouse IL10, IL12 and Interferon γ ELISA kits.

Cytokine	Hours	PBS		VVL15		WRDD	
		Cytokine concentration (pg/ml)	SEM	Cytokine concentration (pg/ml)	SEM	Cytokine concentration (pg/ml)	SEM
IL12	6	3.259	0.358	20.70	1.651	36.44	3.211
	24	4.019	0.293	14.25	1.473	40.90	3.352
	48	3.217	0.243	11.91	1.176	36.01	3.4703
IFNγ	6	0.000	0.000	0.000	0.000	0.371	0.0508
	24	0.000	0.000	0.000	0.000	1.336	0.0731
	48	0.000	0.000	0.159	0.057	1.569	0.1500
IL10	6	0.000	0.000	22.76	3.183	0.875	0.3665
	24	1.291	0.636	91.08	4.954	1.767	0.6233
	48	1.486	0.620	138.24	4.816	1.699	0.5983

Table 13. Concentration of multiple pro-inflammatory cytokines of CMT93 tissue culture samples following viral infection *in vitro*. $2x10^5$ cells per well were infected with 1 PFU/cell of virus. Cell lysates were harvested at 6, 24 and 48 hour intervals. Cytokine concentration was quantified in triplicate using R&D Systems Quantikine Mouse IL10, IL12 and Interferon γ ELISA kits. Mean cytokine concentrations ± SEM are shown.

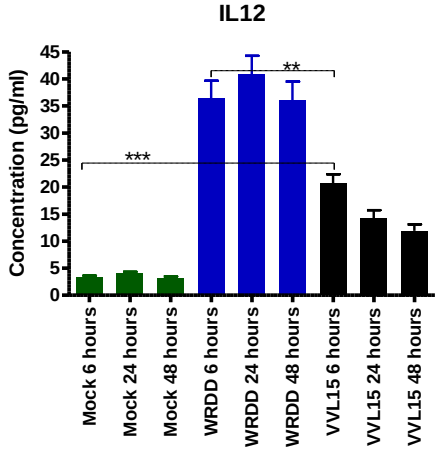

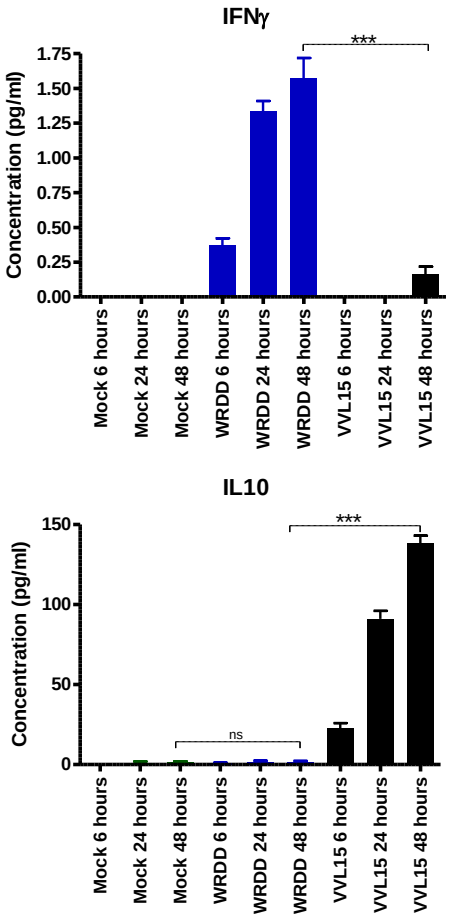

Figure 31. Concentration of multiple pro-inflammatory cytokines of CMT93 tissue culture samples following viral infection *in vitro*. $2x10^5$ cells per well were infected with 1 PFU/cell of virus. Cell lysates were harvested at 6, 24 and 48 hour intervals. Cytokine concentration was quantified in triplicate using R&D Systems Quantikine Mouse IL10, IL12 and Interferon γ ELISA kits. Mean cytokine concentrations ± SEM are shown. Statistical analysis was performed using the unpaired T-test with * representing statistical significance at $p<0.05$, ** representing statistical significance at $p<0.01$, *** representing statistical significance at $p<0.001$ and ns indicating no statistical significance.

The above findings confirm the data using the Meso Scale Discovery multi-spot assay system. Raised pro-inflammatory IL12 and IFNγ levels with WRDD infection; and elevated anti-inflammatory IL10 levels with VVL15 infection. Again this is suggestive of a greater pro-inflammatory response as a result of the WRDD infection leading to increased viral clearance and diminished anti-tumour potency.

5.7 Chapter Conclusions

- Assessment of several pro-inflammatory cytokines, including IL12, IFNγ, and TNFα, demonstrated a greater pro-inflammatory response to WRDD treatment both locally and systemically in an immunocompetent CMT93flank tumour model following IT virus delivery compared to VVL15.
- Assessment of the anti-inflammatory cytokine IL10 showed higher levels locally and systemically with VVL15 treatment in an immunocompetent CMT93flank tumour model following IT virus delivery compared to WRDD.

6. Results: Effect of IL10 expression on Lister strain anti-tumour efficacy and biodistribution.

The above data are suggestive of reduced induction of a pro-inflammatory response following Lister strain vaccinia virus treatment compared to Western Reserve. The consequences are reduced viral clearance and improved anti-tumour efficacy *in vivo*, as demonstrated by biodistribution, biological time-points and efficacy studies. Therefore to further improve Lister strain anti-tumour efficacy it was proposed to insert a murine IL10 gene into the VVL15 genome. It has been shown elsewhere that IL10 expressed by an adenovirus can inhibit peritoneal gastric cancer spread. [157]

Therefore a TK-deleted Lister strain vaccinia virus expressing murine IL10 (VVIL10), already demonstrated to reduce the incidence of auto-immune diabetes in a mouse model, [240] was provided by a collaborator.

6.1. Confirmation of expression of the IL10 transgene in VVIL10 and determination of IL10 expression by VVL15 infection using ELISA.

Firstly expression of the IL10 transgene by VVIL10 was confirmed by ELISA of CMT93, PT45 and SCCCVII tissue culture lysates infected with VVIL10, VVL15 and mock infection as controls. WRDD was also included to confirm that no endogenous IL10 was produced by this strain.

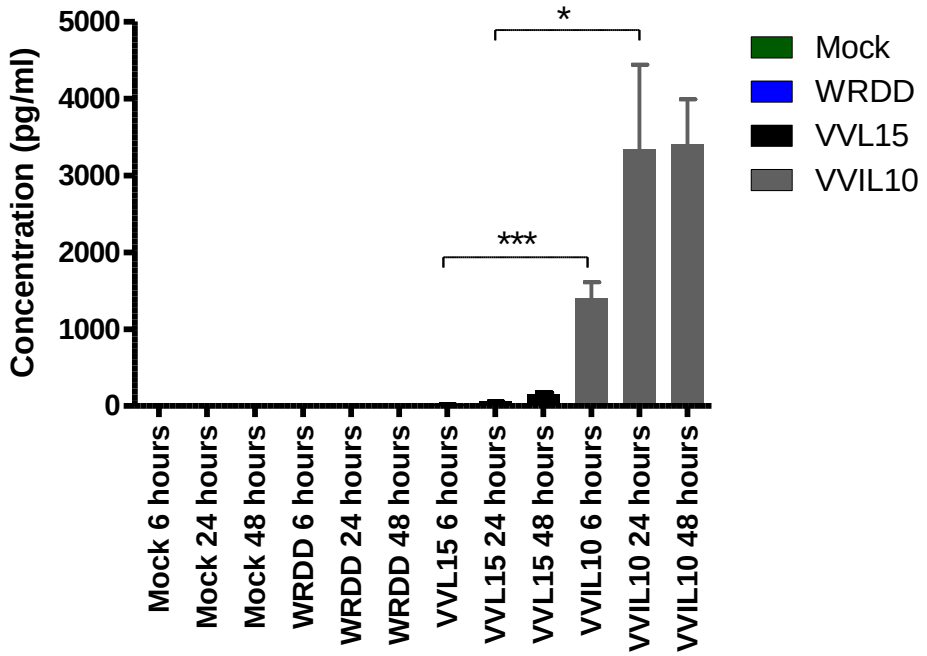

Figure 32. IL10 expression of CMT93 cells infected with VVL15 and VVIL10 at 6, 24 and 48 hours post-infection. 2 x10^5 CMT93 cells per 2ml well were infected with MOI 5 PFU/ml of VVL15, WRDD or VVIL10. Cells and supernatants were harvested at 6, 24 and 48 hours post-infection. Samples were repeatedly freeze-thawed and IL10 expression was quantified using a murine IL10 ELISA. Mean IL10 concentration ± SEM are shown. Statistical analysis of IL10 concentration at stated time-points was performed using the unpaired T-test with * representing statistical significance at $p<0.05$, ** representing statistical significance at $p<0.01$, *** representing statistical significance at $p<0.001$ and ns indicating no statistical significance.

Expression of the IL10 transgene in VVIL10 and to a lesser extent VVL15 was confirmed in the CMT93 cell line. No endogenous IL10 expression by uninfected CMT93 cells was found; nor following WRDD treatment.

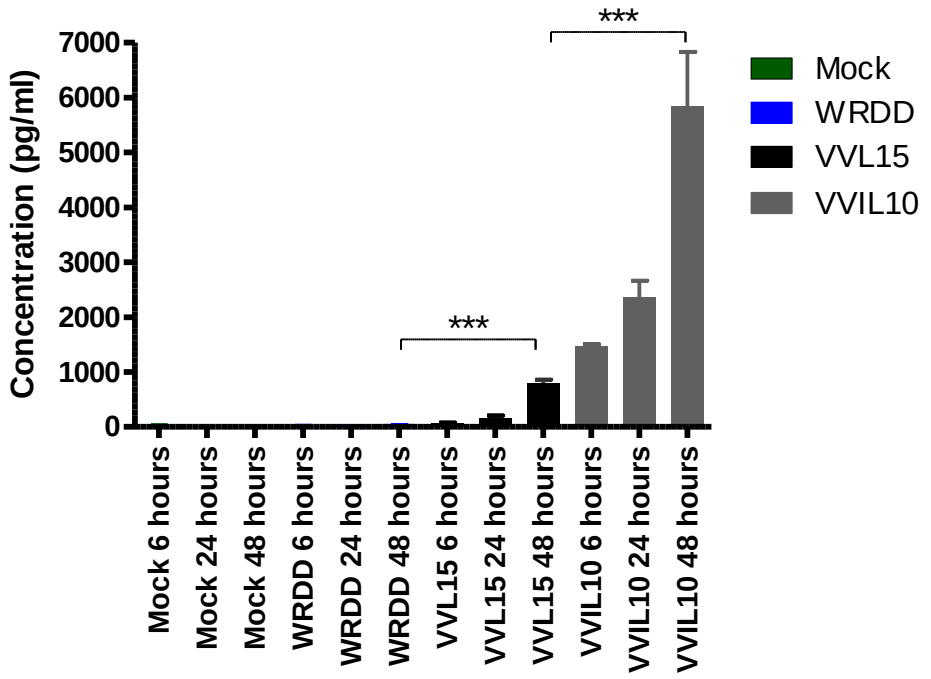

Figure 33. IL10 expression of PT45 cells infected with VVL15 and VVIL10 at 6, 24 and 48 hours post-infection. 2 x10^5 PT45 cells per 2ml well were infected with MOI 5 PFU/ml of VVL15, WRDD or VVIL10. Cells and supernatants were harvested at 6, 24 and 48 hours post-infection. Samples were repeatedly freeze-thawed and IL10 expression was quantified using a murine IL10 ELISA. Mean IL10 concentration ± SEM are shown. Statistical analysis of IL10 concentration at stated time-points was performed using the unpaired T-test with * representing statistical significance at $p<0.05$, ** representing statistical significance at $p<0.01$, *** representing statistical significance at $p<0.001$ and ns indicating no statistical significance.

This experiment measured murine IL10 expression in a human pancreatic cancer cell line. The antibody against murine IL10 detected a signal from samples infected with VVIL10 and to a lesser extent those infected with VVL15. Therefore the measured IL10 was made by the virus rather than the cancer cells themselves in response to the virus. VVIL10 has a murine IL10 gene and therefore would be expected to be detected by a murine-specific ELISA. VVL15 must encode an IL10 homologue that shows sufficient homology to murine IL10 to be detected by the ELISA. This viral IL10 homologue was absent from WRDD vaccinia virus.

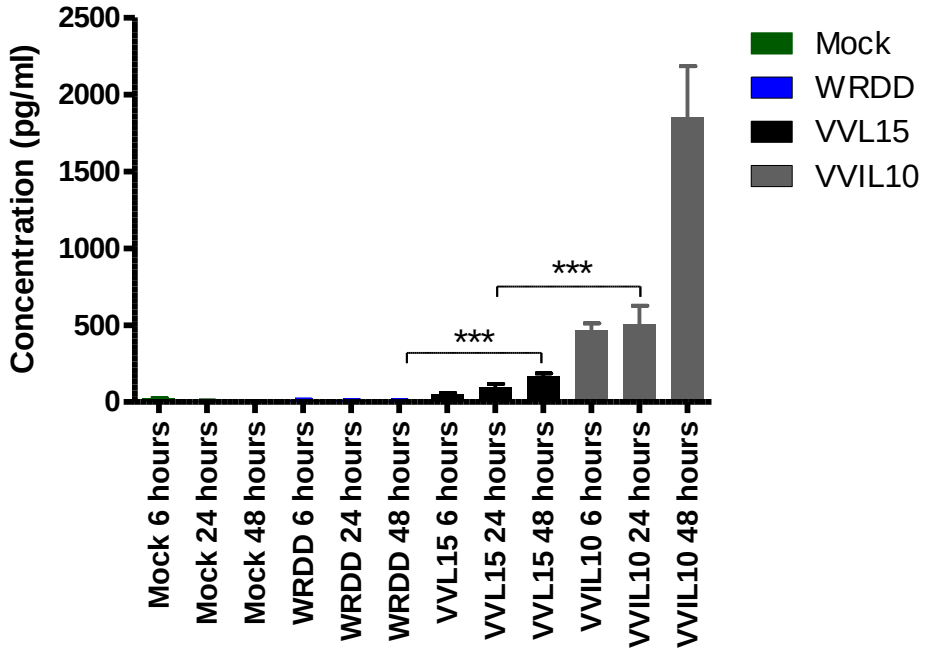

Figure 34. IL10 expression of SCCVII infected with VVL15 and VVIL10 at 6, 24 and 48 hours post-infection. 1 x10^5 SCCVII cells per 2ml well were infected with MOI 5 PFU/ml of VVL15, WRDD or VVIL10. Cells and supernatants were harvested at 6, 24 and 48 hours post infection. Samples were repeatedly freeze-thawed and IL10 expression was quantified using a murine IL10 ELISA. Mean IL10 concentration ± SEM are shown. Statistical analysis of IL10 concentration at stated time-points was performed using the unpaired T-test with * representing statistical significance at $p<0.05$, ** representing statistical significance at $p<0.01$, *** representing statistical significance at $p<0.001$ and ns indicating no statistical significance.

IL10 expression was further confirmed in the murine HNSCC cancer cell line SCCVII after infection with VVL15 and VVIL10.

6.2. Anti-tumour potency of VVL15 and VVIL10 Lister strain vaccinia virus mutants in a selection of cancer cell lines.

The effect of IL10 expression on *in vitro* cytotoxicity was determined using the MTS cell proliferation assay, as before, in a number of murine cancer cell lines and two human cancer cell lines (PT45, MKN45) from multiple organ sites.

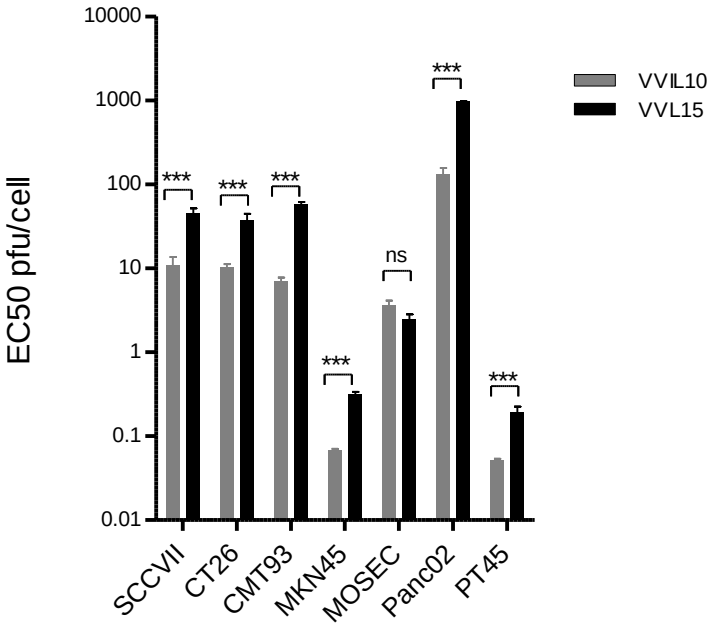

Figure 35. Anti-tumour potency of VVL15 and VVIL10 in panel of cancer cell lines. Comparison of mean EC_{50} values ± SEM generated from sextuplicate MTS cell proliferation assays 6 days after infection; 1000 cells per well and an MOI of 1000 PFU/cell. Statistical analysis was using the unpaired T-test with * representing statistical significance at $p<0.05$, ** representing statistical significance at $p<0.01$, * representing statistical significance at $p<0.001$ and ns indicating no statistical significance.

Of the seven cell lines tested, all of which are murine except MKN45 and PT45, VVIL10 demonstrated greater or equivalent antitumour potency to VVL15.

6.3. Comparison of the viral replication of VVL15 and VVIL10 in a selection of cancer cell lines.

As before when comparing the anti-tumour potency of VVL15 and WRDD, MTS cell proliferation data was compared with viral replication data.

Tumour type	Cell line	VVL15		VVIL10	
		Viral Replication (PFU/cell)	SEM	Viral Replication (PFU/cell)	SEM
HNSCC	SCCVII	**201.30**	70.87	23.70	5.68
Pancreatic	PT45	**1042.95**	242.83	229.81	56.87
	Panc02	60.11	7.08	**84.52**	7.40
Gastro intestinal	CMT93	**142.43**	31.56	80.04	23.74
	CT26	**94.21**	23.73	20.55	6.40

Table 14. Viral replication of VVL15 and VVIL10 vaccinia virus in a panel of human and murine tumour cell lines. Burst assays were infected with 1 PFU/cell of virus ($2x10^5$ cells per well). Cell lysates were harvested at 24 hour intervals typically up to 96 hours. Mean viral replication at 72 hours ± SEM was determined by $TCID_{50}$ assay on CV1 cells are tabulated. Grey shaded cells are murine cell lines; white cells are human cell lines. Bold figures represent the most potent virus overall; underlined figures represent the most potent virus comparing VVL15 and WRDD. Where two viruses are highlighted, they are jointly most potent statistically (i.e. no statistically significant difference).

With the exception of Panc02, VVIL10 demonstrated inferior viral replication compared to VVL15. Panc02 is a very aggressive cancer cell line with a short doubling time. Microscopy of the six well plates following viral infection of PT45 and Panc02 cells prior to cell scraping and cell lysis, showed increased cell death in the VVIL10-treated wells compared to those treated VVL15 (Figures 36. and 37.). Reduced numbers of viable cells results in reduced viral replication as the virus life cycle is dependent on living cells. In cancer cell lines with very high multiplication rate, such as Panc02, cell death does not limit viral replication as there is a plentiful supply of viable cells to support virus progeny.

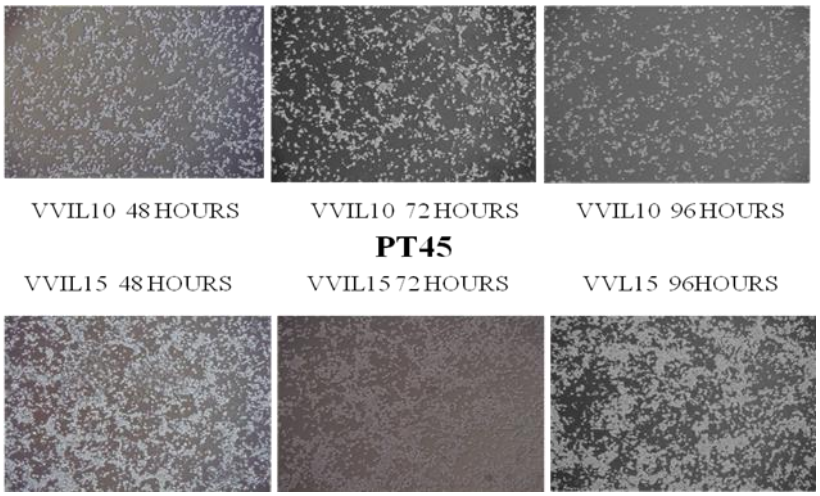

Figure 36. Microscopy of PT45 viral replication 6-well plates infected with VVIL10 and VVL15. $2x10^5$ PT45 cells were seeded in 2ml 6-well plates and infected with VVL15 and VVIL10 (MOI = 1 PFU/ml). Microscopy of plates was performed at 48, 72 and 96 hours post infection. Representative micrographs are shown at 40x magnification.

Figure 37. Microscopy of Panc02 viral replication 6-well plates infected with VVIL10 and VVL15. $2x10^5$ Panc02 cells were seeded in 2ml 6-well plates and infected with VVL15 and VVIL10 (MOI = 1 PFU/ml). Microscopy of plates was performed at 48, 72 and 96 hours post infection. Representative micrographs are shown at 40x magnification.

6.4. Anti-tumour potency of VVL15 and VVIL10 vaccinia virus mutants in a mouse colorectal carcinoma CMT93 nude mouse model.

Having established enhanced anti-tumour potency of VVIL10 over VVL15 *in vitro*, potency was assessed in nude and immunocompetent mouse tumour models.

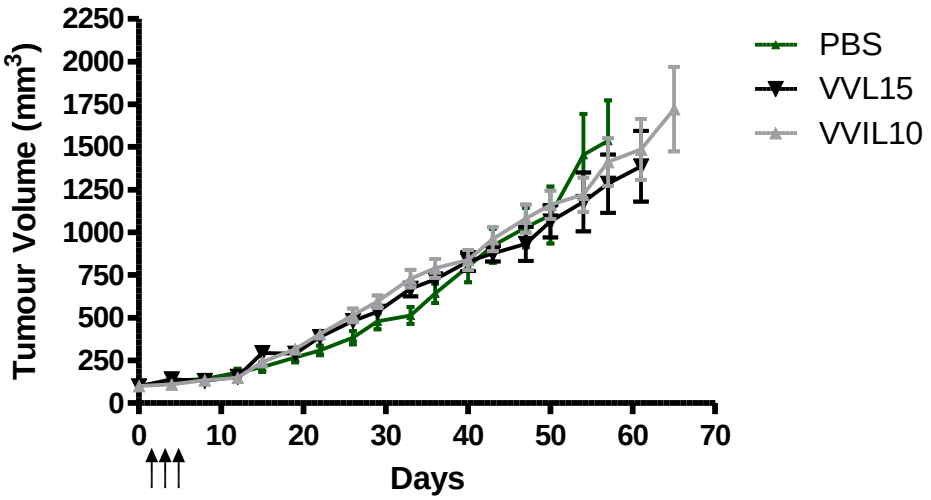

Figure 38a. Growth of established murine colorectal tumours in nude mice after treatment with different vaccinia virus mutants. $5x10^6$ CMT93 cells were seeded by subcutaneous injection into the right flank of 30 ICRF nu/nu mice. When tumours reached 4-5mm in diameter, 10 mice each received IT injections of PBS, VVL15 or VVIL10 on days 1,3,5 (3 x $1x10^7$ PFU). Tumours were measured twice weekly. Mean tumour sizes ± SEM are displayed until the death of the first mouse in each group. Statistical analysis of tumour sizes at stated time-points was performed using the unpaired T-test with * representing statistical significance at $p<0.05$, ** representing statistical significance at $p<0.01$, *** representing statistical significance at $p<0.001$ and ns indicating no statistical significance.

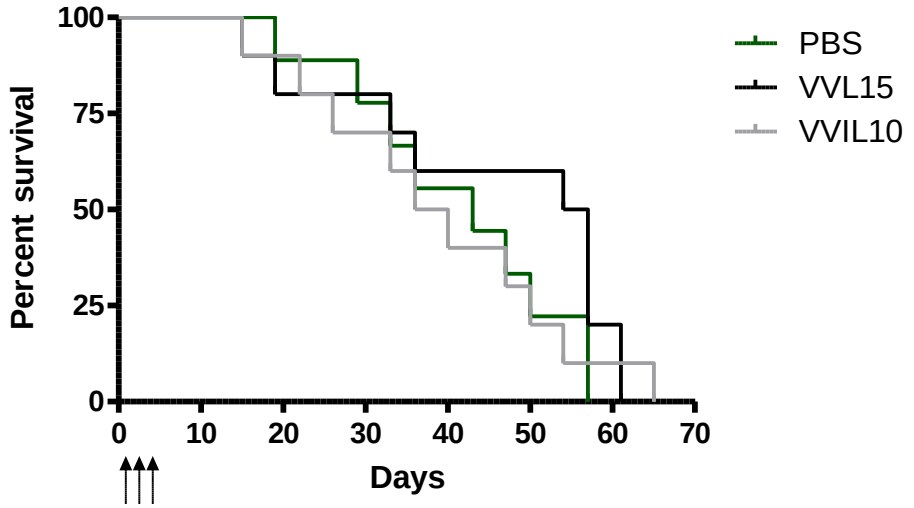

Figure 38b. Animal survival of nude mice bearing established murine colorectal tumours after treatment with different vaccinia virus mutants. $5x10^6$ CMT93 cells were seeded by subcutaneous injection into the right flank of 30 ICRF nu/nu mice. When tumours reached 4-5mm in diameter, 10 mice each received IT injections of PBS, VVL15 or VVIL10 on days 1,3,5 (3 x $1x10^7$ PFU). Kaplan-Meier curves are shown. Log-rank test curve statistical analysis showed no significance between all 3 data sets.

In the nude mouse CMT93 model no difference in animal survival or tumour progression was noted between the virus-treated animals and those subjected to mock infections with PBS.

6.5. Anti-tumour potency of VVL15 and VVIL10 vaccinia virus mutants in a mouse colorectal carcinoma CMT93 immunocompetent mouse model.

To assess the anti-tumour potency efficacy studies were performed using a C57BL/6 immunocompetent mouse model. CMT93 flank tumours were grown and viruses ($1x10^8$) were administered IT on a 3 day (days 1,3,5) and 5 day (1,2,3,4,5) injection regime. Our hypothesis was that the anti-tumour effect would be enhanced with the 5 day injection regime; whilst being well tolerated by the mice.

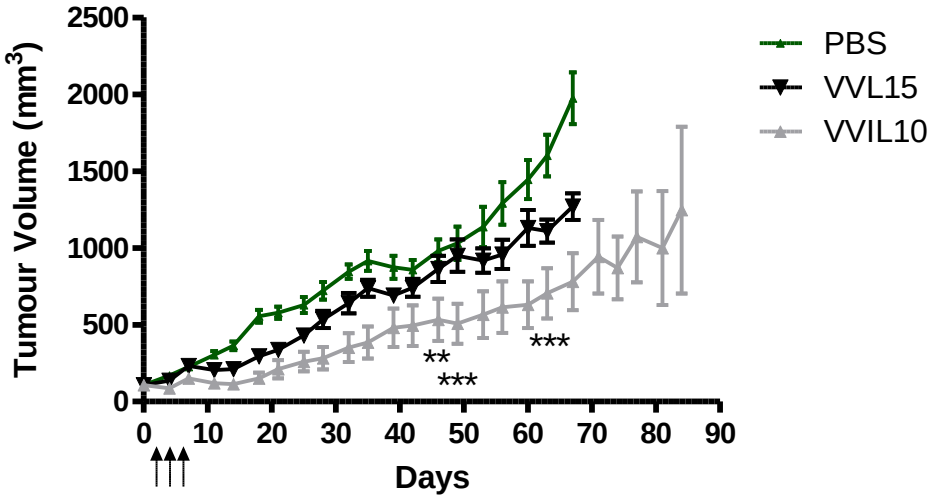

Figure 39a. Growth of established murine colorectal tumours in immunocompetent mice after treatment with different vaccinia virus mutants. $5x10^6$ CMT93 cells were seeded by subcutaneous injection into the right flank of 30 C57BL/6 mice. When tumours reached 4-5mm in diameter, 10 mice each received IT injections of PBS, VVL15 or VVIL10 (3 x $1x10^8$ PFU) on days 1,3,5. Tumours were measured twice weekly. Mean tumour sizes ± SEM are displayed until the death of the first mouse in each group. Statistical analysis of tumour sizes at stated time-points was performed using the unpaired T-test with * representing statistical significance at $p<0.05$, ** representing statistical significance at $p<0.01$, *** representing statistical significance at $p<0.001$ and ns indicating no statistical significance.

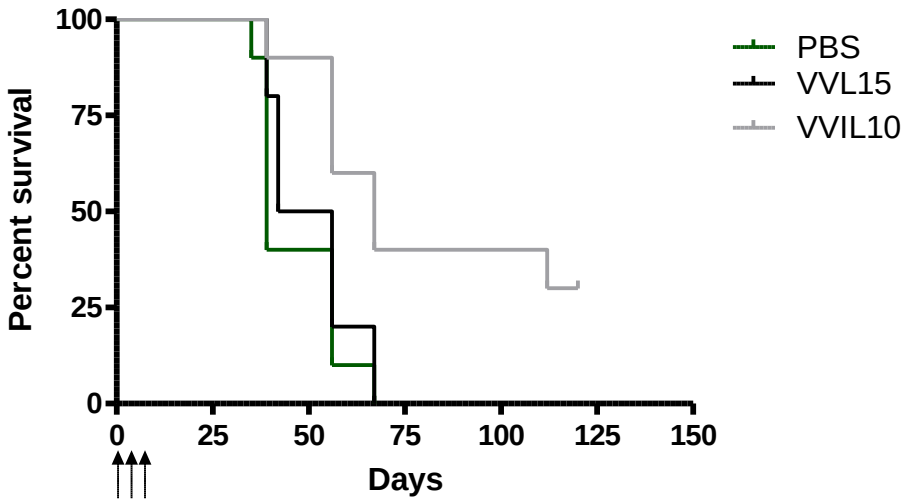

Figure 39b. Animal survival of immunocompetent mice bearing established murine colorectal tumours after treatment with different vaccinia virus mutants.

$5x10^6$ CMT93 cells were seeded by subcutaneous injection into the right flank of 30 C57BL/6 mice. When tumours reached 4-5mm in diameter, 10 mice each received IT injections of PBS, VVL15 or VVIL10 (3 x $1x10^8$ PFU) on days 1,3,5. Tumours were measured twice weekly. Kaplan-Meier curves are shown. Log-rank test curve statistical analysis showed significance at the 0.1% level between PBS and VVL15 data sets; and at the 5% level between VVL15 and VVIL10.

In the immunocompetent model, statistically significant differences in tumour growth were noted between the PBS, VVL15 and VVIL10 treatment regimes. The VVIL10 treated mice showed reduced tumour progression and enhanced survival compared to PBS and VVL15.

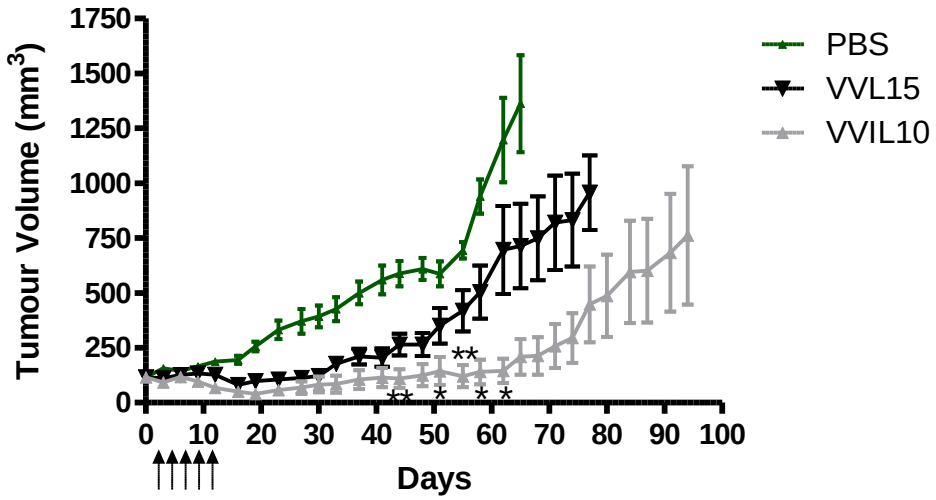

Figure 40a. Growth of established murine colorectal tumours in immunocompetent mice after treatment with different vaccinia virus mutants. $5x10^6$ CMT93 cells were seeded by subcutaneous injection into the right flank of 30 C57BL/6 mice. When tumours reached 4-5mm in diameter, 10 mice each received IT injections of PBS, VVL15 or VVIL10 (5 x $1x10^8$ PFU) on days 1,2,3,4,5. Tumours were measured twice weekly. Mean tumour sizes ± SEM are displayed until the death of the first mouse in each group. Statistical analysis of tumour sizes at stated time-points was performed using the unpaired T-test with * representing statistical significance at $p<0.05$, ** representing statistical significance at $p<0.01$, *** representing statistical significance at $p<0.001$ and ns indicating no statistical significance.

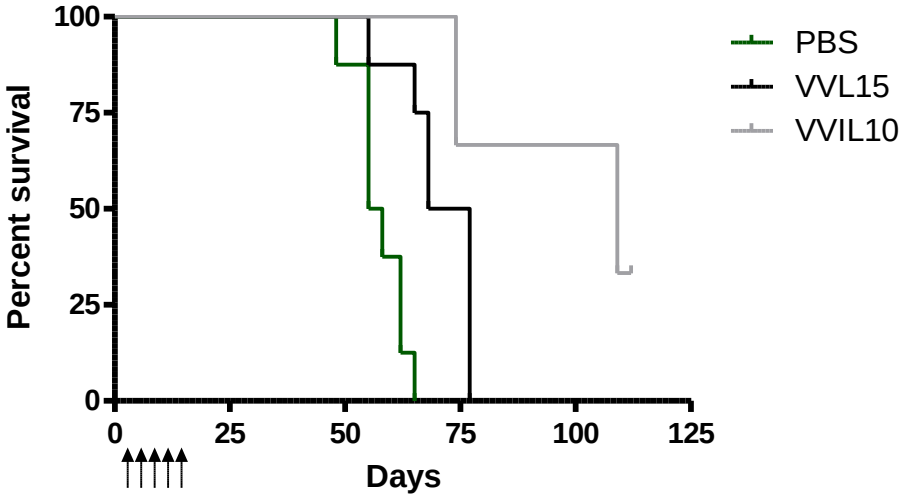

Figure 40b. Animal survival of immunocompetent mice bearing established murine colorectal tumours after treatment with different vaccinia virus mutants. $5x10^6$ CMT93 cells were seeded by subcutaneous injection into the right flank of 30 C57BL/6 mice. When tumours reached 4-5mm in diameter, 10 mice each received IT injections of PBS, VVL15 or VVIL10 (5 x $1x10^8$ PFU) on days 1,2,3,4,5. Kaplan-Meier curves are shown. Log-rank test curve statistical analysis showed significance at the 5% level between VVL15 vs PBS and at the 1% level between VVL15 and VVIL10 data sets.

With the five-day regime of injections reduced tumour progression was again noted with the VVIL10-treated group; indeed 6/10 animals showed complete tumour regression.

6.6. Anti-tumour potency of VVL15 and VVIL10 vaccinia virus mutants in a mouse colorectal carcinoma CT26 immunocompetent mouse model.

Having demonstrated reduced tumour progression with VVIL10-treated mice in the immunocompetent CMT93 models compared to VVL15, virus anti-tumour efficacy was investigated in a further immunocompetent model.

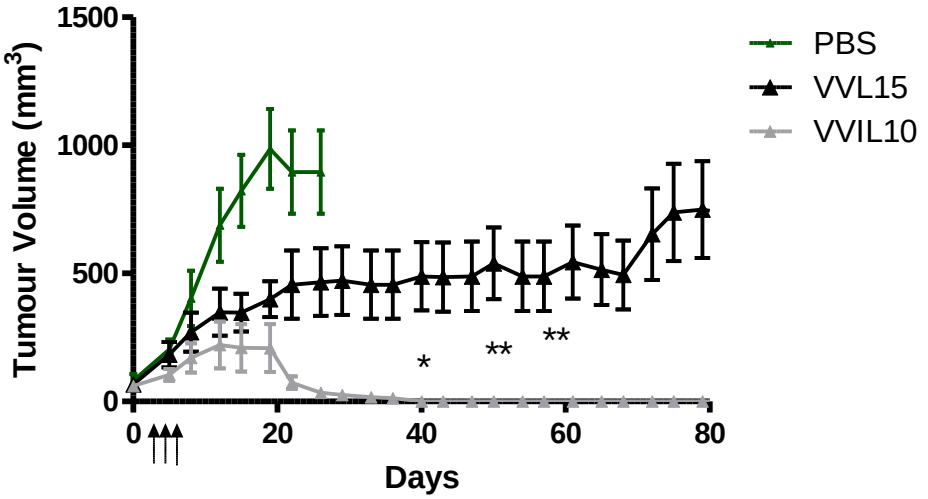

Figure 41a. Growth of established murine colorectal tumours in immunocompetent mice after treatment with different vaccinia virus mutants. $1x10^6$ CT26 cells were seeded by subcutaneous injection into the right flank of 30 BALB/c immunocompetent mice. When tumours reached 4-5mm in diameter, 10 mice each received IT injections of PBS, VVIL10 or VVL15 on days 1,3,5 (3 x $1x10^8$ PFU). Tumours were measured twice weekly. Mean tumour sizes ± SEM are displayed until the death of the first mouse in each group. Statistical analysis of tumour sizes at stated time-points was performed using the unpaired T-test with * representing statistical significance at $p<0.05$, ** representing statistical significance at $p<0.01$, *** representing statistical significance at $p<0.001$ and ns indicating no statistical significance.

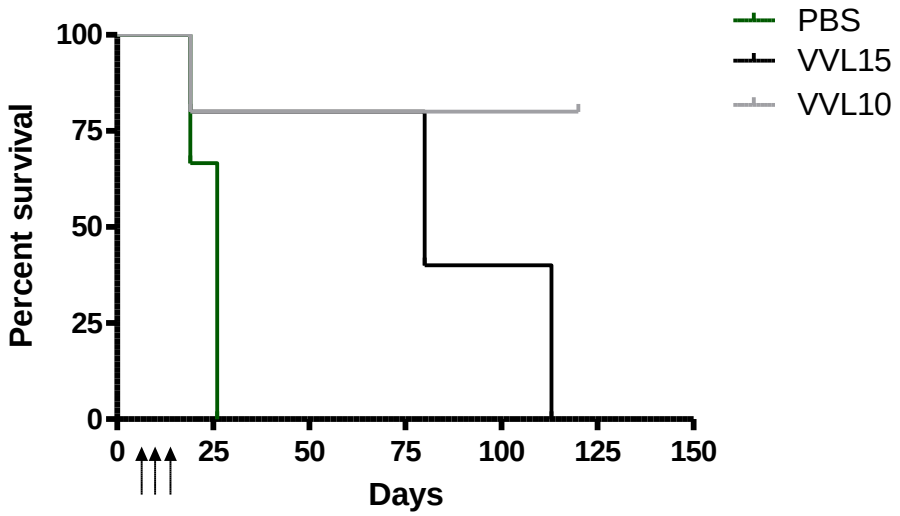

Figure 41b. Animal survival of immunocompetent mice bearing established murine colorectal tumours after treatment with different vaccinia virus mutants. $1x10^6$ CT26 cells were seeded by subcutaneous injection into the right flank of 30 BALB/c immunocompetent mice. When tumours reached 4-5mm in diameter, 10 mice each received IT injections of PBS, VVIL10 or VVL15 on days 1,3,5 (3 x $1x10^8$ PFU). Kaplan-Meier curves are shown. . Log-rank test curve statistical analysis showed significance at the 0.1% level between VVL15 and VVIL10 treated mice, and at the 1% level between VVL15 and PBS.

In a different immunocompetent model, CT26 colorectal carcinoma, statistically significant differences in tumour progression between VVL15- and VVIL10-treated mice were again recorded. VVIL10 treated m ice showed marked tumour regression and prolonged animal survival.

6.7. Anti-tumour potency of VVL15 and VVIL10 vaccinia virus mutants in a human pancreatic carcinoma PT45 nude mouse model.

VVIL10 anti-tumour potency was further investigated in the model of human pancreatic PT45 flank tumours in ICRF nu/nu mice.

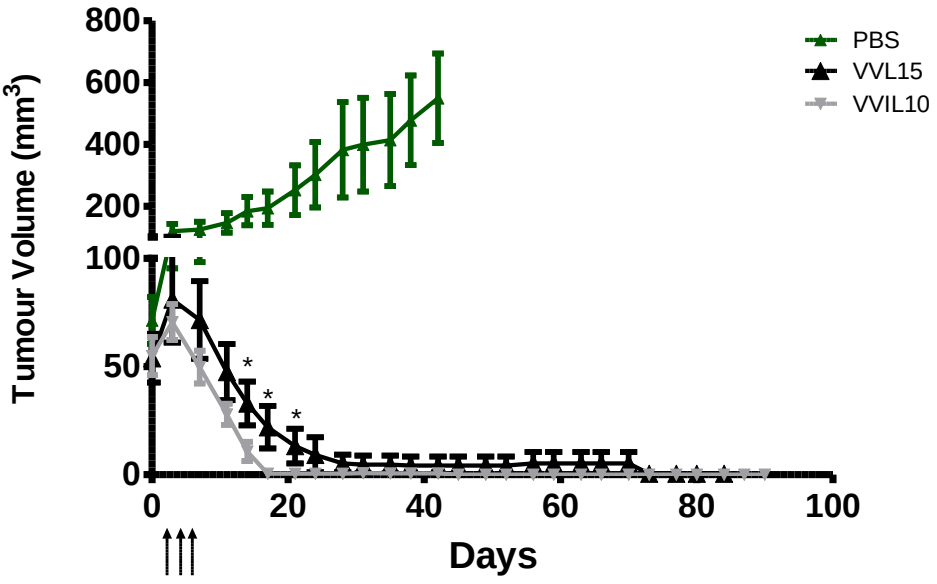

Figure 42a. Growth of established human pancreatic tumours in nude mice after treatment with different vaccinia virus mutants. $5x10^6$ PT45 cells were seeded by

subcutaneous injection into the right flank of 30 ICRF nude mice. When tumours reached 4-5mm in diameter, 10 mice each received IT injections of PBS, VVIL10 or VVL15 on days 1,3,5 (3 x $1x10^7$ PFU). Tumours were measured twice weekly. Mean tumour sizes ± SEM are displayed until the death of the first mouse in each group. Statistical analysis of tumour sizes at stated time-points was performed using the unpaired T-test with * representing statistical significance at $p<0.05$, ** representing statistical significance at $p<0.01$, *** representing statistical significance at $p<0.001$ and ns indicating no statistical significance.

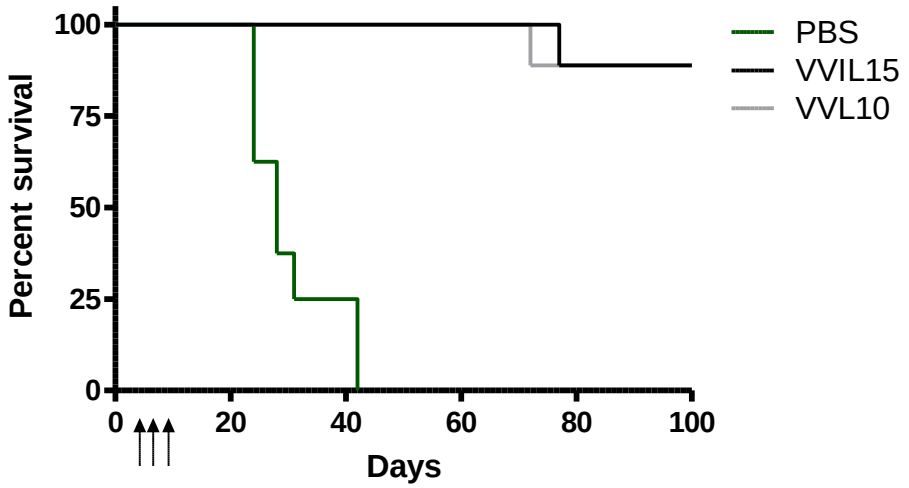

Figure 42b. Animal survival of nude mice bearing established human pancreatic tumours after treatment with different vaccinia virus mutants. $5x10^6$ PT45 cells were seeded by subcutaneous injection into the right flank of 30 ICRF nude mice. When tumours reached 4-5mm in diameter, 10 mice each received IT injections of PBS, VVIL10 and VVL15 on days 1,3,5 (3 x $1x10^7$ PFU). Kaplan-Meier curves are shown. Log-rank test curve statistical analysis showed significance at the 0.1% level between PBS and VVL15 & VVIL10 data sets.

Marked tumour regression was demonstrated in the virus treated groups; with all tumours becoming virtually undetectable after 17 days. VVIL10 treated mice showed more enhanced tumour regression compared to VVL15 treated mice during the first 17 days of the experiment.

6.8. Biodistribution of VVL15 and VVIL10 vaccinia virus mutants in immunocompetent C57BL/6 mice bearing flank CMT93 tumours, as determined by qRT-PCR.

As before the behaviour of the virus in a mouse model was assessed through biodistribution studies in immunocompetent mice bearing CMT93 flank tumours. A single tail vein injection was used to deliver the viruses and control. Tumours and organs were harvested at specific time-points and subjected to virus quantification using qRT-PCR; which I have previously validated as an accurate method of virus measurement.

Tumour Site	**PBS**		**VVL15**		**VVIL10**	
	Viral Recovery (PFU/ml/g)	**SEM**	**Viral Recovery** (PFU/ml/g)	**SEM**	**Viral Recovery** (PFU/ml/g)	**SEM**
Tumour	0	0	23237.07	8439.10	282895.700	129522.5
Ovary	0	0	26.13	2.398	33.361	7.319
Lung	0	0	4292.67	691.937	285.553	47.499
Liver	0	0	166.99	34.239	126.608	28.974
Spleen	0	0	78.04	18.0735	19.363	1.9812
Brain	0	0	0	0	0	0
Bone Marrow	0	0	130.96	51.817	5.402	5.402

Table 15. Vaccinia virus genome copy number of harvested CMT93 tumours in C57BL/6 immunocompetent mice following IV vaccinia virus treatment. $5x10^6$ CMT93 cells were seeded by subcutaneous injection into the right flank of 36 C57BL/6 immunocompetent mice. When tumours reached 4-5mm in diameter, 12 mice each received single IV injections of PBS, VVIL10 or VVL15 (2×10^8 PFU). On days 4, 8, and 12 four mice from each group were sacrificed and the tumours were harvested and frozen. Samples were then homogenised and repeatedly freeze-thawed. Lysates underwent DNA extraction. Mean viral genome copy numbers ± SEM were determined by qRT-PCR using the vaccinia late gene (VLTF-1); data for day 8 are tabulated.

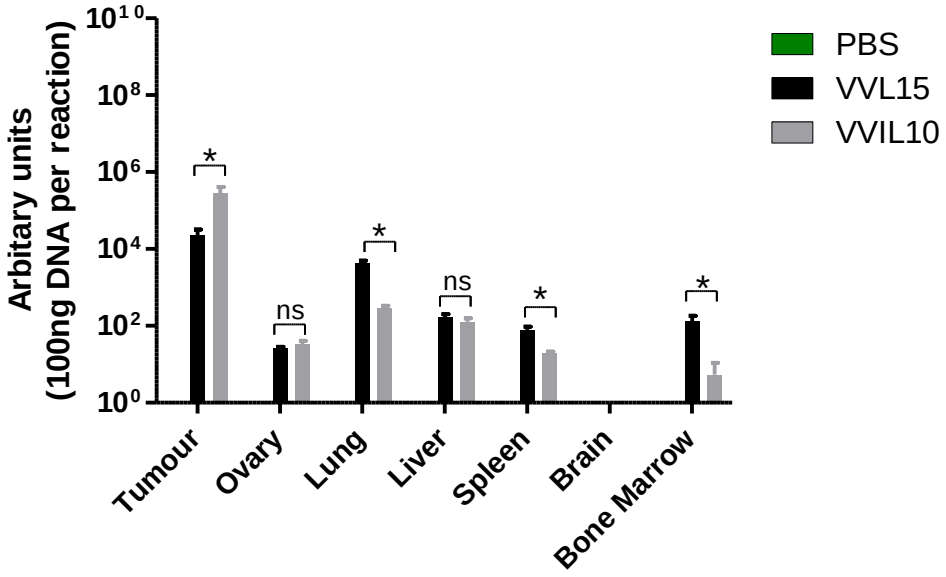

Figure 43. Vaccinia virus genome copy number of harvested CMT93 tumours in C57BL/6 immunocompetent mice following IV vaccinia virus treatment. $5x10^6$ CMT93 cells were seeded by subcutaneous injection into the right flank of 36 C57BL/6 immunocompetent mice. When tumours reached 4-5mm in diameter, 12 mice each received single IV injections of PBS, VVIL10 or VVL15 (2×10^8 PFU). On days 4, 8, and 12 four mice from each group were sacrificed and the tumours were harvested and frozen. Samples were then homogenised and repeatedly freeze-thawed. Lysates underwent DNA extraction. Mean viral genome copy numbers ± SEM were determined by qRT-PCR using the vaccinia late gene (VLTF-1); data for day 8 are shown. Statistical analysis of viral genome copy number at stated time-points was performed using the unpaired T-test with * representing statistical significance at $p<0.05$, ** representing statistical significance at $p<0.01$, *** representing statistical significance at $p<0.001$ and ns indicating no statistical significance.

VVIL10 biodistribution in a CMT93 flank tumour immunocompetent model demonstrated significantly higher viral replication in the tumours, with equivalent levels in the ovaries and liver, and reduced levels in the bone marrow, lungs and spleen. Therefore not only is VVIL10 likely to be more efficacious than VVL15 due to higher achieved tumour concentrations following systemic delivery, the side effect profile is likely to be better due to reduced viral titres in the bone marrow, lungs and spleen.

6.9. Biological time-points of vaccinia virus mutants in C57BL/6 immunocompetent mice bearing CMT93 flank tumours determined by qRT-PCR.

Following assessment of VVL15 and VVIL10 biodistribution in an immunocompetent murine tumour model, investigation into the behaviour of IT delivered viruses was examined.

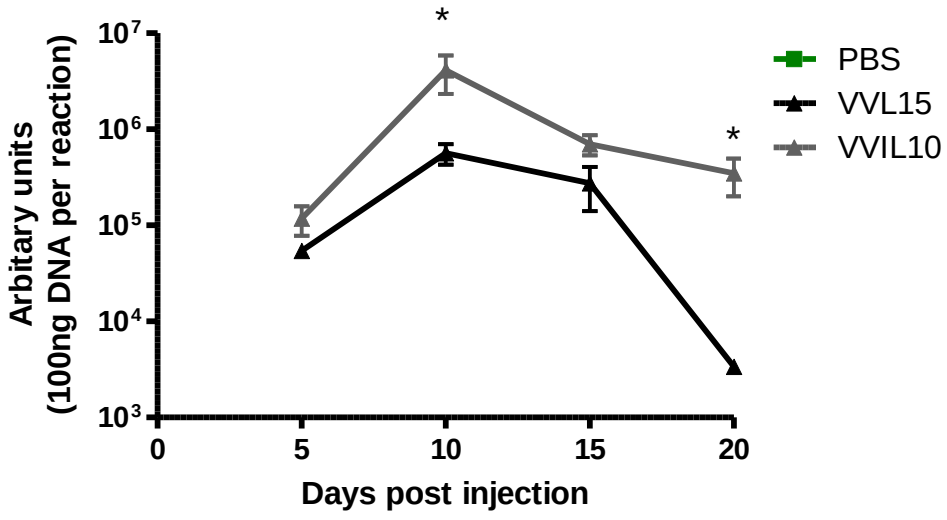

Figure 44. Vaccinia virus genome copy number of harvested tumours in C57BL/6 immunocompetent mice bearing CMT93 flank tumours following IT vaccinia virus treatment. $5x10^6$ CMT93 cells were seeded by subcutaneous injection into the right flank of 36 C57BL/6 immunocompetent mice. When tumours reached 4-5mm in diameter, 12 mice each received single IT injections of PBS, VVIL10 or VVL15 (3 x

1x10^8 PFU). On days 5, 10, 15 and 20 three mice from each group were sacrificed and the tumours were harvested and frozen. Samples were then homogenised and repeatedly freeze-thawed. Lysates underwent DNA extraction. Mean viral genome copy numbers ± SEM were determined by qRT-PCR using the vaccinia late gene (VLTF-1). Statistical analysis of viral genome copy number at stated time-points was performed using the unpaired T-test with * representing statistical significance at $p<0.05$, ** representing statistical significance at $p<0.01$, *** representing statistical significance at $p<0.001$ and ns indicating no statistical significance.

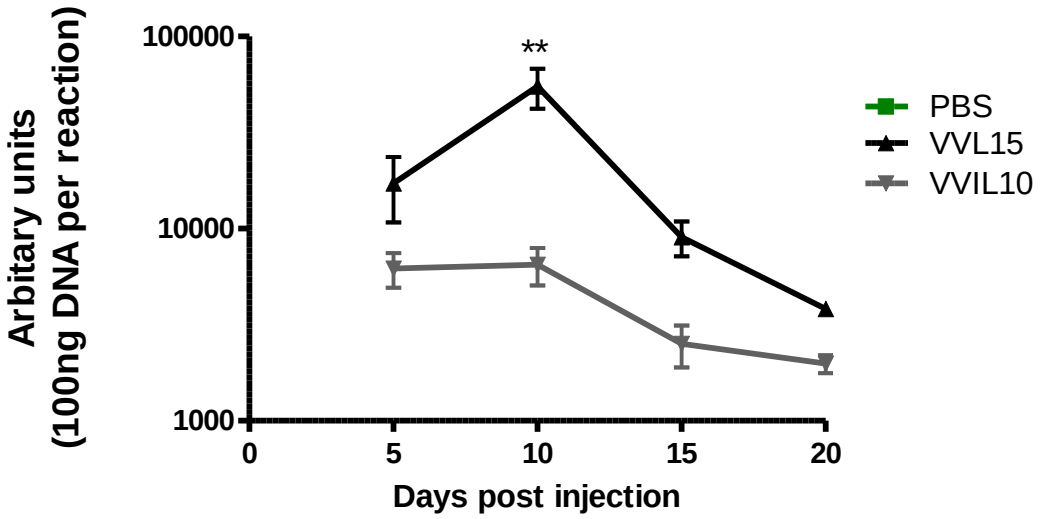

Figure 45. Vaccinia virus genome copy number of harvested ovaries in C57BL/6 immunocompetent mice bearing CMT93 flank tumours following IT vaccinia virus treatment. 5x10^6 CMT93 cells were seeded by subcutaneous injection into the right flank of 36 C57BL/6 immunocompetent mice. When tumours reached 4-5mm in diameter, 12 mice each received single IT injections of PBS, VVIL10 or VVL15 (3 x 1x10^8 PFU). On days 5, 10, 15 and 20 three mice from each group were sacrificed and the ovaries were harvested and frozen. Samples were then homogenised and repeatedly freeze-thawed. Lysates underwent DNA extraction. Mean viral genome copy numbers ± SEM were determined by qRT-PCR using the vaccinia late gene (VLTF-1). Statistical analysis of viral genome copy number at stated time-points was performed using the unpaired T-test with * representing statistical significance at $p<0.05$, ** representing

statistical significance at p<0.01, *** representing statistical significance at p<0.001 and ns indicating no statistical significance.

Biological time-points studies showed that VVIL10 delivered IT replicated better than VVL15 in the flank tumours of immunocompetent mouse. This would explain why better anti-tumour efficacy was demonstrated *in vivo*. VVL15 delivered IT, and to a much lesser extent VVIL10, was able to spread to and replicate within the mouse ovaries.

6.10. Biodistribution of vaccinia virus mutants in nude mice bearing human pancreatic carcinoma PT45 flank tumours determined by qRT-PCR.

Following assessment of VVL15 and VVIL10 biodistribution in immunocompetent murine tumour models, investigation into the biodistribution of the viruses in a model of human cancer was undertaken. The human pancreatic tumour PT45 was chosen and flank tumours in ICRF nu/nu mice were grown.

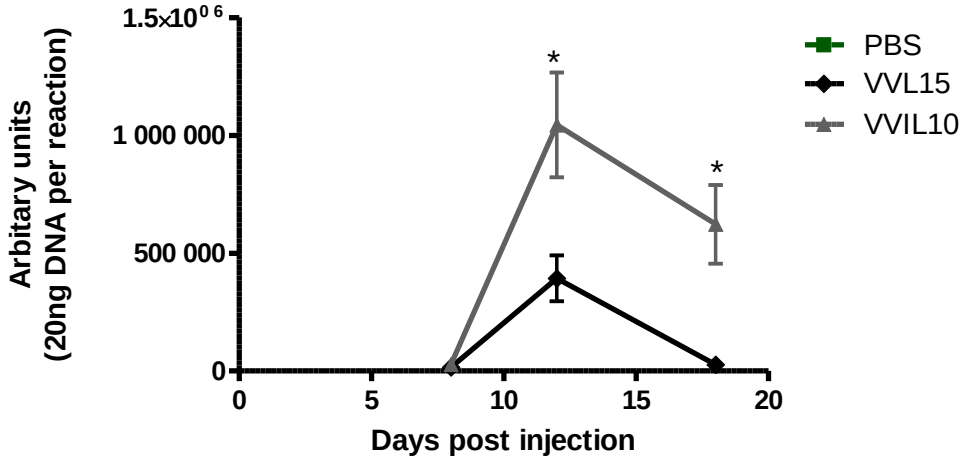

Figure 46. Vaccinia virus genome copy number of harvested tumours in ICRF nu/nu mice bearing PT45 flank tumours following IV vaccinia virus treatment. $5x10^6$ PT45 cells were seeded by subcutaneous injection into the right flank of 27 ICRF nu/nu mice. When tumours reached 4-5mm in diameter, 9 mice each received single IV

injections of PBS, VVIL10 or VVL15 ($1x10^7$ PFU). On days 8, 12 and 18 three mice from each group were sacrificed and the tumours were harvested and frozen. Samples were then homogenised and repeatedly freeze-thawed. Lysates underwent DNA extraction. Mean viral genome copy numbers ± SEM were determined by qRT-PCR using the vaccinia late gene (VLTF-1).

The biodistribution results are in keeping with the PT45 *in vitro* cell proliferation assays, which showed superior anti-tumour potency of VVIL10 over VVL15; and the *in vivo* efficacy studies, where reduced tumour growth and improved animal survival was recorded in a nude model of human pancreatic cancer.

6.11. Biological time-points of vaccinia virus mutants in ICRF nu/nu mice bearing PT45 flank tumours determined by qRT-PCR.

Assessment of viruses delivered IT was also made in the mouse ICRF nu/nu PT45 human pancreatic cancer model.

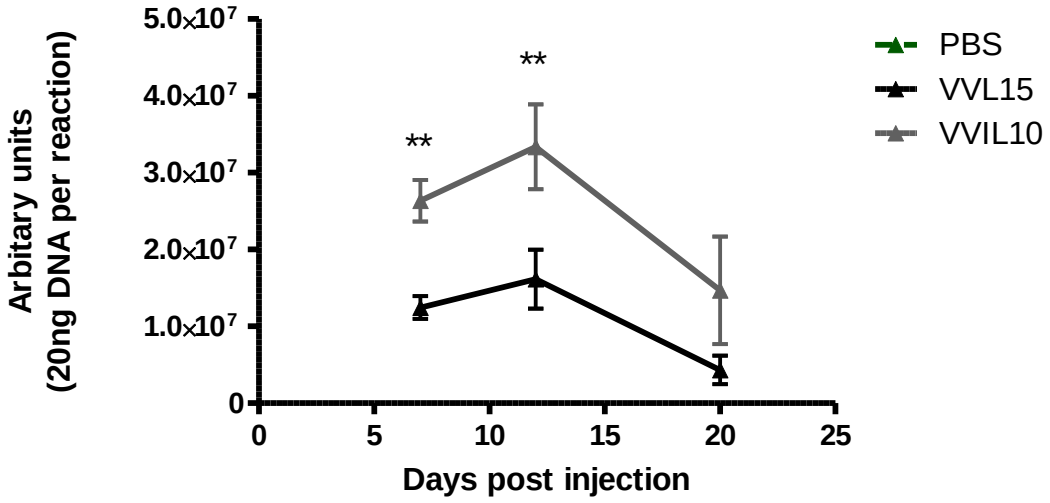

Figure 47. Vaccinia virus genome copy number of harvested tumours in ICRF nu/nu mice bearing PT45 flank tumours following IT vaccinia virus treatment. $5x10^6$ PT45 cells were seeded by subcutaneous injection into the right flank of 30 ICRF nu/nu mice. When tumours reached 4-5mm in diameter, 12 mice each received single IT injections of PBS, VVIL10 or VVL15 (3 x $1x10^7$ PFU). On days 7, 12 and 20 three mice from each group were sacrificed and the tumours were harvested and frozen. Samples were then homogenised and repeatedly freeze-thawed. Lysates underwent

DNA extraction. Mean viral genome copy numbers ± SEM were determined by qRT-PCR using the vaccinia late gene (VLTF-1).

Higher viral titres for VVIL10 were recovered compared to VVL15; indicating that VVIL10 is better able to replicate in cancer cells *in vivo*. This result is in keeping with the *in vitro* cytotoxicity studies, as well as the PT45 efficacy study.

6.12 Chapter Conclusions

- IL10 is expressed at high levels when CMT93. PT45, SCCVII cells are infected with VVIL10, a TK-deleted Lister mutant encoding a murine IL10 gene.
- A lower level of IL10 expression was demonstrated following VVL15 infection of the same cell lines.
- No IL10 expression was demonstrated by WRDD infection of the same cell lines.
- Higher levels of VVL15 were found in cell lines following viral infection compared to VVIL10, except Panc02.
- No differences in tumour progression and animal survival were demonstrated in a nude CMT93 cancer model following IT virus delivery to flank tumours.
- In the immunocompetent model VVIL10 IT treated mice demonstrated reduced tumour progression and improved animal survival compared to VVL15 treated mice bearing CMT93 tumours. This effect was enhanced with five consecutive days of injections ($5 \times 1x10^8$ PFU) compared to three ($3 \times 1x10^8$ PFU).
- Biodistribution data in an immunocompetent murine CMT93 flank tumour model shows higher levels of virus following VVIL10 treatment within the tumours with less off-target virus, compared to VVL15 treated mice. This was also the case with the human PT45nude model following systemic delivery of both viruses..
- Local delivery of viruses to nude and immunocompetent mice bearing PT45 and CMT93 flank tumours respectively, demonstrated higher levels of VVIL10 compared to VVL15 within harvested tumours.

7. Results: Investigation into the mechanism of enhanced VVIL10 anti-tumour potency over VVL15.

Having demonstrated that VVIL10 has greater anti-tumour potency over VVL15 *in vitro* and *in vivo*, possible mechanisms for this observation were then investigated.

7.1. Anti-tumour potency of recombinant IL10 on CMT93 colorectal cancer cell line *in vitro*.

Firstly investigation was made into whether the effect of IL10 on cancer cells was a direct action, independent of the virus. To determine this, CMT93 cells were exposed to murine unconjugated recombinant IL10 (rIL10) at a range of concentrations in an MTS cell proliferation assay.

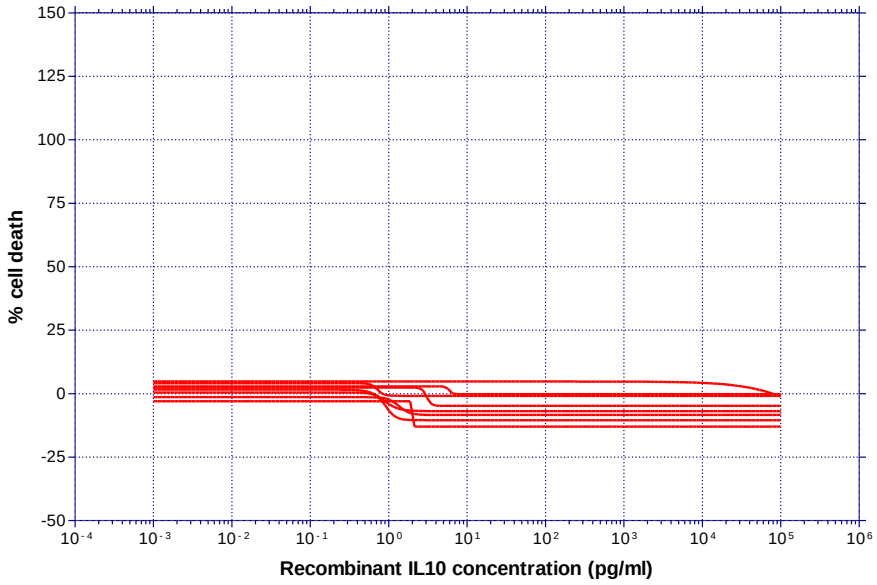

Figure 48. Effect of recombinant IL10 on CMT93 cancer cells. 5000 cells were seeded per well and serial dilutions of recombinant IL10 were applied, with a starting concentration of $1x10^5$pg/ml. Following 3 days of incubation, the viable cells were assayed with MTS reagent and graphed as a dose-response curve using non-linear regression analysis.

No cytopathic effect of recombinant IL10 was demonstrated on CMT93 cells in a concentration range 0.001 - $1x10^5$pg/ml. This corroborates data from another group that used rIL10 directly applied to CT26 cells, with a concentration range from 800 – $3x10^6$pg/ml, with no effect on cell proliferation. [59]

7.2. Anti-tumour potency of recombinant IL10 in conjunction with VVL15 compared to VVL15 and VVIL10 alone infected CMT93 colorectal cancer cells.

As no cytopathic effect was observed with recombinant IL10 directly applied to cancer cells, it was investigated whether an effect would be demonstrated in conjunction with viruses. Specifically I sought to determine if rIL10 and VVL15 was able to result in equivalent cytotoxicity to VVIL10.

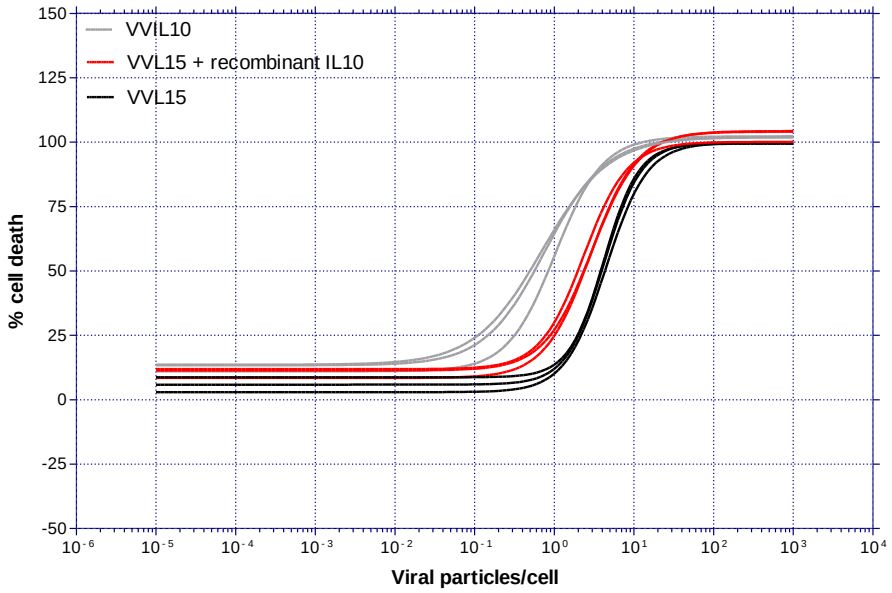

Figure 49. Anti-tumour potency of recombinant IL10 in conjunction with VVL15 compared to VVL15 and VVIL0 alone infected CMT93 colorectal cancer cells. 5000 CMT93 cells were seeded per well and infected with vaccinia virus at a series of increasing MOI (highest MOI of 1000 PFU/cell). Recombinant IL10 ($1x10^6$pg/ml) was added to the VVL15 + rIL10 group wells immediately prior to infection. Following 3 days of incubation, cell proliferation MTS assays were performed and the results graphed as a dose-response curve.

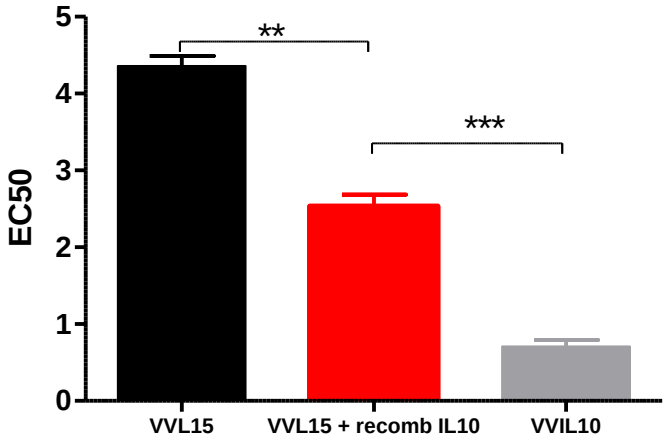

Figure 50. Anti-tumour potency of VVL15 + rIL10, VVL15 and VVIL10 infected CMT93 colorectal cancer cells. Comparison of mean EC_{50} values ± SEM generated from sextuplicate. 5000 CMT93 cells were seeded per well and infected with vaccinia virus at a series of increasing MOI (highest MOI of 1000 PFU/cell). MTS cell proliferation assays were performed 3 days after infection. Statistical analysis was performed using the unpaired T-test with * representing statistical significance at $p<0.05$, ** representing statistical significance at $p<0.01$, *** representing statistical significance at $p<0.001$ and ns indicating no statistical significance.

As demonstrated before VVIL10 exhibited superior cytotoxicity *in vitro* compared to VVL15. However VVL15 with rIL10 showed an intermediate level potency. Therefore, to a degree the rIL10, was able to improve VVL15 potency; partially compensating for the lack of IL10 expression compared to VVIL10. This may suggest the concentration of rIL10 on its own was insufficient in the previous experiment to exert a direct, non-virally mediated, cytotoxic effect; or further unknown factors produced by the vaccinia virus work in conjunction with IL10 to induce an elevated cytotoxic effect compared to VVL15.

7.3. Analysis of multiple pro-inflammatory cytokines of the serum in C57BL/6 immunocompetent mice bearing CMT93 flank tumours following intratumoural viral injection.

To assess the differences in pro-inflammatory cytokines of the serum in C57BL/6 immunocompetent mice bearing CMT93 flank tumours, serum was sampled at various

time-points following different IT viral treatments. Serum samples were subjected to cytokine quantification using a mouse proinflammatory ultra-sensitive kit for the Meso Scale Discovery multi-spot assay system.

Cytokine	**PBS**		**VVL15**		**VVIL10**	
	Cytokine concentration (pg/ml)	**SEM**	**Cytokine concentration** (pg/ml)	**SEM**	**Cytokine concentration** (pg/ml)	**SEM**
IL1β	0.000	0.000	0.04157703	0.04157703	2.793901	0.3649448
TNFα	0.000	0.000	1.005828	0.3554596	8.915852	0.9564027
IFNγ	1.409787	0.09003938	2.398584	0.32478	58.30131	12.67154
IL10	14.97578	1.881992	84.60355	5.741311	165.0063	6.791869
IL12	0.000	0.000	0.000	0.000	35.9429	4.252429
IL6	11.38702	1.2283	29.93359	4.15731	159.2583	5.413141
IL8	189.8381	6.495094	204.7455	11.96176	85.29649	5.474484

Table 16. Concentration of multiple pro-inflammatory cytokines of sampled serum in C57BL/6 immunocompetent mice bearing CMT93 flank tumours following intratumoural viral injection. $5x10^6$ CMT93 cells were seeded by subcutaneous injection into the right flank of 27 C57BL/6 mice. When tumours reached 4-5mm in diameter, 9 mice each received IT injections of PBS, VVL15 or VVIL10 on days 1,3,5 (3 x $1x10^8$ PFU). At days 5, 10 and 15, 3 animals from each group were sacrificed and the serum was sampled. The cytokine concentration was quantified using a mouse pro-inflammatory ultra-sensitive kit for the Meso Scale Discovery multi-spot assay system (2 animals per group in sample duplicate). Mean cytokine concentrations at day 10 ± SEM are shown.

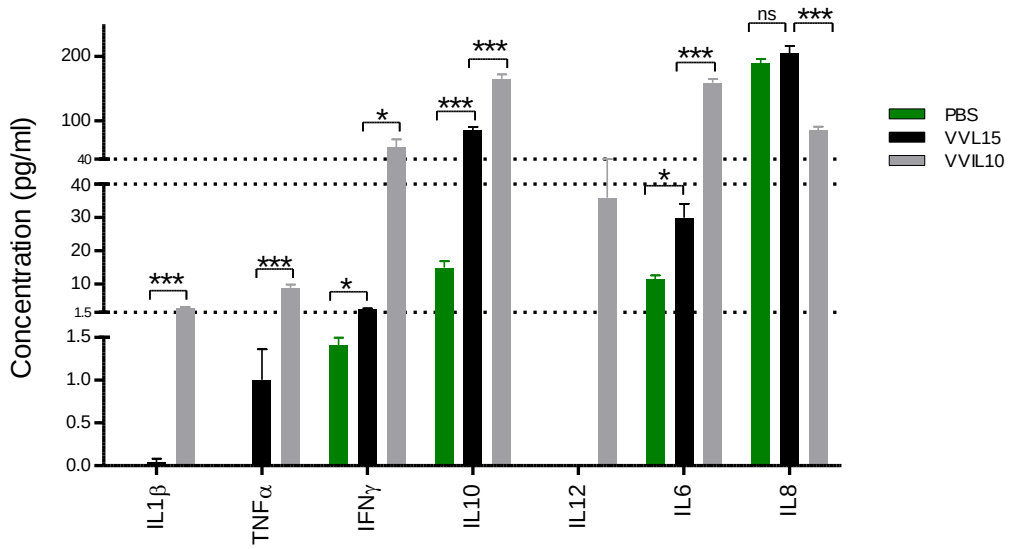

Figure 51. Concentration of multiple pro-inflammatory cytokines of sampled serum in C57BL/6 immunocompetent mice bearing CMT93 flank tumours following intratumoural viral injection. $5x10^6$ CMT93 cells were seeded by subcutaneous injection into the right flank of 27 C57BL/6 mice. When tumours reached 4-5mm in diameter, 9 mice each received IT injections of PBS, VVL15 or VVIL10 on days 1,3,5 (3 x $1x10^8$ PFU). At days 5, 10 and 15, 3 animals from each group were sacrificed and the serum was sampled. The cytokine concentration was quantified using a mouse pro-inflammatory ultra-sensitive kit for the Meso Scale Discovery multi-spot assay system (2 animals per group in sample duplicate). Mean cytokine concentrations at day 10 ± SEM are shown. Statistical analysis was performed using the unpaired T-test with * representing statistical significance at $p<0.05$, ** representing statistical significance at $p<0.01$, *** representing statistical significance at $p<0.001$ and ns indicating no statistical significance.

The serum cytokine levels reveal higher pro-inflammatory levels for VVIL10 compared to VVL15, with the exception of IL8. This is difficult to explain given the greater tumour biodistribution and superior anti-tumour efficacy of VVIL10 over VVL15. However in contrast to the previous experiments comparing cytokine responses following VVL15 and WRDD treatment, these high pro-inflammatory cytokines levels now occur in conjunction with high IL10 levels. Although this may explain why the viral titres of VVIL10 were less than VVL15 in the highly vascular bone marrow,

spleen and lungs; with the induction of a pro-inflammatory response clearing the virus from the circulation. Again the relative levels and combinations of cytokines may be important in explaining viral persistence and anti-tumour potency of the viruses tested.

7.4. Analysis of multiple pro-inflammatory cytokines in CMT93 flank tumour homogenates following intratumoural viral injection of C57BL/6 immunocompetent mice.

To assess the differences in pro-inflammatory cytokines in the tumour microenvironment, CMT93 flank tumours were grown in C57BL/6 immunocompetent mice and different viral treatments were applied intratumourally. Harvested tumours from sacrificed mice were weighed, homogenised and subjected to cytokine quantification using a Meso Scale Discovery multi-spot assay system mouse pro-inflammatory ultra-sensitive kit.

Cytokine	**PBS**		**VVL15**		**VVIL10**	
	Cytokine concentration (pg/ml/g)	**SEM**	**Cytokine concentration** (pg/ml/g)	**SEM**	**Cytokine concentration** (pg/ml/g)	**SEM**
IL1β	374.89	41.03	2105.35	347.6	2121.22	102.27
TNFα	8.359	0.810	15.34	1.407	1.458	0.3791
IFNγ	37.73	5.974	76.37	9.292	239.15	19.800
IL10	60.25	10.93	132.54	13.59	426.90	80.919
IL12	4.574	0.380	59.29	16.04	87.998	17.980
IL6	360.82	8.625	370.64	66.40	215.97	40.302
IL8	83.35	9.717	1509.98	261.9	510.93	61.936

Table 17. Concentration of multiple pro-inflammatory cytokines of harvested and homogenised CMT93 flank tumour samples following IT viral infection in C57BL/6 immunocompetent mice. $5x10^6$ CMT93 cells were seeded by subcutaneous injection into the right flank of 27 C57BL/6 mice. When tumours reached 4-5mm in diameter, 9 mice each received IT injections of PBS, VVL15 or VVIL10 on days 1,3,5 (3 x $1x10^8$ PFU). At days 5, 10 and 15 (day 15 samples not analysed here), 3 animals from each group were sacrificed and the tumours were harvested. The tumours were weighed, homogenised and subjected to cytokine quantification using a mouse proinflammatory ultra-sensitive kit for the Meso Scale Discovery multi-spot assay

system (2 animals per group in sample duplicate). Mean cytokine concentrations at day 10 ± SEM are shown. Cytokine concentration was corrected for tumour weight.

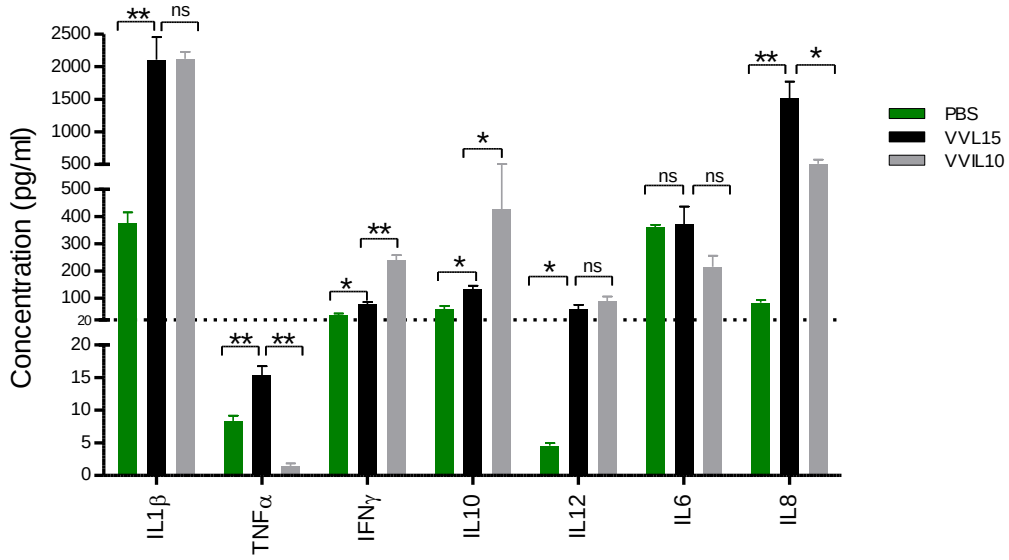

Figure 52. Concentration of multiple pro-inflammatory cytokines of harvested and homogenised CMT93 flank tumour samples following IT viral infection in C57BL/6 immunocompetent mice. $5x10^6$ CMT93 cells were seeded by subcutaneous injection into the right flank of 27 C57BL/6 mice. When tumours reached 4-5mm in diameter, 9 mice each received IT injections of PBS, VVL15 or VVIL10 on days 1,3,5 (3 x $1x10^8$ PFU). At days 5, 10 and 15 (day 15 samples not analysed here), 3 animals from each group were sacrificed and the tumours were harvested. The tumours were weighed, homogenised and subjected to cytokine quantification using a mouse proinflammatory ultra-sensitive kit for the Meso Scale Discovery multi-spot assay system (2 animals per group in sample duplicate). Mean cytokine concentrations at day 10 ± SEM are shown. Cytokine concentration was corrected for tumour weight. Statistical analysis was performed using the unpaired T-test with * representing statistical significance at $p<0.05$, ** representing statistical significance at $p<0.01$, *** representing statistical significance at $p<0.001$ and ns indicating no statistical significance.

When considering the cytokine levels found within tumours the cytokine profile is more complicated, as it was with WRDD and VVL15. VVIL10-treated tumours exhibited

higher levels of IL10 and IFNγ; whilst VVL15-infected tumours resulted in higher IL8 and TNFα. Insignificant differences were found between the two virus treatments for IL12, IL1β and IL6. Both IFNγ and TNFα have anti-tumour and anti-viral functions; but, as discussed before, cytokines are considered part of a "cytokine network", and therefore the relative levels and combinations of cytokines may be important in explaining viral persistence and anti-tumour potency of the viruses tested.

7.5. Analysis of multiple pro-inflammatory cytokines of CMT93 tissue culture samples following viral infection.

To further investigate the observed differences in anti-tumour potency between VVL15 and VVIL10 an analysis of multiple pro-inflammatory cytokines was performed using a mouse pro-inflammatory ultra-sensitive kit for the Meso Scale Discovery multi-spot assay system. Samples were analysed from supernatants of tissue cultured CMT93 cells infected with viruses.

Cytokine	**PBS**		**VVL15**		**VVIL10**	
	Cytokine concentration (pg/ml)	**SEM**	**Cytokine concentration** (pg/ml)	**SEM**	**Cytokine concentration** (pg/ml)	**SEM**
IL1β	0.000	0.000	5.081	0.094	16.790	0.408
TNFα	0.000	0.000	0.000	0.000	0.000	0.000
IFNγ	0.000	0.000	0.000	0.000	8.1655	0.309
IL10	4.795	4.795	337.7298	32.75	7250.18	855.46
IL12	11.270	5.687	48.63353	4.555	219.63	6.961
IL6	14.355	2.346	0.000	0.000	241.40	8.880
IL8	55.253	7.221	266.4881	9.017	193.39	9.361

Table 18. Concentration of multiple pro-inflammatory cytokines of CMT93 tissue culture samples following viral infection *in vitro*. $2x10^5$ cells per well were infected with 1 PFU/cell of virus. Cell lysates were harvested at 6 and 24 hour intervals. Cytokine concentration was quantified in triplicate using a Meso Scale Discovery multi-spot assay system mouse proinflammatory 7-plex ultra-sensitive kit. Mean cytokine concentrations at 24 hours ± SEM are shown.

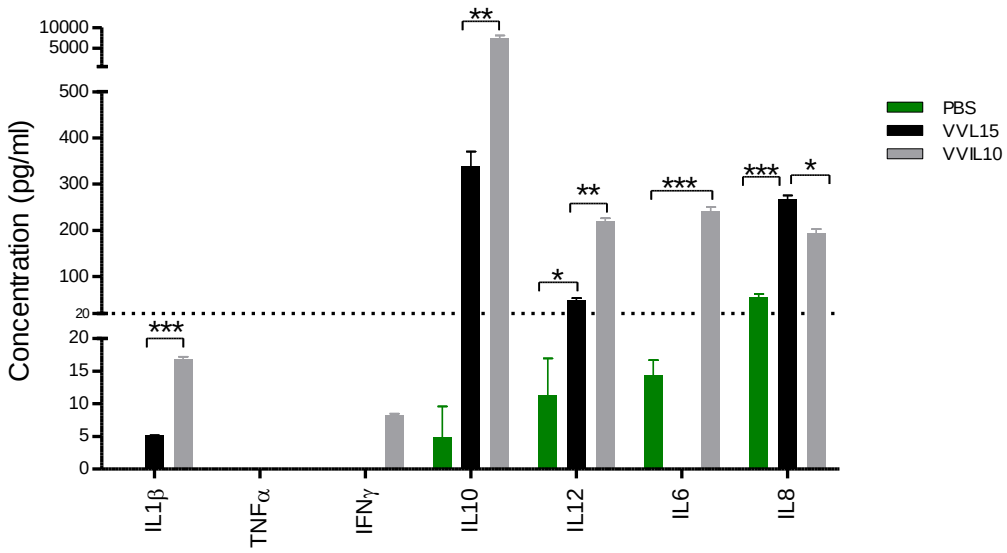

Figure 53. Concentration of multiple pro-inflammatory cytokines of CMT93 tissue culture samples following viral infection *in vitro*. $2x10^5$ cells per well were infected with 1 PFU/cell of virus. Cell lysates were harvested at 6 and 24 hour intervals. Cytokine concentration was quantified in triplicate using a Meso Scale Discovery multi-spot assay system mouse proinflammatory 7-plex ultra-sensitive kit. Mean cytokine concentrations at 24 hours ± SEM are shown. Statistical analysis was performed using the unpaired T-test with * representing statistical significance at $p<0.05$, ** representing statistical significance at $p<0.01$, *** representing statistical significance at $p<0.001$ and ns indicating no statistical significance.

Comparing VVIL10 to VVL15 higher levels of IFNγ, IL10, IL12, IL1β and IL6 were demonstrated with VVIL10 infected cells. VVL15-infected cultures had higher levels of IL8, and no TNFα was detected. This pattern was similar to the serum pattern.

Having reviewed the different cytokines and virus combinations, the cytokines that showed most promise as to explain the different anti-tumour potencies between VVL15 and VVIL10 *in vitro* and *in vivo* were IL10, IL12 and Interferon γ. More samples from an additional time-points and in sample triplicate were analysed.

7.6. Analysis of IL10, IL12 and Interferon γ cytokine concentrations of the serum in C57BL/6 immunocompetent mice bearing CMT93 flank tumours following intratumoural viral injection.

IL10, IL12 and Interferon γ cytokine concentrations in the serum of C57BL/6 immunocompetent mice bearing CMT93 flank tumours following different IT viral treatments were quantified using R&D Systems Quantikine ELISA kits.

Cytokine	Day	PBS		VVL15		VVIL10	
		Cytokine concentration (pg/ml)	SEM	Cytokine concentration (pg/ml)	SEM	Cytokine concentration (pg/ml)	SEM
IL12	5	0.000	0.000	0.000	0.000	9.079	0.416
	10	0.6228	0.0736	0.000	0.000	10.901	1.283
	15	0.8979	0.1031	0.1299	0.045	21.547	1.371
IFNγ	5	0.3376	0.0230	0.5186	0.023	15.356	1.682
	10	0.3543	0.0169	0.5765	0.042	16.393	1.932
	15	0.9062	0.0357	0.4263	0.026	20.915	1.419
IL10	5	0.0993	0.0628	23.746	2.882	50.240	3.170
	10	0.000	0.000	10.099	0.886	48.025	2.987
	15	0.000	0.000	3.0025	0.395	29.596	3.717

Table 19. Concentration of multiple pro-inflammatory cytokines of sampled serum in C57BL/6 immunocompetent mice bearing CMT93 flank tumours following intratumoural viral injection. $5x10^6$ CMT93 cells were seeded by subcutaneous injection into the right flank of 27 C57BL/6 mice. When tumours reached 4-5mm in diameter, 9 mice each received IT injections of PBS, WRDD, VVL15 or VVIL10 on days 1,3,5 (3 x $1x10^8$ PFU). At days 5, 10 and 15, 3 animals from each group were sacrificed and the serum was sampled. The cytokine concentration was quantified using R&D Systems Quantikine Mouse IL10, IL12 and Interferon γ ELISA kits (3 animals per group in sample duplicate). Mean cytokine concentrations ± SEM are shown.

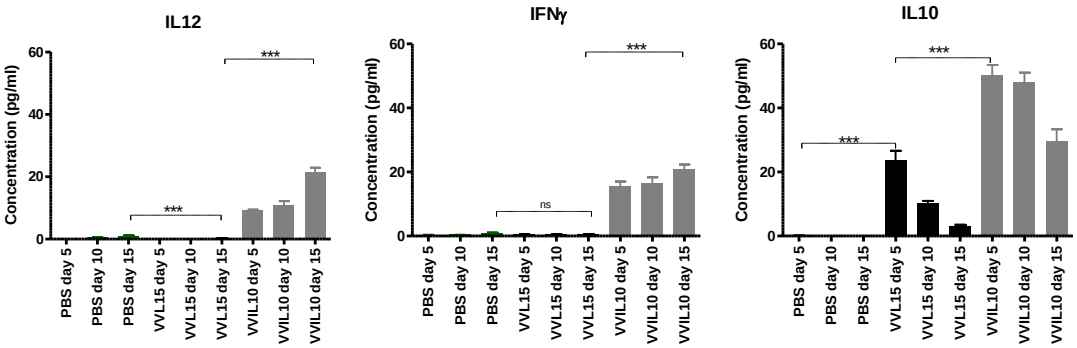

Figure 54. Concentration of multiple pro-inflammatory cytokines of sampled serum in C57BL/6 immunocompetent mice bearing CMT93 flank tumours following intratumoural viral injection. $5x10^6$ CMT93 cells were seeded by subcutaneous injection into the right flank of 27 C57BL/6 mice. When tumours reached 4-5mm in diameter, 9 mice each received IT injections of PBS, WRDD, VVL15 or VVIL10 on days 1,3,5 (3 x $1x10^8$ PFU). At days 5, 10 and 15, 3 animals from each group were sacrificed and the serum was sampled. The cytokine concentration was quantified using R&D Systems Quantikine Mouse IL10, IL12 and Interferon γ ELISA kits (3 animals per group in sample duplicate). Mean cytokine concentrations ± SEM are shown. Statistical analysis was performed using the unpaired T-test with * representing statistical significance at $p<0.05$, ** representing statistical significance at $p<0.01$, *** representing statistical significance at $p<0.001$ and ns indicating no statistical significance.

The above data confirm the previous pattern of multiple cytokine data over two time-points.

7.7. Analysis of IL10, IL12 and Interferon γ cytokine concentrations from CMT93 flank tumour homogenates following intratumoural viral injection in C57BL/6 immunocompetent mice.

In order to assess IL10, IL12 and Interferon γ cytokine concentrations in the tumour microenvironment, CMT93 flank tumours were grown in C57BL/6 immunocompetent mice and different viral treatments were applied intratumourally. Harvested tumours from sacrificed mice were weighed, homogenised and subjected to cytokine quantification using R&D Systems Quantikine ELISA kits.

Cytokine	Day	PBS		VVL15		VVIL10	
		Cytokine concentration (pg/ml)	**SEM**	**Cytokine concentration** (pg/ml)	**SEM**	**Cytokine concentration** (pg/ml)	**SEM**
IL12	5	0.9225	0.070	18.07	2.640	54.527	10.02
	10	1.1699	0.055	19.83	2.552	41.733	4.631
	15	0.892	0.114	20.33	1.963	48.382	4.393
IFNγ	5	14.419	0.700	30.88	2.092	73.486	8.780
	10	10.487	0.960	19.10	1.329	109.01	9.824
	15	14.249	0.599	15.94	0.713	91.810	5.929
IL10	5	11.737	1.611	82.54	7.448	244.30	27.33
	10	12.442	1.404	43.02	3.140	214.76	15.7
	15	9.081	0.778	47.06	4.460	96.206	8.946

Table 20. Concentration of multiple pro-inflammatory cytokines of harvested and homogenised CMT93 flank tumour samples following IT viral infection in C57BL/6 immunocompetent mice. $5x10^6$ CMT93 cells were seeded by subcutaneous injection into the right flank of 27 C57BL/6 mice. When tumours reached 4-5mm in diameter, 9 mice each received IT injections of PBS, VVL15 or VVIL10 on days 1,3,5 ($3 \times 1x10^8$ PFU). At days 5, 10 and 15, 3 animals from each group were sacrificed and the tumours were harvested. The tumours were weighed, homogenised and subjected to cytokine quantification using R&D Systems Quantikine Mouse IL10, IL12 and Interferon γ ELISA kits (3 animals per group in sample duplicate). Cytokine concentration was corrected for tumour weight. Mean cytokine concentrations ± SEM are shown.

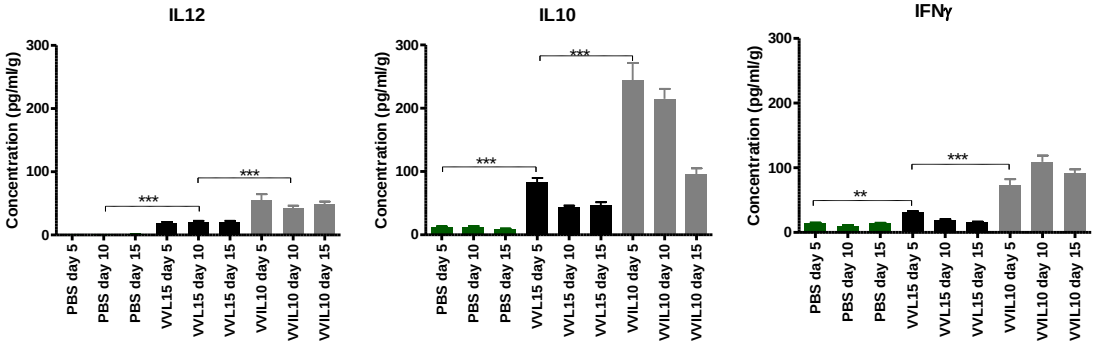

Figure 55. Concentration of multiple pro-inflammatory cytokines of harvested and homogenised CMT93 flank tumour samples following IT viral infection in C57BL/6 immunocompetent mice. $5x10^6$ CMT93 cells were seeded by subcutaneous injection into the right flank of 27 C57BL/6 mice. When tumours reached 4-5mm in

diameter, 9 mice each received IT injections of PBS, VVL15 or VVIL10 on days 1,3,5 (3 x $1x10^8$ PFU). At days 5, 10 and 15, 3 animals from each group were sacrificed and the tumours were harvested. The tumours were weighed, homogenised and subjected to cytokine quantification using R&D Systems Quantikine Mouse IL10, IL12 and Interferon γ ELISA kits (3 animals per group in sample duplicate). Cytokine concentration was corrected for tumour weight. Mean cytokine concentrations ± SEM are shown. Statistical analysis was performed using the unpaired T-test with * representing statistical significance at $p<0.05$, ** representing statistical significance at $p<0.01$, *** representing statistical significance at $p<0.001$ and ns indicating no statistical significance.

These data compared to the multiple cytokine data over two time-points show the same pattern for IL10 and IFNγ; with VVIL10 inducing higher levels of these cytokines. However now there are significant differences in IL12 levels, with VVIL10 inducing higher levels.

7.8. Analysis of IL10, IL12 and Interferon γ cytokine concentrations in CMT93 tissue culture supernatants following viral infection.

IL10, IL12 and Interferon γ cytokine concentrations of CMT93 tissue culture supernatants infected 6, 24 and 48 hours following mock, VVL15 and VVIL10 infection were quantified using R&D Systems Quantikine ELISA kits.

Cytokine	Hours	PBS		VVL15		VVIL10	
		Cytokine concentration (pg/ml)	**SEM**	**Cytokine concentration** (pg/ml)	**SEM**	**Cytokine concentration** (pg/ml)	**SEM**
IL12	6	3.259	0.358	20.700	1.651	55.623	1.9947
	24	4.019	0.293	14.251	1.473	62.156	5.1402
	48	3.217	0.243	11.911	1.176	68.847	4.5780
IFNγ	6	0.000	0.000	0.000	0.000	1.378	0.1332
	24	0.000	0.000	0.000	0.000	3.323	0.3093
	48	0.000	0.000	0.159	0.057	4.698	0.2195
IL10	6	0.000	0.000	22.769	3.183	548.350	28.919
	24	1.291	0.636	91.082	4.954	2433.62	296.10
	48	1.486	0.620	138.249	4.816	3225.154	155.32

Table 21. Concentration of multiple pro-inflammatory cytokines in CMT93 tissue culture samples following viral infection *in vitro*. $2x10^5$ cells per well were infected with 1 PFU/cell of virus. Cell lysates were harvested at 6, 24 and 48 hour intervals. Cytokine concentration was quantified in triplicate using R&D Systems Quantikine Mouse IL10, IL12 and Interferon γ ELISA kits. Mean cytokine concentrations ± SEM are shown.

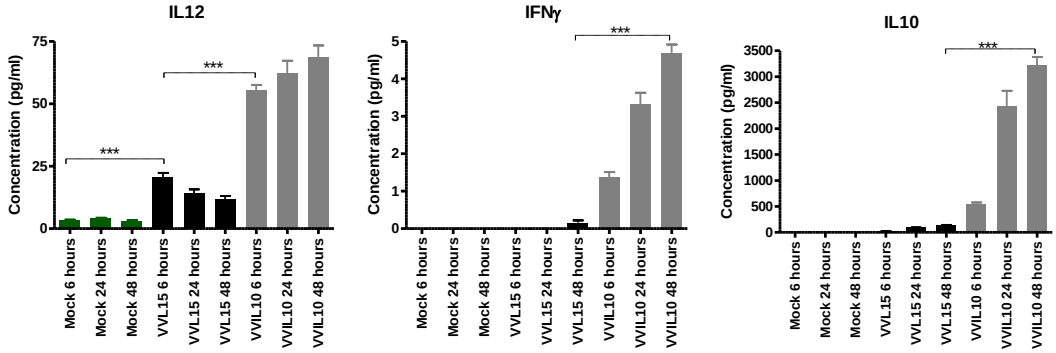

Figure 56. Concentration of multiple pro-inflammatory cytokines in CMT93 tissue culture samples following viral infection *in vitro*. $2x10^5$ cells per well were infected with 1 PFU/cell of virus. Cell lysates were harvested at 6, 24 and 48 hour intervals. Cytokine concentration was quantified in triplicate using R&D Systems Quantikine Mouse IL10, IL12 and Interferon γ ELISA kits. Mean cytokine concentrations ± SEM are shown. Statistical analysis was performed using the unpaired T-test with * representing statistical significance at $p<0.05$, ** representing statistical significance at $p<0.01$, *** representing statistical significance at $p<0.001$ and ns indicating no statistical significance.

These data compared to the multiple cytokine data over two time-points show the same pattern for VVL15- and VVIL10-treated mice.

7.9. Analysis of tumour homogenate IL10 concentrations in nude mouse bearing PT45 flank tumours following IT vaccinia virus treatment.

Having assessed IL10 expression *in vitro* and *in vivo* in a murine colorectal CMT93 immunocompetent tumour model following IT virus injection, expression was analysed in a human cancer model in nude mice. As employed before a PT45 human pancreatic

flank tumour model was used and harvested tumours and serum were subjected to IL10 quantification using an R&D Systems Quantikine Mouse IL10 ELISA kit, following homogenisation.

Day	PBS		WRDD		VVL15		VVIL10	
	Cytokine concent-ration (pg/ml/g)	**SEM**	**Cytokine concent-ration** (pg/ml)	**SEM**	**Cytokine concent-ration** (pg/ml)	**SEM**	**Cytokine concent-ration** (pg/ml)	**SEM**
7	214.8	21.55	894.5	216.2	4869	450.6	743.9	743.9
12	1016	72.90	386.8	43.78	6680	330.4	1006	1006
20	708.3	133.7	409.4	189.0	1446	226.5	87.19	87.19

Table 22. Concentration of IL10 in harvested tumours from ICRF nu/nu mice bearing PT45 flank tumours following intratumoural viral injection. $5x10^6$ PT45 cells were seeded by subcutaneous injection into the right flank of 36 ICRF nu/nu mice. When tumours reached 4-5mm in diameter, 9 mice each received IT injections of PBS, WRDD, VVL15 or VVIL10 on days 1,3,5 (3 x $1x10^7$ PFU). At days 7, 12 and 20, 3 animals from each group were sacrificed and the serum was sampled. The cytokine concentration was quantified using R&D Systems Quantikine Mouse IL10 ELISA kit (3 animals per group in sample duplicate). Mean cytokine concentrations ± SEM are shown.

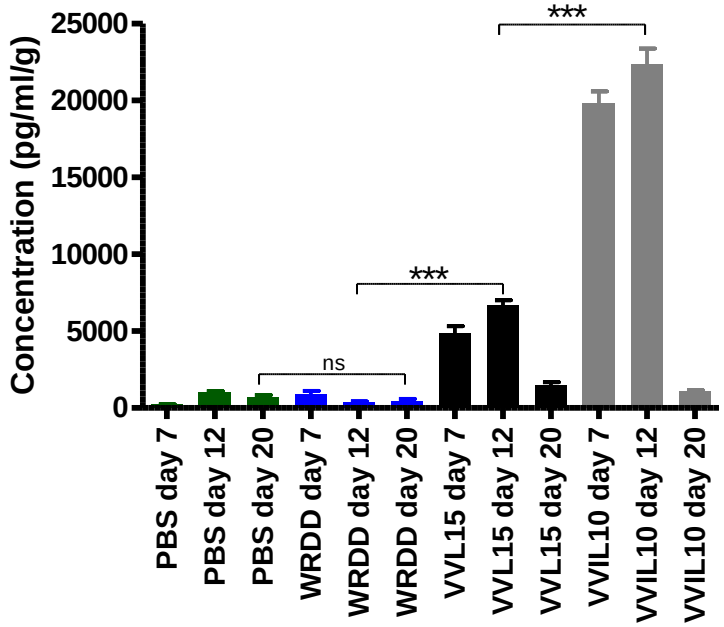

Figure 57. Concentration of IL10 in harvested tumours from ICRF nu/nu mice bearing PT45 flank tumours following intratumoural viral injection. $5x10^6$ PT45 cells were seeded by subcutaneous injection into the right flank of 36 ICRF nu/nu mice. When tumours reached 4-5mm in diameter, 9 mice each received IT injections of PBS, WRDD, VVL15 or VVIL10 on days 1,3,5 (3 x $1x10^7$ PFU). At days 7, 12 and 20, 3 animals from each group were sacrificed and the serum was sampled. The cytokine concentration was quantified using R&D Systems Quantikine Mouse IL10 ELISA kit (3 animals per group in sample duplicate). Mean cytokine concentrations ± SEM are shown. Statistical analysis was performed using the unpaired T-test with * representing statistical significance at $p<0.05$, ** representing statistical significance at $p<0.01$, *** representing statistical significance at $p<0.001$ and ns indicating no statistical significance.

These data show the same pattern as in the CMT93 model data, with high IL10 levels in VVIL10-treated tumours and moderate levels in VVL15-treated tumours. Negligible levels were found with WRDD and mock infection. This again suggests the IL10 detected in VVIL10-treated mice is virally encoded and not produced by the host cell in response to the viral infection. Furthermore, it is likely Lister strain vaccinia virus produces an IL10 homologue able to react with the murine IL10 antibody.

7.10. Analysis of serum IL10 concentrations in nude mouse bearing PT45 flank tumours following IT vaccinia virus treatment

IL10 expression in the serum of nude mice bearing PT45 tumours was also assessed following IT vaccinia virus administration.

Day	PBS		WRDD		VVL15		VVIL10	
	Cytokine concent-ration (pg/ml)	**SEM**	**Cytokine concent-ration** (pg/ml)	**SEM**	**Cytokine concent-ration** (pg/ml)	**SEM**	**Cytokine concent-ration** (pg/ml)	**SEM**
7	103.8	24.46	94.91	15.14	1081	130.8	3220	314.8
12	194.4	21.73	195.2	61.78	1115	85.07	4247	172.7
20	131.3	23.05	157.7	29.59	574.0	108.2	1891	235.3

Table 23. Concentration of IL10 in sampled serum of ICRF nu/nu mice bearing PT45 flank tumours following intratumoural viral injection. $5x10^6$ PT45 cells were seeded by subcutaneous injection into the right flank of 36 ICRF nu/nu mice. When tumours reached 4-5mm in diameter, 9 mice each received IT injections of PBS, WRDD, VVL15 or VVIL10 on days 1,3,5 (3 x $1x10^7$ PFU). At days 7, 12 and 20, 3 animals from each group were sacrificed and the serum was sampled. The cytokine concentration was quantified using R&D Systems Quantikine Mouse IL10 ELISA kit (3 animals per group in sample duplicate). Mean cytokine concentrations ± SEM are shown.

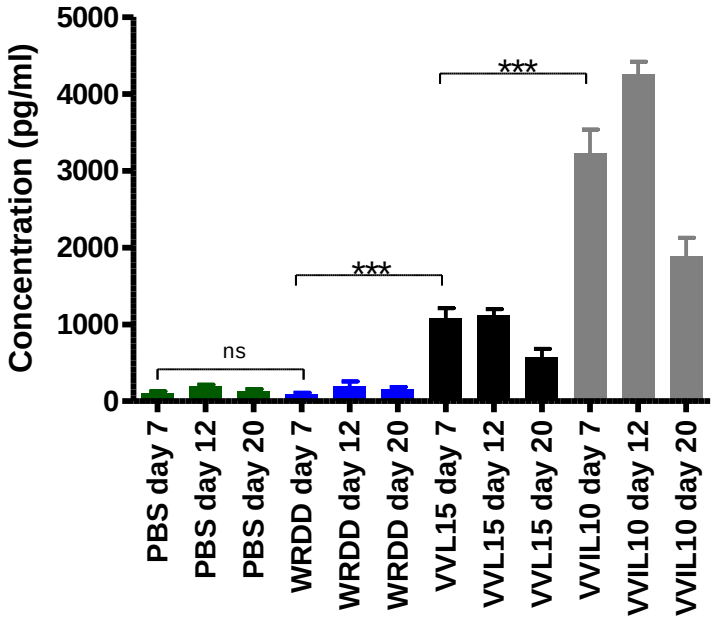

Figure 58. Concentration of IL10 in sampled serum of ICRF nu/nu mice bearing PT45 flank tumours following intratumoural viral injection. $5x10^6$ PT45 cells were seeded by subcutaneous injection into the right flank of 36 ICRF nu/nu mice. When tumours reached 4-5mm in diameter, 9 mice each received IT injections of PBS, WRDD, VVL15 or VVIL10 on days 1,3,5 (3 x $1x10^7$ PFU). At days 7, 12 and 20, 3 animals from each group were sacrificed and the serum was sampled. The cytokine concentration was quantified using R&D Systems Quantikine Mouse IL10 ELISA kit (3 animals per group in sample duplicate). Statistical analysis was performed using the unpaired T-test with * representing statistical significance at $p<0.05$, ** representing statistical significance at $p<0.01$, *** representing statistical significance at $p<0.001$ and ns indicating no statistical significance.

This finding is the same as found in the CMT93 immunocompetent mouse model. High IL10 levels are found with VVIL10 infection, albeit lower than the level measured from the tumour samples, moderate levels with VVL15 infections, and negligible levels with WRDD and PBS.

7.11 Chapter Conclusions

- Recombinant IL10 has no effect on CMT93 cells *in vitro* at the concentration range of 0.001 - $1x10^5$pg/ml.
- Recombinant IL10 ($1x10^6$pg/ml) in combination with VVL15 (MOI $1x10^{-5}$ to 1000 PFU/cell) had an intermediate EC_{50} compared to VVIL10 alone (higher) and VVL15 alone (lower).
- Serum cytokine profiles of immunocompetent mice bearing CMT93 flank tumours following IT viral treatments revealed higher levels of pro-inflammatory cytokines in conjunction with higher IL10 anti-inflammatory cytokine with VVIL10 compared to VVL15.
- Tumour homongenates of immunocompetent mice bearing CMT93 flank tumours following IT treatments revealed high IL10 and IFNγ, whilst VVL15 had high IL8 and TNFα.
- High IL10 expression from serum and tumours was demonstrated in a human model of pancreatic cancer, PT45, following VVIL10 and to a lesser extent VVL15, treatment of flank tumours with IT virus.

Discussion

Key Findings

- Lister strain vaccinia virus demonstrated superior anti-tumour potency and cancer-selective replication in vitro and in vivo, compared to Western Reserve; especially in human cancer cell lines.
- Greater tumour-selective replication following local and systemic delivery of Lister strain virus to immunocompetent mice compared to Western Reserve.
- Reduced local and systemic pro-inflammatory response with Lister strain virus treatment; with associated heightened anti-inflammatory IL10 response.
- An IL10 expressing Lister strain mutant has increased anti-tumour potency and tumour selective replication.

The Western Reserve (WR) strain of vaccinia virus is the dominant vaccinia strain in oncolytic viral gene therapy research due to its perceived superior anti-tumour potency and selectivity following publication of recent evidence comparing ten wild-type vaccinia virus strains *in vitro*. [82] However this paper compared wild-type viruses which we know from clinical trials in the 1970s and 1990s are well tolerated, but exhibit poor efficacy. [60] Additionally the basis for the conclusion of WR superiority was founded on *in vitro* viral replication studies in two human cancer cell lines. An ovarian carcinoma cell line, A2780, and colorectal carcinoma cell line, HCT116, compared to replication in two normal cell lines; normal human bronchial epithelial (NHBE) and small airway bronchial epithelial (SAEC) cells. This is not a comprehensive panel of cancer cell lines to draw such a broad conclusion and relies on a single technique, measuring viral replication. A more robust comparison strategy would present data for several cancer cell lines and use a variety of techniques, including *in vivo* experiments.

I present, in this study, experiments using cancer cell lines from multiple organ primary sites, both human and murine. Additionally I have utilised two *in vitro* methods to demonstrate anti-tumour potency, both viral replication assays and MTS cell proliferation assays; as well as evidence of comparative *in vivo* efficacy. Although I have demonstrated higher anti-tumour potency of WR strains in five murine cancer cell lines from multiple primary sites (head & neck, pancreatic, colorectal and ovarian),

Lister strain, VVL15, showed greater anti-tumour potency compared to WR strain, WRDD, in 11 out of 14 human cancer cell lines. Of the remaining three human cancer cell lines, one showed equivalent EC_{50} values between VVL15 and WRDD (MKN45 human gastric adenocarcinoma cell line) and the other two exhibited greater anti-tumour potency for WRDD compared to VVL15 (A2780 and HCT116). Interestingly these two cancer cell lines were used by Steve Thorne's group to evidence WR superiority over all other vaccinia virus strains, [82] but appear to be outliers to the general trend. The apparent murine tropism of the WR strain is not surprising given it was developed by repeated passage of the Wyeth vaccinia virus strain in mice brains. [246]

Wild-type poxviruses demonstrate wide tissue tropism, [89] but some strains have inherent tumour selectivity that can be further enhanced by deletions of genes such as thymidine kinase [241] and vaccinia growth factor. [83] To test the tumour selectivity of Lister and WR vaccinia virus strains, replication in normal human bronchial epithelial (NHBE) cells was compared to replication in specific human cancer cell lines. NHBE was chosen as poxviruses generally spread via the respiratory tract or direct skin inoculation, and therefore must replicate to some extent in normal epithelial cells of the skin and lung. In MiaPaCa2, PT45, PANC1 and SUIT2 human cancer cell lines VVL15 demonstrated higher ratios of replication in cancer cells compared to NHBE cell lines; indicating superior tumour selectivity. This cancer-selective viral replication was significantly better for VVL15 compared to WRDD in equivalent cell lines.

To assess *in vivo* anti-tumour efficacy, Lister and WR vaccinia virus mutants were then administered IT to nude and immunocompetent mice bearing FaDu human HNSCC, PT45 human pancreatic carcinoma, CMT93 and CT26 murine colorectal flank tumours. In nude mouse human cancer models, FaDu (HNSCCC) and PT45 (pancreatic), the Lister strain VVL15 showed superior anti-cancer activity compared to Western Reserve WRDD virus; in keeping with the cytotoxicity and viral replication *in vitro* data. In nude mice bearing murine CMT93 flank tumours, there was reduced tumour progression in the WRDD-treated mice. Changing the mouse model to immunocompetent C57BL/6 mice bearing CMT93 flank tumours as before, and with two treatment regimes of 3 x IT virus injections (days 1,3,5) and 5 x IT virus injections (days 1,2,3,4,5), a different pattern was seen where VVL15 showed superior anti-tumour efficacy over WRDD. This effect seemed dose-responsive with the 5 x IT injection regime enhancing the anti-tumour potency with VVL15 treatment. Testing in

another immunocompetent murine colorectal cancer model (CT26) improved anti-tumour efficacy was demonstrated in VVL15-treated mice.

To define the mechanism of enhanced Lister strain anti-tumour potency and evaluate viral replication in other, non-tumour, tissues (which may result in host treatment side-effects/complications), biodistribution studies were performed using IV viral treatment in nude and immunocompetent mice bearing CMT93 flank tumours. In the nude mouse model, WRDD demonstrated higher levels of replication than VVL15 in the tumour as determined by $TCID_{50}$, qRT-PCR and immunohistochemistry. However WRDD also exhibited higher levels of viral replication in the ovary and to lesser extent lungs, liver, spleen, brain and bone marrow. Therefore it is apparent that WRDD is able to replicate better in all murine tissues compared to VVL15; which again is probably unsurprising given the origins of the WR strain.

In the immunocompetent model the titre of virus measured in the tumour samples was higher with VVL15 compared to WRDD; with similar levels of both viruses in the lungs, liver and spleen. Again WRDD showed very high concentrations in the ovaries, which was not seen with VVL15. This finding in the immunocompetent model is suggestive of Lister strain having a greater ability than WR strain to replicate in the presence of an intact immune system, with the exception of ovarian tissues. Vaccinia viruses are known to have a number of strategies to suppress the host immune system and therefore reduce their clearance. These include interferon decoy receptors, [128,129] TNF receptors, [132] IL1 receptor blocker, [108] IL18 binding protein, [261] CC chemokine inhibitor, [136] and serine protease inhibitors. [137] More of these immunomodulatory proteins have been identified in the Lister strain virus compared to the WR strain, and as such may have more powerful mechanisms to subdue the host immune response, and hence reduce Lister strain virus clearance.

To investigate functional mechanisms for Lister mutant superiority over WR, inflammatory responses to the two viruses were examined through cytokine analysis of cancer cells in tissue culture, and *in vivo* tumours and serum following IT viral treatment of flank tumours in immunocompetent mice. Interestingly, WR strain induced much higher levels of pro-inflammatory cytokines compared to Lister. IL10 was the only cytokine that recorded higher levels in VVL15-treated mice compared to WRDD-treated animals. IL10 is considered an anti-inflammatory cytokine. This suggested that

VVL15 was able to induce a less pro-inflammatory response, explaining the higher viral titres of this virus in the immunocompetent mouse biodistribution model and consequently the superior anti-tumour efficacy seen in the immunocompetent animal models.

To further improve the anti-tumour efficacy of the Lister strain vaccinia virus, a transgene was sought to arm the Lister viral backbone. As viral clearance by the host immune system is a key factor in determining viral efficacy, mechanisms to suppress this immunity were investigated. IL10 is an anti-inflammatory cytokine that has been demonstrated to inhibit tumour growth and metastasis. [157] A Lister vaccinia virus expressing murine IL10 (VVIL10) was constructed; with the IL10 transgene inserted into the TK region driven by the synthetic early/late promoter pE/L. [240] IL10 expression was confirmed by ELISA in CMT93, SCCVII and PT45 cells infected with this virus. Endogenous IL10 expression was found with VVL15 (lacking the exogenous IL10 gene)-infected cells, suggesting a Lister viral IL10 homologue. No endogenous IL10 expression was found in cells infected with WR strain. Viral IL10 homologues have been discovered to be expressed by human cytomegalovirus, human herpes virus 4 and Yaba-like disease virus (poxvirus), but not to date by vaccinia virus. [262] MTS cell proliferation assays demonstrated increased potency of the Lister strain virus encoding murine IL10 (VVIL10) compared to control virus (VVL15). Viral replication assays were complicated by the effect of marked cell death in the VVIL10-treated group, limiting the number of viable cells available for virus replication. The mechanism for an *in vitro* action of IL10 is unclear.

To further investigate the *in vitro* anti-tumour function of IL10, the effect of recombinant IL10 (rIL10) alone and in combination with VVL15 on CMT93 cancer cells was examined. Using an MTS cytotoxicity assay technique, there was no evidence of a direct cytotoxic effect of rIL10 following a single application at a starting maximum concentration of $1x10^5$pg/ml. This finding was also been reported using direct application of rIL10 to CT26 cells (concentration range: 800 - $3x10^6$ pg/ml).[59] The half-life of recombinant IL10 *in vitro* is unclear. In mice following intravenous administration it has a half life of no more than 20 minutes. [263] rIL10 in conjunction with VVL15, and compared to VVL15 and VVIL10 alone, demonstrated an intermediate cytotoxicity result, between the high EC_{50} value of VVL15 alone and low EC_{50} value of VVIL10 alone. Clearly rIL10 is able to partially compensate for the lack

of the IL10 transgene in VVL15. It is feasible that administering more rIL10 may be able to bring the EC_{50} value of VVL15 + rIL10 closer to VVIL10.

Having established superior cytotoxicity of VVIL10 *in vitro* compared to VVL15, evaluation of VVIL10 *in vivo* required investigation. Using identical mouse cancer models as in the previous WR versus Lister efficacy studies this was achieved. The potency of VVIL10 compared to VVL15 and PBS in a nude CMT93 mouse model, demonstrated no significant difference in tumour progression. However, in the immunocompetent model diminished tumour progression was noted with the VVIL10-treated mice compared to VVL15 and PBS. This effect was enhanced by increasing the dose of VVIL10 administered from a three-day to a five-day regime. Further supportive evidence of VVIL10 superiority was obtained in a CT26 murine colorectal model in immunocompetent mice. Anti-tumour efficacy was also assessed a human pancreatic model of cancer (PT45) in nude mice. Interestingly, in contrast to the nude CMT93 mouse model, tumour progression was more limited with the VVIL10-treated mice compared to VVL15 and PBS. Clearly the effects of IL10 are not restricted to the cell-mediated immune system, with influences on the residual immune system of nude mice (NK cells,[234] macrophages [170]) and tumour angiogenesis, as suggested elsewhere. [167]

VVIL10 was further examined using similar methodology to the investigation of WR and Lister biodistribution and biological time-points studies following IV and IT delivery respectively. Biodistribution in an immunocompetent CMT93 mouse model demonstrated higher viral concentrations within the tumours for VVIL10-, compared to VVL15-, treated mice. This suggests that IL10 transgene expression was able to reduce systemic viral clearance allowing more of the virus dose to reach the tumours. Additionally when the VVIL10 virus started replicating within the tumour microenvironment, IL10 reduced viral clearance locally as demonstrated by the biological time-points data. There is also evidence of enhanced tumour selectivity of VVIL10 compared to VVL15 with reduced viral concentrations in the spleen, bone marrow and lung. Biodistribution and biological time-points were further examined in the PT45 human pancreatic model in nude mice. Higher tumour viral concentrations were recorded for VVIL10 compared to VVL15 following IT and IV administration, again suggesting the importance of the innate immune system in clearing invading viruses and how IL10 is able to subdue this response.

Investigation of an anti-tumour mechanism of IL10 focused on differences in the cytokine profiles following VVL15 and VVIL10 infections. CMT93 cells infected in tissue culture, and tumour and serum samples from mouse CMT93 flank tumours injected intratumourally were analysed. Cytokine levels from tissue culture and serum samples showed a marked elevation of several pro-inflammatory cytokines, including IFNγ, IL12, IL6, and IL1β, and elevation of the anti-inflammatory cytokine IL10 following VVIL10 infection compared to VVL15. These raised pro-inflammatory cytokines following VVIL10 infection correlate with higher viral titres from biodistribution and biological time-points studies, and superior anti-tumour potency in efficacy studies, compared to VVL15. Other studies looked at effect of macrophage cytokine expression *in vitro* following recombinant IL10 administration. [264-266] These experiments showed a depression of pro-inflammatory cytokines. However these experiments did not use virally mediated expression of IL10 and were *in vitro* studies only. IL4 is another important Th2 cytokine that inhibits cell-mediated immune responses, like IL10. IL4 vaccinia virus mediated expression has been shown to result in reduced pro-inflammatory cytokines following IV virus injection.[156] Therefore my findings would seem contradictory when correlating with higher viral titres and enhanced anti-tumour potency following VVIL10 infection, given the findings for WRDD and VVL15. Higher levels of pro-inflammatory cytokines were recorded with WRDD-treatment, which also demonstrated increased viral clearance and inferior anti-tumour efficacy compared to VVL15. However the levels of these pro-inflammatory cytokines are much higher following VVIL10-treatment than WRDD, and occur in the context of high IL10 levels. The roles of cytokines in tumourigenesis are poorly understood and can be paradoxical. They should be considered as a "cytokine network", rather than individual cytokines acting independently.[267] The effect of dose, timing, cell-type, effect of other cytokines, nutritional factors and other local mediators are all thought to be significant in determining an overall pro- or anti-inflammatory response. [260]

Finally, a recurrent finding of WR strain vaccinia virus biodistribution research relates to the high levels of virus found in ovarian tissue. [83,96,239,241,268] Smallpox was known to replicate preferentially in areas of increased vascular permeability secondary to injury and histamine release. [269] It has also been shown that increases in vascular permeability induced by hyperthermia leads to increased uptake of vaccinia virus. [270] Furthermore ovarian tissue has been shown to have high levels of VEGF, which increases vascular

permeability and hence vaccinia virus uptake. [271] However this does not explain why ovary tropism is not demonstrated with VVL15, but tumour tropism is preserved. Research has shown partial dependence on asialo-GM_1 for WR strain viruses to enter cells. [272] This potential accessory receptor is widely expressed in ovarian and brain tissue; and anti-serum to asialo-GM_1 has been shown to abrogate ovarian infection. [272] Further studies have shown that two viral proteins, A27L and H3L, interact with heparan sulphate to infect host cells.[92,93] Heparan sulphate is found abundantly in ovarian follicular basal lamina and is a potential candidate for supporting WR vaccinia virus entry into ovarian follicles.

9. Future work

This study challenges the dogma that the most promising vaccinia virus strain for human viral oncolytic gene therapy is Western Reserve. Lister strain virus has a number of characteristics, identified in this study, that suggest it might represent a preferred choice to WR. IL10 has been shown to have a powerful augmentative effect to the Lister strain, improving anti-tumour efficacy and tumour-selectivity. However a number of questions remain following this study.

The most significant question arising from my study is the functional mechanism of IL10 that results in improved anti-tumour efficacy. I have demonstrated that viral persistence is improved with IL10 expressing Lister strain virus. Other groups have reported conflicting data. One group demonstrated that administration of murine IL10 12 hours after vaccinia virus in a mouse model of pulmonary metastases enhanced viral effectiveness; however this was not through an immunosuppressive mechanism as vaccinia virus titres were found to be reduced following IL10 adjuvant therapy and CTL activity was increased. [59] Another group found that the use of an IL10R-blocking antibody resulted in reduced viral titres in immunocompetent mice infected with lymphocytic choriomeningitis virus. [237] Comparison of the biodistribution and anti-tumour efficacy in immunocompetent IL10R-knockout mice bearing flank tumours following IT and IV VVIL10 administration would provide further evidence for the effect on IL10 on viral persistence. Administration of IL10R-blocking antibody to immunocompetent mice bearing flank tumours following VVIL10 administration would also be informative.

IL10 expressed from an adenoviral vector has been shown to inhibit angiogenesis in a gastric cancer mouse model. [157] This was demonstrated using immunohistochemical staining of peritoneal nodules with monoclonal rat anti-CD31 antibody and calculation of microvascular density. Similar experiments could be performed on the samples from my CMT93 mouse model to evidence repression of angiogenesis following IT virus delivery. Furthermore, measurement of angiogenesis-mediating VEGF has been shown to be downregulated in a human melanoma cell line transfected with an IL10 expression vector and subsequent implantation into nude mice. [273] ELISA techniques are available to measure VEGF and other angiogenesis mediators such as MMP, as well as tissue inhibitors of MMP (TIMP) on existing tumour samples. Angiogenesis inhibition can

also be demonstrated *in vitro* through the effect of virally-infected cancer cell tissue culture supernatants on HUVEC tube formation and proliferation. [245]

Further proposed mechanisms of IL10 include effects on nitric oxide and the immune system. Nitric oxide is released by activated macrophages and neutrophils, and is a major defensive weapon against many pathogens. [274] IL10 gene transfer has been associated with increased inducible nitric oxide synthase (iNOS) protein expression and enzymatic activity *in vitro* and *in vivo*. [236] The *in vitro* effect of VVIL10 infection on cancer cell nitric oxide could be measured using a Greiss reagent, as previously described. [236] To assess nitric oxide or NOS levels *in vivo* Greiss reagents could be used on existing samples, or iNOS antibody on paraffin embedded tumour samples. Additionally anti-tumour efficacy of VVIL10 in iNOS knockout and control mice could be compared. The anti-tumour immune mechanisms of IL10 have been demonstrated to be dependent on natural killer cells, cytotoxic lymphocytes and macrophages. [233,234,236,275,276] Localisation of these cell types to tumours following VVIL10 administration compared to control virus using immunohistochemistry or FACS would be highly suggestive of their role in the mediation of an IL10 effect. Knockout mice or neutralising antibodies could also be used to determine the significance of specific immune cells on IL10 anti-tumour efficacy.

Finally, the ovarian tropism demonstrated by WR strain vaccinia virus, but not Lister strain, requires further investigation. Electron microscopy of the two viruses would determine the feasibility of a physical explanation of this tropism; based on the relative size of the viruses affecting their ability to pass through the ovarian vasculature endothelium. A molecular mechanism could be studied by comparing the infectability of ovarian follicular cells using fluorescence microscopy for detection of viral protein expression, real time PCR for viral mRNA expression and DNA amplification. Yeast hybridisation could also be used to identify new host factors or viral proteins that affect the tropism of WR strain vaccinia virus to ovaries.

Further studies using anti-asialo-GM_1 antibody and soluble heparan will determine the role of asialo-GM_1 and heparan sulphate in WR strain follicular attachment and uptake. Co-immunoprecipitation or a two-hybrid approach followed by mass spectrometry could identify a candidate protein at the surface of the follicular cell that interacts with WR proteins.

10. References

1. Cancer Facts & Figures 2009. Atlanta: American Cancer Society, 2009.
2. UK Health Research Analysis.
3. Available at: http://info.cancerresearchuk.org/cancerstats/survival/latestrates/index.htm. Accessed 01.05.2010 2010.
4. Peng Z. Current status of gendicine in China: recombinant human Ad-p53 agent for treatment of cancers. Hum Gene Ther 2005; 16:1016-1027.
5. Mathis JM, Stoff-Khalili MA, Curiel DT. Oncolytic adenoviruses - selective retargeting to tumor cells. Oncogene 2005; 24:7775-7791.
6. Hanahan D, Weinberg RA. Hallmarks of cancer: the next generation. Cell 2011; 144:646-674.
7. Hanahan D, Weinberg RA. The hallmarks of cancer. Cell 2000; 100:57-70.
8. Curto M, Cole BK, Lallemand D, Liu CH, McClatchey AI. Contact-dependent inhibition of EGFR signaling by Nf2/Merlin. J Cell Biol 2007; 177:893-903.
9. Partanen JI, Nieminen AI, Klefstrom J. 3D view to tumor suppression: Lkb1, polarity and the arrest of oncogenic c-Myc. Cell Cycle 2009; 8:716-724.
10. Adams JM, Cory S. The Bcl-2 apoptotic switch in cancer development and therapy. Oncogene 2007; 26:1324-1337.
11. Junttila MR, Evan GI. p53--a Jack of all trades but master of none. Nat Rev Cancer 2009; 9:821-829.
12. Levine B, Kroemer G. Autophagy in the pathogenesis of disease. Cell 2008; 132:27-42.
13. White E, DiPaola RS. The double-edged sword of autophagy modulation in cancer. Clin Cancer Res 2009; 15:5308-5316.
14. Grivennikov SI, Greten FR, Karin M. Immunity, inflammation, and cancer. Cell 2010; 140:883-899.
15. Blasco MA. Telomeres and human disease: ageing, cancer and beyond. Nat Rev Genet 2005; 6:611-622.
16. Kawai T, Hiroi S, Nakanishi K, Meeker AK. Telomere length and telomerase expression in atypical adenomatous hyperplasia and small bronchioloalveolar carcinoma of the lung. Am J Clin Pathol 2007; 127:254-262.
17. Artandi SE, Chang S, Lee SLet al. Telomere dysfunction promotes non-reciprocal translocations and epithelial cancers in mice. Nature 2000; 406:641-645.
18. Kang HJ, Choi YS, Hong SBet al. Ectopic expression of the catalytic subunit of telomerase protects against brain injury resulting from ischemia and NMDA-induced neurotoxicity. J Neurosci 2004; 24:1280-1287.
19. Baeriswyl V, Christofori G. The angiogenic switch in carcinogenesis. Semin Cancer Biol 2009; 19:329-337.
20. Zumsteg A, Christofori G. Corrupt policemen: inflammatory cells promote tumor angiogenesis. Curr Opin Oncol 2009; 21:60-70.
21. Kazerounian S, Yee KO, Lawler J. Thrombospondins in cancer. Cell Mol Life Sci 2008; 65:700-712.
22. Talmadge JE, Fidler IJ. AACR centennial series: the biology of cancer metastasis: historical perspective. Cancer Res 2010; 70:5649-5669.
23. Berx G, van Roy F. Involvement of members of the cadherin superfamily in cancer. Cold Spring Harb Perspect Biol 2009; 1:a003129.

24. Polyak K, Weinberg RA. Transitions between epithelial and mesenchymal states: acquisition of malignant and stem cell traits. Nat Rev Cancer 2009; 9:265-273.
25. Yang J, Weinberg RA. Epithelial-mesenchymal transition: at the crossroads of development and tumor metastasis. Dev Cell 2008; 14:818-829.
26. Joyce JA, Pollard JW. Microenvironmental regulation of metastasis. Nat Rev Cancer 2009; 9:239-252.
27. Kessenbrock K, Plaks V, Werb Z. Matrix metalloproteinases: regulators of the tumor microenvironment. Cell 2010; 141:52-67.
28. Naumov GN, Folkman J, Straume O. Tumor dormancy due to failure of angiogenesis: role of the microenvironment. Clin Exp Metastasis 2009; 26:51-60.
29. Kenific CM, Thorburn A, Debnath J. Autophagy and metastasis: another double-edged sword. Curr Opin Cell Biol 2010; 22:241-245.
30. Barkan D, Green JE, Chambers AF. Extracellular matrix: a gatekeeper in the transition from dormancy to metastatic growth. Eur J Cancer 2010; 46:1181-1188.
31. Teng MW, Swann JB, Koebel CM, Schreiber RD, Smyth MJ. Immune-mediated dormancy: an equilibrium with cancer. J Leukoc Biol 2008; 84:988-993.
32. Warburg O. On the origin of cancer cells. Science 1956; 123:309-314.
33. Potter VR. The biochemical approach to the cancer problem. Fed Proc 1958; 17:691-697.
34. Pages F, Galon J, Dieu-Nosjean MC, Tartour E, Sautes-Fridman C, Fridman WH. Immune infiltration in human tumors: a prognostic factor that should not be ignored. Oncogene 2010; 29:1093-1102.
35. Yang L, Pang Y, Moses HL. TGF-beta and immune cells: an important regulatory axis in the tumor microenvironment and progression. Trends Immunol 2010; 31:220-227.
36. Department Of Health. Genetics White Paper "Our inheritance, our future - realising the potential of genetics in the NHS". 2003.
37. Lehrman S. Virus treatment questioned after gene therapy death. Nature 1999; 401:517-518.
38. Young LS, Searle PF, Onion D, Mautner V. Viral gene therapy strategies: from basic science to clinical application. J Pathol 2006; 208:299-318.
39. Edelstein ML, Abedi MR, Wixon J. Gene therapy clinical trials worldwide to 2007--an update. J Gene Med 2007; 9:833-842.
40. Vile RG, Russell SJ, Lemoine NR. Cancer gene therapy: hard lessons and new courses. Gene Ther 2000; 7:2-8.
41. Shiraishi K, Kato S, Han SYet al. Isolation of temperature-sensitive p53 mutations from a comprehensive missense mutation library. J Biol Chem 2004; 279:348-355.
42. Liu CC, Shen Z, Kung HF, Lin MC. Cancer gene therapy targeting angiogenesis: an updated review. World J Gastroenterol 2006; 12:6941-6948.
43. Zitvogel L, Tesniere A, Kroemer G. Cancer despite immunosurveillance: immunoselection and immunosubversion. Nat Rev Immunol 2006; 6:715-727.
44. Bai XF, Liu J, Li O, Zheng P, Liu Y. Antigenic drift as a mechanism for tumor evasion of destruction by cytolytic T lymphocytes. J Clin Invest 2003; 111:1487-1496.
45. Bubenik J. MHC class I down-regulation: tumour escape from immune surveillance? (review). Int J Oncol 2004; 25:487-491.

46. Lehmann C, Zeis M, Schmitz N, Uharek L. Impaired binding of perforin on the surface of tumor cells is a cause of target cell resistance against cytotoxic effector cells. Blood 2000; 96:594-600.
47. Real LM, Jimenez P, Kirkin Aet al. Multiple mechanisms of immune evasion can coexist in melanoma tumor cell lines derived from the same patient. Cancer Immunol Immunother 2001; 49:621-628.
48. Shin MS, Kim HS, Lee SHet al. Mutations of tumor necrosis factor-related apoptosis-inducing ligand receptor 1 (TRAIL-R1) and receptor 2 (TRAIL-R2) genes in metastatic breast cancers. Cancer Res 2001; 61:4942-4946.
49. Kowalczyk DW. Tumors and the danger model. Acta Biochim Pol 2002; 49:295-302.
50. Elpek KG, Lacelle C, Singh NP, Yolcu ES, Shirwan H. CD4+CD25+ T regulatory cells dominate multiple immune evasion mechanisms in early but not late phases of tumor development in a B cell lymphoma model. J Immunol 2007; 178:6840-6848.
51. Ryschich E, Schmidt J, Hammerling GJ, Klar E, Ganss R. Transformation of the microvascular system during multistage tumorigenesis. Int J Cancer 2002; 97:719-725.
52. Uyttenhove C, Pilotte L, Theate Iet al. Evidence for a tumoral immune resistance mechanism based on tryptophan degradation by indoleamine 2,3-dioxygenase. Nat Med 2003; 9:1269-1274.
53. Zhang XM, Xu Q. Metastatic melanoma cells escape from immunosurveillance through the novel mechanism of releasing nitric oxide to induce dysfunction of immunocytes. Melanoma Res 2001; 11:559-567.
54. Beck C, Schreiber H, Rowley D. Role of TGF-beta in immune-evasion of cancer. Microsc Res Tech 2001; 52:387-395.
55. Kawamura K, Bahar R, Natsume W, Sakiyama S, Tagawa M. Secretion of interleukin-10 from murine colon carcinoma cells suppresses systemic antitumor immunity and impairs protective immunity induced against the tumors. Cancer Gene Ther 2002; 9:109-115.
56. Whiteside TL. Tumor-induced death of immune cells: its mechanisms and consequences. Semin Cancer Biol 2002; 12:43-50.
57. Gallina G, Dolcetti L, Serafini Pet al. Tumors induce a subset of inflammatory monocytes with immunosuppressive activity on CD8+ T cells. J Clin Invest 2006; 116:2777-2790.
58. Chen B, Timiryasova TM, Haghighat Pet al. Low-dose vaccinia virus-mediated cytokine gene therapy of glioma. J Immunother 2001; 24:46-57.
59. Kaufman HL, Rao JB, Irvine KR, Bronte V, Rosenberg SA, Restifo NP. Interleukin-10 enhances the therapeutic effectiveness of a recombinant poxvirus-based vaccine in an experimental murine tumor model. J Immunother 1999; 22:489-496.
60. Kirn DH, Thorne SH. Targeted and armed oncolytic poxviruses: a novel multi-mechanistic therapeutic class for cancer. Nat Rev Cancer 2009; 9:64-71.
61. Kaneda Y, Tabata Y. Non-viral vectors for cancer therapy. Cancer Sci 2006; 97:348-354.
62. Everts B, van der Poel HG. Replication-selective oncolytic viruses in the treatment of cancer. Cancer Gene Ther 2005; 12:141-161.
63. Vorburger SA, Hunt KK. Adenoviral gene therapy. Oncologist 2002; 7:46-59.
64. Parato KA, Senger D, Forsyth PA, Bell JC. Recent progress in the battle between oncolytic viruses and tumours. Nat Rev Cancer 2005; 5:965-976.
65. Dock G. Influence of complicating diseases upon leukaemia. Am J Med Sci 1904; 127:563-592.

66. Wong HH, Lemoine NR, Wang Y. Oncolytic Viruses for Cancer Therapy: Overcoming the Obstacles. Viruses 2010; 2:78-106.
67. Martuza RL, Malick A, Markert JM, Ruffner KL, Coen DM. Experimental therapy of human glioma by means of a genetically engineered virus mutant. Science 1991; 252:854-856.
68. Garber K. China approves world's first oncolytic virus therapy for cancer treatment. J Natl Cancer Inst 2006; 98:298-300.
69. Nemunaitis J, Ganly I, Khuri Fet al. Selective replication and oncolysis in p53 mutant tumors with ONYX-015, an E1B-55kD gene-deleted adenovirus, in patients with advanced head and neck cancer: a phase II trial. Cancer Res 2000; 60:6359-6366.
70. Mulvihill S, Warren R, Venook Aet al. Safety and feasibility of injection with an E1B-55 kDa gene-deleted, replication-selective adenovirus (ONYX-015) into primary carcinomas of the pancreas: a phase I trial. Gene Ther 2001; 8:308-315.
71. Douglas JT, Kim M, Sumerel LA, Carey DE, Curiel DT. Efficient oncolysis by a replicating adenovirus (ad) in vivo is critically dependent on tumor expression of primary ad receptors. Cancer Res 2001; 61:813-817.
72. Pesonen S, Kangasniemi L, Hemminki A. Oncolytic adenoviruses for the treatment of human cancer: focus on translational and clinical data. Mol Pharm 2011; 8:12-28.
73. Xu Z, Tian J, Smith JS, Byrnes AP. Clearance of adenovirus by Kupffer cells is mediated by scavenger receptors, natural antibodies, and complement. J Virol 2008; 82:11705-11713.
74. Wang Y, Gangeswaran R, Zhao Xet al. CEACAM6 attenuates adenovirus infection by antagonizing viral trafficking in cancer cells. J Clin Invest 2009; 119:1604-1615.
75. Moss B. Genetically engineered poxviruses for recombinant gene expression, vaccination, and safety. Proc Natl Acad Sci U S A 1996; 93:11341-11348.
76. Baxby D. The origins of vaccinia virus. J Infect Dis 1977; 136:453-455.
77. Fenner F HD AI, Jezek Z, Ladnyi ID. Smallpox and its eradication. Geneva: WHO, 1988.
78. Moss B. Poxvirus entry and membrane fusion. Virology 2006; 344:48-54.
79. Harrington KJ, Pandha H, Vile RG. Viral therapy of cancer. Hoboken, N.J.: Wiley ; Chichester : John Wiley [distributor], 2008.
80. ET. S. Adenoviruses: The viruses and their replication. . Philadelphia: Lipincott, Williams and Wilkins, 2001.
81. Hiley CT, Yuan M, Lemoine NR, Wang Y. Lister strain vaccinia virus, a potential therapeutic vector targeting hypoxic tumours. Gene Ther; 17:281-287.
82. Thorne SH, Hwang TH, O'Gorman WEet al. Rational strain selection and engineering creates a broad-spectrum, systemically effective oncolytic poxvirus, JX-963. J Clin Invest 2007; 117:3350-3358.
83. McCart JA, Ward JM, Lee Jet al. Systemic cancer therapy with a tumor-selective vaccinia virus mutant lacking thymidine kinase and vaccinia growth factor genes. Cancer Res 2001; 61:8751-8757.
84. Hayasaka D, Ennis FA, Terajima M. Pathogeneses of respiratory infections with virulent and attenuated vaccinia viruses. Virol J 2007; 4:22.
85. Luker KE, Hutchens M, Schultz T, Pekosz A, Luker GD. Bioluminescence imaging of vaccinia virus: effects of interferon on viral replication and spread. Virology 2005; 341:284-300.
86. Goebel SJ, Johnson GP, Perkus ME, Davis SW, Winslow JP, Paoletti E. The complete DNA sequence of vaccinia virus. Virology 1990; 179:247-266, 517-263.

87. Smith GL, Vanderplasschen A, Law M. The formation and function of extracellular enveloped vaccinia virus. J Gen Virol 2002; 83:2915-2931.
88. Smith GL, Vanderplasschen A. Extracellular enveloped vaccinia virus. Entry, egress, and evasion. Adv Exp Med Biol 1998; 440:395-414.
89. McFadden G. Poxvirus tropism. Nat Rev Microbiol 2005; 3:201-213.
90. Moss B. Poxviridae: The viruses and their replication. . Philadelphia: Lippincott Williams and Wilkins, 2001.
91. Hsiao JC, Chung CS, Chang W. Vaccinia virus envelope D8L protein binds to cell surface chondroitin sulfate and mediates the adsorption of intracellular mature virions to cells. J Virol 1999; 73:8750-8761.
92. Chung CS, Hsiao JC, Chang YS, Chang W. A27L protein mediates vaccinia virus interaction with cell surface heparan sulfate. J Virol 1998; 72:1577-1585.
93. Lin CL, Chung CS, Heine HG, Chang W. Vaccinia virus envelope H3L protein binds to cell surface heparan sulfate and is important for intracellular mature virion morphogenesis and virus infection in vitro and in vivo. J Virol 2000; 74:3353-3365.
94. Blasco R, Sisler JR, Moss B. Dissociation of progeny vaccinia virus from the cell membrane is regulated by a viral envelope glycoprotein: effect of a point mutation in the lectin homology domain of the A34R gene. J Virol 1993; 67:3319-3325.
95. McIntosh AA, Smith GL. Vaccinia virus glycoprotein A34R is required for infectivity of extracellular enveloped virus. J Virol 1996; 70:272-281.
96. Whitman ED, Tsung K, Paxson J, Norton JA. In vitro and in vivo kinetics of recombinant vaccinia virus cancer-gene therapy. Surgery 1994; 116:183-188.
97. Jain RK. Barriers to drug delivery in solid tumors. Sci Am 1994; 271:58-65.
98. Shen Y, Nemunaitis J. Fighting cancer with vaccinia virus: teaching new tricks to an old dog. Mol Ther 2005; 11:180-195.
99. Moroziewicz D, Kaufman HL. Gene therapy with poxvirus vectors. Curr Opin Mol Ther 2005; 7:317-325.
100. Hengstschlager M, Knofler M, Mullner EW, Ogris E, Wintersberger E, Wawra E. Different regulation of thymidine kinase during the cell cycle of normal versus DNA tumor virus-transformed cells. J Biol Chem 1994; 269:13836-13842.
101. Tzahar E, Moyer JD, Waterman Het al. Pathogenic poxviruses reveal viral strategies to exploit the ErbB signaling network. EMBO J 1998; 17:5948-5963.
102. Buller RM, Chakrabarti S, Moss B, Fredrickson T. Cell proliferative response to vaccinia virus is mediated by VGF. Virology 1988; 164:182-192.
103. de Magalhaes JC, Andrade AA, Silva PNet al. A mitogenic signal triggered at an early stage of vaccinia virus infection: implication of MEK/ERK and protein kinase A in virus multiplication. J Biol Chem 2001; 276:38353-38360.
104. Symons JA, Alcami A, Smith GL. Vaccinia virus encodes a soluble type I interferon receptor of novel structure and broad species specificity. Cell 1995; 81:551-560.
105. Colamonici OR, Domanski P, Sweitzer SM, Larner A, Buller RM. Vaccinia virus B18R gene encodes a type I interferon-binding protein that blocks interferon alpha transmembrane signaling. J Biol Chem 1995; 270:15974-15978.
106. Kirn DH, Wang Y, Le Boeuf F, Bell J, Thorne SH. Targeting of interferon-beta to produce a specific, multi-mechanistic oncolytic vaccinia virus. PLoS Med 2007; 4:e353.
107. Kettle S, Alcami A, Khanna A, Ehret R, Jassoy C, Smith GL. Vaccinia virus serpin B13R (SPI-2) inhibits interleukin-1beta-converting enzyme and protects

virus-infected cells from TNF- and Fas-mediated apoptosis, but does not prevent IL-1beta-induced fever. J Gen Virol 1997; 78 (Pt 3):677-685.
108. Alcami A, Smith GL. A soluble receptor for interleukin-1 beta encoded by vaccinia virus: a novel mechanism of virus modulation of the host response to infection. Cell 1992; 71:153-167.
109. Taylor JM, Quilty D, Banadyga L, Barry M. The vaccinia virus protein F1L interacts with Bim and inhibits activation of the pro-apoptotic protein Bax. J Biol Chem 2006; 281:39728-39739.
110. Prestwich RJ, Errington F, Diaz RMet al. The case of oncolytic viruses versus the immune system: waiting on the judgment of Solomon. Hum Gene Ther 2009; 20:1119-1132.
111. Biron CA. Role of early cytokines, including alpha and beta interferons (IFN-alpha/beta), in innate and adaptive immune responses to viral infections. Semin Immunol 1998; 10:383-390.
112. Boehm U, Klamp T, Groot M, Howard JC. Cellular responses to interferon-gamma. Annu Rev Immunol 1997; 15:749-795.
113. van den Broek MF, Muller U, Huang S, Aguet M, Zinkernagel RM. Antiviral defense in mice lacking both alpha/beta and gamma interferon receptors. J Virol 1995; 69:4792-4796.
114. Karupiah G, Buller RM, Van Rooijen N, Duarte CJ, Chen J. Different roles for CD4+ and CD8+ T lymphocytes and macrophage subsets in the control of a generalized virus infection. J Virol 1996; 70:8301-8309.
115. See DM, Khemka P, Sahl L, Bui T, Tilles JG. The role of natural killer cells in viral infections. Scand J Immunol 1997; 46:217-224.
116. Brutkiewicz RR, Klaus SJ, Welsh RM. Window of vulnerability of vaccinia virus-infected cells to natural killer (NK) cell-mediated cytolysis correlates with enhanced NK cell triggering and is concomitant with a decrease in H-2 class I antigen expression. Nat Immun 1992; 11:203-214.
117. Bukowski JF, Woda BA, Habu S, Okumura K, Welsh RM. Natural killer cell depletion enhances virus synthesis and virus-induced hepatitis in vivo. J Immunol 1983; 131:1531-1538.
118. Puhlmann M, Gnant M, Brown CK, Alexander HR, Bartlett DL. Thymidine kinase-deleted vaccinia virus expressing purine nucleoside phosphorylase as a vector for tumor-directed gene therapy. Hum Gene Ther 1999; 10:649-657.
119. Fenner F, Wittek R, Dumbell KR. The orthopoxviruses. San Diego ; London: Academic Press, 1989.
120. Fujiwara H, Shimizu Y, Takai Yet al. The augmentation of tumor-specific immunity by virus help. I. Demonstration of vaccinia virus-reactive helper T cell activity involved in enhanced induction of cytotoxic T lymphocyte and antibody responses. Eur J Immunol 1984; 14:171-175.
121. Seet BT, Johnston JB, Brunetti CRet al. Poxviruses and immune evasion. Annu Rev Immunol 2003; 21:377-423.
122. Park BH, Hwang T, Liu TCet al. Use of a targeted oncolytic poxvirus, JX-594, in patients with refractory primary or metastatic liver cancer: a phase I trial. Lancet Oncol 2008; 9:533-542.
123. Mastrangelo MJ, Maguire HC, Jr., Eisenlohr LCet al. Intratumoral recombinant GM-CSF-encoding virus as gene therapy in patients with cutaneous melanoma. Cancer Gene Ther 1999; 6:409-422.
124. Smith GL. Vaccinia virus immune evasion. Immunol Lett 1999; 65:55-62.
125. Kirn DH, Wang Y, Liang W, Contag CH, Thorne SH. Enhancing poxvirus oncolytic effects through increased spread and immune evasion. Cancer Res 2008; 68:2071-2075.

126. Deonarain R, Alcami A, Alexiou M, Dallman MJ, Gewert DR, Porter AC. Impaired antiviral response and alpha/beta interferon induction in mice lacking beta interferon. J Virol 2000; 74:3404-3409.
127. Thorne SH, Bartlett DL, Kirn DH. The use of oncolytic vaccinia viruses in the treatment of cancer: a new role for an old ally? Curr Gene Ther 2005; 5:429-443.
128. Jackson SS, Ilyinskii P, Philippon Vet al. Role of genes that modulate host immune responses in the immunogenicity and pathogenicity of vaccinia virus. J Virol 2005; 79:6554-6559.
129. Alcami A, Smith GL. Vaccinia, cowpox, and camelpox viruses encode soluble gamma interferon receptors with novel broad species specificity. J Virol 1995; 69:4633-4639.
130. Chang HW, Watson JC, Jacobs BL. The E3L gene of vaccinia virus encodes an inhibitor of the interferon-induced, double-stranded RNA-dependent protein kinase. Proc Natl Acad Sci U S A 1992; 89:4825-4829.
131. Davies MV, Chang HW, Jacobs BL, Kaufman RJ. The E3L and K3L vaccinia virus gene products stimulate translation through inhibition of the double-stranded RNA-dependent protein kinase by different mechanisms. J Virol 1993; 67:1688-1692.
132. Alcami A, Khanna A, Paul NL, Smith GL. Vaccinia virus strains Lister, USSR and Evans express soluble and cell-surface tumour necrosis factor receptors. J Gen Virol 1999; 80 (Pt 4):949-959.
133. Bowie A, Kiss-Toth E, Symons JA, Smith GL, Dower SK, O'Neill LA. A46R and A52R from vaccinia virus are antagonists of host IL-1 and toll-like receptor signaling. Proc Natl Acad Sci U S A 2000; 97:10162-10167.
134. DiPerna G, Stack J, Bowie AGet al. Poxvirus protein N1L targets the I-kappaB kinase complex, inhibits signaling to NF-kappaB by the tumor necrosis factor superfamily of receptors, and inhibits NF-kappaB and IRF3 signaling by toll-like receptors. J Biol Chem 2004; 279:36570-36578.
135. Ng A, Tscharke DC, Reading PC, Smith GL. The vaccinia virus A41L protein is a soluble 30 kDa glycoprotein that affects virus virulence. J Gen Virol 2001; 82:2095-2105.
136. Reading PC, Symons JA, Smith GL. A soluble chemokine-binding protein from vaccinia virus reduces virus virulence and the inflammatory response to infection. J Immunol 2003; 170:1435-1442.
137. Kotwal GJ, Moss B. Vaccinia virus encodes two proteins that are structurally related to members of the plasma serine protease inhibitor superfamily. J Virol 1989; 63:600-606.
138. Rosengard AM, Alonso LC, Korb LCet al. Functional characterization of soluble and membrane-bound forms of vaccinia virus complement control protein (VCP). Mol Immunol 1999; 36:685-697.
139. van Den Broek M, Bachmann MF, Kohler Get al. IL-4 and IL-10 antagonize IL-12-mediated protection against acute vaccinia virus infection with a limited role of IFN-gamma and nitric oxide synthetase 2. J Immunol 2000; 164:371-378.
140. Yu YA, Shabahang S, Timiryasova TMet al. Visualization of tumors and metastases in live animals with bacteria and vaccinia virus encoding light-emitting proteins. Nat Biotechnol 2004; 22:313-320.
141. Hunter-Craig I, Newton KA, Westbury G, Lacey BW. Use of vaccinia virus in the treatment of metastatic malignant melanoma. Br Med J 1970; 2:512-515.
142. Roenigk HH, Jr., Deodhar S, St Jacques R, Burdick K. Immunotherapy of malignant melanoma with vaccinia virus. Arch Dermatol 1974; 109:668-673.

143. Belisario JC, Milton GW. The experimental local therapy of cutaneous metastases of malignant melanoblastomas with cow pox vaccine or colcemid (demecolcine or omaine). Aust J Dermatol 1961; 6:113-118.
144. Lee SS, Eisenlohr LC, McCue PA, Mastrangelo MJ, Lattime EC. Intravesical gene therapy: in vivo gene transfer using recombinant vaccinia virus vectors. Cancer Res 1994; 54:3325-3328.
145. Katsafanas GC, Moss B. Vaccinia virus intermediate stage transcription is complemented by Ras-GTPase-activating protein SH3 domain-binding protein (G3BP) and cytoplasmic activation/proliferation-associated protein (p137) individually or as a heterodimer. J Biol Chem 2004; 279:52210-52217.
146. Gnant MF, Noll LA, Irvine KRet al. Tumor-specific gene delivery using recombinant vaccinia virus in a rabbit model of liver metastases. J Natl Cancer Inst 1999; 91:1744-1750.
147. Guo ZS, Naik A, O'Malley MEet al. The enhanced tumor selectivity of an oncolytic vaccinia lacking the host range and antiapoptosis genes SPI-1 and SPI-2. Cancer Res 2005; 65:9991-9998.
148. Denes B, Gridley DS, Fodor N, Takatsy Z, Timiryasova TM, Fodor I. Attenuation of a vaccine strain of vaccinia virus via inactivation of interferon viroceptor. J Gene Med 2006; 8:814-823.
149. Davison AJ, Moss B. Structure of vaccinia virus late promoters. J Mol Biol 1989; 210:771-784.
150. Scholl SM, Balloul JM, Le Goc Get al. Recombinant vaccinia virus encoding human MUC1 and IL2 as immunotherapy in patients with breast cancer. J Immunother 2000; 23:570-580.
151. Pantuck AJ, van Ophoven A, Gitlitz BJet al. Phase I trial of antigen-specific gene therapy using a recombinant vaccinia virus encoding MUC-1 and IL-2 in MUC-1-positive patients with advanced prostate cancer. J Immunother 2004; 27:240-253.
152. Kaufman HL, Cohen S, Cheung Ket al. Local delivery of vaccinia virus expressing multiple costimulatory molecules for the treatment of established tumors. Hum Gene Ther 2006; 17:239-244.
153. Zitvogel L, Apetoh L, Ghiringhelli F, Andre F, Tesniere A, Kroemer G. The anticancer immune response: indispensable for therapeutic success? J Clin Invest 2008; 118:1991-2001.
154. Mukherjee S, Haenel T, Himbeck Ret al. Replication-restricted vaccinia as a cytokine gene therapy vector in cancer: persistent transgene expression despite antibody generation. Cancer Gene Ther 2000; 7:663-670.
155. Qin H, Valentino J, Manna Set al. Gene therapy for head and neck cancer using vaccinia virus expressing IL-2 in a murine model, with evidence of immune suppression. Mol Ther 2001; 4:551-558.
156. Sharma DP, Ramsay AJ, Maguire DJ, Rolph MS, Ramshaw IA. Interleukin-4 mediates down regulation of antiviral cytokine expression and cytotoxic T-lymphocyte responses and exacerbates vaccinia virus infection in vivo. J Virol 1996; 70:7103-7107.
157. Tanaka F, Tominaga K, Shiota Met al. Interleukin-10 gene transfer to peritoneal mesothelial cells suppresses peritoneal dissemination of gastric cancer cells due to a persistently high concentration in the peritoneal cavity. Cancer Gene Ther 2008; 15:51-59.
158. McCart JA, Puhlmann M, Lee Jet al. Complex interactions between the replicating oncolytic effect and the enzyme/prodrug effect of vaccinia-mediated tumor regression. Gene Ther 2000; 7:1217-1223.

159. McCart JA, Mehta N, Scollard Det al. Oncolytic vaccinia virus expressing the human somatostatin receptor SSTR2: molecular imaging after systemic delivery using 111In-pentetreotide. Mol Ther 2004; 10:553-561.
160. Weissleder R, Moore A, Mahmood Uet al. In vivo magnetic resonance imaging of transgene expression. Nat Med 2000; 6:351-355.
161. Heo J, Reid T, Ruo Let al. Randomized dose-finding clinical trial of oncolytic immunotherapeutic vaccinia JX-594 in liver cancer. Nature medicine 2013; 19:329-336.
162. Kelly KJ, Woo Y, Brader Pet al. Novel oncolytic agent GLV-1h68 is effective against malignant pleural mesothelioma. Hum Gene Ther 2008; 19:774-782.
163. Fiorentino DF, Bond MW, Mosmann TR. Two types of mouse T helper cell. IV. Th2 clones secrete a factor that inhibits cytokine production by Th1 clones. J Exp Med 1989; 170:2081-2095.
164. O'Garra A, Barrat FJ, Castro AG, Vicari A, Hawrylowicz C. Strategies for use of IL-10 or its antagonists in human disease. Immunol Rev 2008; 223:114-131.
165. Kohno T, Mizukami H, Suzuki Met al. Interleukin-10-mediated inhibition of angiogenesis and tumor growth in mice bearing VEGF-producing ovarian cancer. Cancer Res 2003; 63:5091-5094.
166. Cervenak L, Morbidelli L, Donati Det al. Abolished angiogenicity and tumorigenicity of Burkitt lymphoma by interleukin-10. Blood 2000; 96:2568-2573.
167. Huang S, Ullrich SE, Bar-Eli M. Regulation of tumor growth and metastasis by interleukin-10: the melanoma experience. J Interferon Cytokine Res 1999; 19:697-703.
168. Spits H, de Waal Malefyt R. Functional characterization of human IL-10. Int Arch Allergy Immunol 1992; 99:8-15.
169. Asadullah K, Sterry W, Volk HD. Interleukin-10 therapy--review of a new approach. Pharmacol Rev 2003; 55:241-269.
170. Moore KW, de Waal Malefyt R, Coffman RL, O'Garra A. Interleukin-10 and the interleukin-10 receptor. Annu Rev Immunol 2001; 19:683-765.
171. Platzer C, Volk HD, Platzer M. 5' noncoding sequence of human IL-10 gene obtained by oligo-cassette PCR walking. DNA Seq 1994; 4:399-401.
172. Woiciechowsky C, Asadullah K, Nestler Det al. Sympathetic activation triggers systemic interleukin-10 release in immunodepression induced by brain injury. Nat Med 1998; 4:808-813.
173. Platzer C, Docke W, Volk H, Prosch S. Catecholamines trigger IL-10 release in acute systemic stress reaction by direct stimulation of its promoter/enhancer activity in monocytic cells. J Neuroimmunol 2000; 105:31-38.
174. Platzer C, Meisel C, Vogt K, Platzer M, Volk HD. Up-regulation of monocytic IL-10 by tumor necrosis factor-alpha and cAMP elevating drugs. Int Immunol 1995; 7:517-523.
175. Platzer C, Fritsch E, Elsner T, Lehmann MH, Volk HD, Prosch S. Cyclic adenosine monophosphate-responsive elements are involved in the transcriptional activation of the human IL-10 gene in monocytic cells. Eur J Immunol 1999; 29:3098-3104.
176. Meisel C, Vogt K, Platzer C, Randow F, Liebenthal C, Volk HD. Differential regulation of monocytic tumor necrosis factor-alpha and interleukin-10 expression. Eur J Immunol 1996; 26:1580-1586.
177. Riese U, Brenner S, Docke WDet al. Catecholamines induce IL-10 release in patients suffering from acute myocardial infarction by transactivating its promoter in monocytic but not in T-cells. Mol Cell Biochem 2000; 212:45-50.

178. Kotenko SV, Krause CD, Izotova LS, Pollack BP, Wu W, Pestka S. Identification and functional characterization of a second chain of the interleukin-10 receptor complex. EMBO J 1997; 16:5894-5903.
179. Weber-Nordt RM, Meraz MA, Schreiber RD. Lipopolysaccharide-dependent induction of IL-10 receptor expression on murine fibroblasts. J Immunol 1994; 153:3734-3744.
180. Liu Y, Wei SH, Ho AS, de Waal Malefyt R, Moore KW. Expression cloning and characterization of a human IL-10 receptor. J Immunol 1994; 152:1821-1829.
181. Michel G, Gailis A, Jarzebska-Deussen B, Muschen A, Mirmohammadsadegh A, Ruzicka T. 1,25-(OH)2-vitamin D3 and calcipotriol induce IL-10 receptor gene expression in human epidermal cells. Inflamm Res 1997; 46:32-34.
182. Ho AS, Liu Y, Khan TA, Hsu DH, Bazan JF, Moore KW. A receptor for interleukin 10 is related to interferon receptors. Proc Natl Acad Sci U S A 1993; 90:11267-11271.
183. Finbloom DS, Winestock KD. IL-10 induces the tyrosine phosphorylation of tyk2 and Jak1 and the differential assembly of STAT1 alpha and STAT3 complexes in human T cells and monocytes. J Immunol 1995; 155:1079-1090.
184. Vieira P, de Waal-Malefyt R, Dang MNet al. Isolation and expression of human cytokine synthesis inhibitory factor cDNA clones: homology to Epstein-Barr virus open reading frame BCRFI. Proc Natl Acad Sci U S A 1991; 88:1172-1176.
185. Jankovic D, Kullberg MC, Feng CGet al. Conventional T-bet(+)Foxp3(-) Th1 cells are the major source of host-protective regulatory IL-10 during intracellular protozoan infection. J Exp Med 2007; 204:273-283.
186. Anderson CF, Oukka M, Kuchroo VJ, Sacks D. CD4(+)CD25(-)Foxp3(-) Th1 cells are the source of IL-10-mediated immune suppression in chronic cutaneous leishmaniasis. J Exp Med 2007; 204:285-297.
187. O'Garra A, Vieira P. T(H)1 cells control themselves by producing interleukin-10. Nat Rev Immunol 2007; 7:425-428.
188. Trinchieri G. Interleukin-10 production by effector T cells: Th1 cells show self control. J Exp Med 2007; 204:239-243.
189. Kuhn R, Lohler J, Rennick D, Rajewsky K, Muller W. Interleukin-10-deficient mice develop chronic enterocolitis. Cell 1993; 75:263-274.
190. Sellon RK, Tonkonogy S, Schultz Met al. Resident enteric bacteria are necessary for development of spontaneous colitis and immune system activation in interleukin-10-deficient mice. Infect Immun 1998; 66:5224-5231.
191. Briere F, Bridon JM, Chevet Det al. Interleukin 10 induces B lymphocytes from IgA-deficient patients to secrete IgA. J Clin Invest 1994; 94:97-104.
192. Briere F, Chevet D, Bridon JM, Souillet G, Rifle G, Banchereau J. [B lymphocytes of patients with complete IgA deficiency secrete IgA in response to interleukin 10]. Nephrologie 1996; 17:289-295.
193. Defrance T, Vanbervliet B, Briere F, Durand I, Rousset F, Banchereau J. Interleukin 10 and transforming growth factor beta cooperate to induce anti-CD40-activated naive human B cells to secrete immunoglobulin A. J Exp Med 1992; 175:671-682.
194. Rousset F, Garcia E, Defrance Tet al. Interleukin 10 is a potent growth and differentiation factor for activated human B lymphocytes. Proc Natl Acad Sci U S A 1992; 89:1890-1893.
195. Thompson-Snipes L, Dhar V, Bond MW, Mosmann TR, Moore KW, Rennick DM. Interleukin 10: a novel stimulatory factor for mast cells and their progenitors. J Exp Med 1991; 173:507-510.

196. O'Garra A, Stapleton G, Dhar Vet al. Production of cytokines by mouse B cells: B lymphomas and normal B cells produce interleukin 10. Int Immunol 1990; 2:821-832.
197. Chen WF, Zlotnik A. IL-10: a novel cytotoxic T cell differentiation factor. J Immunol 1991; 147:528-534.
198. Pestka S, Krause CD, Sarkar D, Walter MR, Shi Y, Fisher PB. Interleukin-10 and related cytokines and receptors. Annu Rev Immunol 2004; 22:929-979.
199. Groux H, Bigler M, de Vries JE, Roncarolo MG. Inhibitory and stimulatory effects of IL-10 on human CD8+ T cells. J Immunol 1998; 160:3188-3193.
200. Groux H, Cottrez F, Rouleau Met al. A transgenic model to analyze the immunoregulatory role of IL-10 secreted by antigen-presenting cells. J Immunol 1999; 162:1723-1729.
201. Schottelius AJ, Mayo MW, Sartor RB, Baldwin AS, Jr. Interleukin-10 signaling blocks inhibitor of kappaB kinase activity and nuclear factor kappaB DNA binding. J Biol Chem 1999; 274:31868-31874.
202. Ito S, Ansari P, Sakatsume Met al. Interleukin-10 inhibits expression of both interferon alpha- and interferon gamma- induced genes by suppressing tyrosine phosphorylation of STAT1. Blood 1999; 93:1456-1463.
203. Yamaoka K, Otsuka T, Niiro Het al. Selective DNA-binding activity of interleukin-10-stimulated STAT molecules in human monocytes. J Interferon Cytokine Res 1999; 19:679-685.
204. Lee TS, Chau LY. Heme oxygenase-1 mediates the anti-inflammatory effect of interleukin-10 in mice. Nat Med 2002; 8:240-246.
205. Tilg H, van Montfrans C, van den Ende Aet al. Treatment of Crohn's disease with recombinant human interleukin 10 induces the proinflammatory cytokine interferon gamma. Gut 2002; 50:191-195.
206. Asadullah K, Friedrich M, Hanneken Set al. Effects of systemic interleukin-10 therapy on psoriatic skin lesions: histologic, immunohistologic, and molecular biology findings. J Invest Dermatol 2001; 116:721-727.
207. Samoilova EB, Horton JL, Chen Y. Acceleration of experimental autoimmune encephalomyelitis in interleukin-10-deficient mice: roles of interleukin-10 in disease progression and recovery. Cell Immunol 1998; 188:118-124.
208. Kennedy MK, Torrance DS, Picha KS, Mohler KM. Analysis of cytokine mRNA expression in the central nervous system of mice with experimental autoimmune encephalomyelitis reveals that IL-10 mRNA expression correlates with recovery. J Immunol 1992; 149:2496-2505.
209. Bettelli E, Das MP, Howard ED, Weiner HL, Sobel RA, Kuchroo VK. IL-10 is critical in the regulation of autoimmune encephalomyelitis as demonstrated by studies of IL-10- and IL-4-deficient and transgenic mice. J Immunol 1998; 161:3299-3306.
210. Cua DJ, Hutchins B, LaFace DM, Stohlman SA, Coffman RL. Central nervous system expression of IL-10 inhibits autoimmune encephalomyelitis. J Immunol 2001; 166:602-608.
211. Whiteside TL. Immune suppression in cancer: effects on immune cells, mechanisms and future therapeutic intervention. Semin Cancer Biol 2006; 16:3-15.
212. Herber DL, Nagaraj S, Djeu JY, Gabrilovich DI. Mechanism and therapeutic reversal of immune suppression in cancer. Cancer Res 2007; 67:5067-5069.
213. Dunn GP, Old LJ, Schreiber RD. The three Es of cancer immunoediting. Annu Rev Immunol 2004; 22:329-360.

214. Balkwill F, Charles KA, Mantovani A. Smoldering and polarized inflammation in the initiation and promotion of malignant disease. Cancer Cell 2005; 7:211-217.
215. Baniyash M. Chronic inflammation, immunosuppression and cancer: new insights and outlook. Semin Cancer Biol 2006; 16:80-88.
216. Lun XQ, Jang JH, Tang Net al. Efficacy of systemically administered oncolytic vaccinia virotherapy for malignant gliomas is enhanced by combination therapy with rapamycin or cyclophosphamide. Clin Cancer Res 2009; 15:2777-2788.
217. Yue FY, Dummer R, Geertsen Ret al. Interleukin-10 is a growth factor for human melanoma cells and down-regulates HLA class-I, HLA class-II and ICAM-1 molecules. Int J Cancer 1997; 71:630-637.
218. Matsuda M, Salazar F, Petersson Met al. Interleukin 10 pretreatment protects target cells from tumor- and allo-specific cytotoxic T cells and downregulates HLA class I expression. J Exp Med 1994; 180:2371-2376.
219. Masood R, Zhang Y, Bond MWet al. Interleukin-10 is an autocrine growth factor for acquired immunodeficiency syndrome-related B-cell lymphoma. Blood 1995; 85:3423-3430.
220. Gu ZJ, Costes V, Lu ZYet al. Interleukin-10 is a growth factor for human myeloma cells by induction of an oncostatin M autocrine loop. Blood 1996; 88:3972-3986.
221. Sica A, Bronte V. Altered macrophage differentiation and immune dysfunction in tumor development. J Clin Invest 2007; 117:1155-1166.
222. Sica A, Schioppa T, Mantovani A, Allavena P. Tumour-associated macrophages are a distinct M2 polarised population promoting tumour progression: potential targets of anti-cancer therapy. Eur J Cancer 2006; 42:717-727.
223. Porta C, Subhra Kumar B, Larghi P, Rubino L, Mancino A, Sica A. Tumor promotion by tumor-associated macrophages. Adv Exp Med Biol 2007; 604:67-86.
224. Mantovani A, Schioppa T, Porta C, Allavena P, Sica A. Role of tumor-associated macrophages in tumor progression and invasion. Cancer Metastasis Rev 2006; 25:315-322.
225. Mocellin S, Marincola FM, Young HA. Interleukin-10 and the immune response against cancer: a counterpoint. J Leukoc Biol 2005; 78:1043-1051.
226. Sakamoto T, Saito H, Tatebe Set al. Interleukin-10 expression significantly correlates with minor CD8+ T-cell infiltration and high microvessel density in patients with gastric cancer. Int J Cancer 2006; 118:1909-1914.
227. Lech-Maranda E, Bienvenu J, Michallet ASet al. Elevated IL-10 plasma levels correlate with poor prognosis in diffuse large B-cell lymphoma. Eur Cytokine Netw 2006; 17:60-66.
228. De Vita F, Orditura M, Galizia Get al. Serum interleukin-10 levels as a prognostic factor in advanced non-small cell lung cancer patients. Chest 2000; 117:365-373.
229. De Vita F, Orditura M, Galizia Get al. Serum interleukin-10 is an independent prognostic factor in advanced solid tumors. Oncol Rep 2000; 7:357-361.
230. De Vita F, Orditura M, Galizia Get al. Serum interleukin-10 levels in patients with advanced gastrointestinal malignancies. Cancer 1999; 86:1936-1943.
231. Loser K, Apelt J, Voskort Met al. IL-10 controls ultraviolet-induced carcinogenesis in mice. J Immunol 2007; 179:365-371.
232. Fujii S, Shimizu K, Shimizu T, Lotze MT. Interleukin-10 promotes the maintenance of antitumor CD8(+) T-cell effector function in situ. Blood 2001; 98:2143-2151.

233. Berman RM, Suzuki T, Tahara H, Robbins PD, Narula SK, Lotze MT. Systemic administration of cellular IL-10 induces an effective, specific, and long-lived immune response against established tumors in mice. J Immunol 1996; 157:231-238.
234. Zheng LM, Ojcius DM, Garaud Fet al. Interleukin-10 inhibits tumor metastasis through an NK cell-dependent mechanism. J Exp Med 1996; 184:579-584.
235. Stearns ME, Rhim J, Wang M. Interleukin 10 (IL-10) inhibition of primary human prostate cell-induced angiogenesis: IL-10 stimulation of tissue inhibitor of metalloproteinase-1 and inhibition of matrix metalloproteinase (MMP)-2/MMP-9 secretion. Clin Cancer Res 1999; 5:189-196.
236. Kundu N, Dorsey R, Jackson MJet al. Interleukin-10 gene transfer inhibits murine mammary tumors and elevates nitric oxide. Int J Cancer 1998; 76:713-719.
237. Brooks DG, Trifilo MJ, Edelmann KH, Teyton L, McGavern DB, Oldstone MB. Interleukin-10 determines viral clearance or persistence in vivo. Nat Med 2006; 12:1301-1309.
238. Timiryasova TM, Chen B, Fodor N, Fodor I. Construction of recombinant vaccinia viruses using PUV-inactivated virus as a helper. Biotechniques 2001; 31:534, 536, 538-540.
239. Hung CF, Tsai YC, He Let al. Vaccinia virus preferentially infects and controls human and murine ovarian tumors in mice. Gene Ther 2007; 14:20-29.
240. Denes B, Yu J, Fodor N, Takatsy Z, Fodor I, Langridge WH. Suppression of hyperglycemia in NOD mice after inoculation with recombinant vaccinia viruses. Mol Biotechnol 2006; 34:317-327.
241. Puhlmann M, Brown CK, Gnant Met al. Vaccinia as a vector for tumor-directed gene therapy: biodistribution of a thymidine kinase-deleted mutant. Cancer Gene Ther 2000; 7:66-73.
242. Wright CF, Keck JG, Tsai MM, Moss B. A transcription factor for expression of vaccinia virus late genes is encoded by an intermediate gene. J Virol 1991; 65:3715-3720.
243. Garcel A, Crance JM, Drillien R, Garin D, Favier AL. Genomic sequence of a clonal isolate of the vaccinia virus Lister strain employed for smallpox vaccination in France and its comparison to other orthopoxviruses. J Gen Virol 2007; 88:1906-1916.
244. Mastrangelo MJ, Maguire HC, Lattime EC. Intralesional vaccinia/GM-CSF recombinant virus in the treatment of metastatic melanoma. Adv Exp Med Biol 2000; 465:391-400.
245. Tysome JR, Briat A, Alusi Get al. Lister strain of vaccinia virus armed with endostatin-angiostatin fusion gene as a novel therapeutic agent for human pancreatic cancer. Gene Ther 2009; 16:1223-1233.
246. Williamson JD, Reith RW, Jeffrey LJ, Arrand JR, Mackett M. Biological characterization of recombinant vaccinia viruses in mice infected by the respiratory route. J Gen Virol 1990; 71 (Pt 11):2761-2767.
247. Mohiuddin M, Chendil D, Dey S, Alcock RA, Regine W, Ahmed MM. Influence of p53 status on radiation and 5-flourouracil synergy in pancreatic cancer cells. Anticancer Res 2002; 22:825-830.
248. Eisold S, Linnebacher M, Ryschich Eet al. The effect of adenovirus expressing wild-type p53 on 5-fluorouracil chemosensitivity is related to p53 status in pancreatic cancer cell lines. World J Gastroenterol 2004; 10:3583-3589.
249. Nichols AC, Yoo J, Palma DAet al. Frequent mutations in TP53 and CDKN2A found by next-generation sequencing of head and neck cancer cell lines. Arch Otolaryngol Head Neck Surg 2012; 138:732-739.

250. Hayashi N, Sugimoto Y, Tsuchiya E, Ogawa M, Nakamura Y. Somatic mutations of the MTS (multiple tumor suppressor) 1/CDK4l (cyclin-dependent kinase-4 inhibitor) gene in human primary non-small cell lung carcinomas. Biochemical and biophysical research communications 1994; 202:1426-1430.
251. Sipos B, Moser S, Kalthoff H, Torok V, Lohr M, Kloppel G. A comprehensive characterization of pancreatic ductal carcinoma cell lines: towards the establishment of an in vitro research platform. Virchows Arch 2003; 442:444-452.
252. Moore PS, Sipos B, Orlandini Set al. Genetic profile of 22 pancreatic carcinoma cell lines. Analysis of K-ras, p53, p16 and DPC4/Smad4. Virchows Arch 2001; 439:798-802.
253. Wang Y, Zhang Y, Yang Jet al. Genomic sequencing of key genes in mouse pancreatic cancer cells. Curr Mol Med 2012; 12:331-341.
254. Abaan OD, Polley EC, Davis SRet al. The exomes of the NCI-60 panel: a genomic resource for cancer biology and systems pharmacology. Cancer research 2013; 73:4372-4382.
255. Akama Y, Yasui W, Kuniyasu Het al. Genetic status and expression of the cyclin-dependent kinase inhibitors in human gastric carcinoma cell lines. Jpn J Cancer Res 1996; 87:824-830.
256. Nishizuka S, Tamura G, Maesawa Cet al. Analysis of the DPC4 gene in gastric carcinoma. Jpn J Cancer Res 1997; 88:335-339.
257. Kitamura T, Fujishita T, Loetscher Pet al. Inactivation of chemokine (C-C motif) receptor 1 (CCR1) suppresses colon cancer liver metastasis by blocking accumulation of immature myeloid cells in a mouse model. Proceedings of the National Academy of Sciences of the United States of America 2010; 107:13063-13068.
258. Zhang B, Halder SK, Zhang S, Datta PK. Targeting transforming growth factor-beta signaling in liver metastasis of colon cancer. Cancer Lett 2009; 277:114-120.
259. Saito M, Okamoto A, Kohno Tet al. Allelic imbalance and mutations of the PTEN gene in ovarian cancer. Int J Cancer 2000; 85:160-165.
260. Mocellin S, Wang E, Marincola FM. Cytokines and immune response in the tumor microenvironment. J Immunother 2001; 24:392-407.
261. Smith VP, Bryant NA, Alcami A. Ectromelia, vaccinia and cowpox viruses encode secreted interleukin-18-binding proteins. J Gen Virol 2000; 81:1223-1230.
262. Bartlett NW, Dumoutier L, Renauld JCet al. A new member of the interleukin 10-related cytokine family encoded by a poxvirus. J Gen Virol 2004; 85:1401-1412.
263. Gerard C, Bruyns C, Marchant Aet al. Interleukin 10 reduces the release of tumor necrosis factor and prevents lethality in experimental endotoxemia. J Exp Med 1993; 177:547-550.
264. de Waal Malefyt R, Haanen J, Spits Het al. Interleukin 10 (IL-10) and viral IL-10 strongly reduce antigen-specific human T cell proliferation by diminishing the antigen-presenting capacity of monocytes via downregulation of class II major histocompatibility complex expression. J Exp Med 1991; 174:915-924.
265. Fiorentino DF, Zlotnik A, Mosmann TR, Howard M, O'Garra A. IL-10 inhibits cytokine production by activated macrophages. J Immunol 1991; 147:3815-3822.
266. Bogdan C, Vodovotz Y, Nathan C. Macrophage deactivation by interleukin 10. J Exp Med 1991; 174:1549-1555.

267. Knowles MA, Selby P. Introduction to the cellular and molecular biology of cancer. New York: Oxford University Press, 2005.
268. Karupiah G, Coupar B, Ramshaw I, Boyle D, Blanden R, Andrew M. Vaccinia virus-mediated damage of murine ovaries and protection by virus-expressed interleukin-2. Immunol Cell Biol 1990; 68 (Pt 5):325-333.
269. Ricketts TF. The diagnosis of smallpox. Washington: U. S. Public Health Service, Division of Foreign Quarantine, 1966.
270. Chang E, Chalikonda S, Friedl Jet al. Targeting vaccinia to solid tumors with local hyperthermia. Hum Gene Ther 2005; 16:435-444.
271. Reynolds LP, Grazul-Bilska AT, Redmer DA. Angiogenesis in the corpus luteum. Endocrine 2000; 12:1-9.
272. Karupiah G, Blanden RV. Anti-asialo-GM1 inhibits vaccinia virus infection of murine ovaries: asialo-GM1 as an additional virus receptor? Immunol Cell Biol 1990; 68 (Pt 5):343-346.
273. Huang S, Xie K, Bucana CD, Ullrich SE, Bar-Eli M. Interleukin 10 suppresses tumor growth and metastasis of human melanoma cells: potential inhibition of angiogenesis. Clin Cancer Res 1996; 2:1969-1979.
274. MacMicking J, Xie QW, Nathan C. Nitric oxide and macrophage function. Annu Rev Immunol 1997; 15:323-350.
275. Kundu N, Beaty TL, Jackson MJ, Fulton AM. Antimetastatic and antitumor activities of interleukin 10 in a murine model of breast cancer. J Natl Cancer Inst 1996; 88:536-541.
276. Kundu N, Fulton AM. Interleukin-10 inhibits tumor metastasis, downregulates MHC class I, and enhances NK lysis. Cell Immunol 1997; 180:55-61.